# Macrophages and Endothelial Cells in the Pancreatic Islet Microenvironment Promote β Cell Regeneration

Ву

Kristie Irene Aamodt

Dissertation

Submitted to the Faculty of the
Graduate School of Vanderbilt University
in partial fulfillment of the requirements
for the degree of

**DOCTOR OF PHILOSOPHY** 

in

Molecular Physiology and Biophysics

August, 2015 Nashville, Tennessee

Approved:

Ambra Pozzi, Ph.D., Chair

Alyssa H. Hasty, Ph.D.

Roland W. Stein, Ph.D.

Pampee P. Young, M.D., Ph.D.

To my grandparents, whose decisions made my dreams possible, and whose lives remind me which goals are truly worth the striving.

## **ACKNOWLEDGEMENTS**

First I would like to thank the Vanderbilt Medical Scientist Training Program for giving me the opportunity to pursue this work, and my training as a physician-scientist. Thank you especially to Terry Dermody and members of the leadership team and administrative staff both past and present: Larry Swift, Jim Bills, Michelle Grundy, Danny Winder, Sally York, Lindsay Meyers, and Melissa Krasnove. The greatest strength of this training program is the people involved, and I am so grateful for the endless support and encouragement I have received over the last six years. I am also grateful for the many opportunities I have been given to serve on committees and to develop and participate in programming. I am a better colleague, scientist, and leader because of these experiences. My training and this work has been supported by the National Institutes of Health (T32 GM07347), multiple grants from the National Institute of Diabetes and Digestive and Kidney Disease (including a National Research Service Award F30 DK097921), the U.S. Department of Veterans Affairs, and the Juvenile Diabetes Research Foundation.

I am immeasurably grateful to my mentor of the last four years, AI Powers. Thank you for constantly demonstrating to me what it truly means to be a physician-scientist: passionate about your research on pancreatic islets, and entirely dedicated to caring for your patients and their families. I hope to take those qualities with me throughout my career. Thank you for providing me with many opportunities to present my research, mentor students, work on grants, form collaborations, and for supporting me in my other scientific, teaching, and leadership endeavors. Your encouragement and vision for my training has made me a better writer, speaker, thinker, collaborator, and ultimately a better scientist. Finally, thank you for bringing together and supporting such a strong team of individuals in the lab who have made my experience both enriching and enjoyable, and for truly caring about the well being of each lab member both inside and outside of the lab.

The members of the Powers laboratory, both past and present, have each contributed to this work and I cannot thank them enough for their scientific contributions, conversations, and friendships, that have made it a pleasure to come into the lab every day. I have to especially thank Marcela Brissova, who has not only been a trusted colleague and second mentor to me, but also a dear friend. This work would not have been possible without your generosity in sharing your time, expertise, and knowledge. The discussions we have had over the last four years have shaped my thinking and driven this work forward; and your personal strength and scientific rigor have been an example to me, for which I will be forever grateful. Thanks also to our incredible research technicians, Radhika Armandla, Greg Poffenberger, and Alena Shostak whose technical skills and commitment have helped maintain a high standard of experimental consistency and quality, which is reflected in this work. I am particularly grateful to Radhika; your wholehearted dedication, support, and hard work helped immensely in driving this work forward, and I would not have been able to accomplish even a fraction of this work without your help. Thank you also to Chunhua Dai, whose insights, knowledge, and work ethic have taught me so much during my time in the lab. It is difficult to express how grateful I am to the graduate students— Rachel Reinert, Qing Cai, Nora Kayton, Diane Saunders, and Rachana Haliyur—and post-doctoral fellows—Danielle Dean, Neil Phillips, Nathaniel Hart, and Ana Maria Robledo Reyes—in the lab that

I have been blessed to work with over the last four years. In addition to always being willing to lend a helping hand, you have so generously provided me with knowledge, advice, support and friendship over the years that have made the disappointments we faced less daunting, and the triumphs more sweet. I will forever value our time together. The environment in the lab over the past four years has enriched my life both personally and professionally, and it has been a privilege to work with and learn from each of you.

Thanks also to former post-doctoral fellow Priyanka Brahmachary who I did not have the pleasure of working with, but whose research provided the foundation for mine; and to rotation students Judy Brown, Megan Dumas, and undergraduate Zoya Khan for their contributions to this work, and their patience with me.

A huge thank you is due to both Shawn Levy and Nripesh Prasad at the Genomic Services Laboratory at HudsonAlpha Institute for Biotechnology for an extremely rewarding collaboration. Your technical and analytical expertise not only elevated the quality of this research, but also greatly expanded my knowledge and understanding. I am especially grateful to Nripesh, thank you for the many hours you dedicated to sample processing and analysis, and for your endless patience in explaining and teaching me over conference calls and in person. I look forward to continuing our friendship and collaboration for many years to come.

This research would not be possible without support from the numerous core facilities and divisions at Vanderbilt. The Islet Procurement and Analysis Core was invaluable in performing the massive number of islet isolations required for these studies, and I want to particularly thank Anastasia Coldran for her expertise and dedication. Thanks to Kevin Weller, David Flaherty, and Brittany Matlock at the Flow Cytometry Core for their help in designing experiments and their flexibility in working with our experimental time constraints. I also appreciate the help of Vladimir Babeav at the Vanderbilt Cardiovascular Pathophysiology and Complications Core who performed our bone marrow isolations. Thanks to all of the technicians, administrators, and staff at the Division of Animal Care whose contribution to watching after our animals is much appreciated, and particularly to Patty Chen for always being willing to work with us to ensure our animals stayed as healthy as possible.

Thank you to my thesis committee members Ambra Pozzi, Alyssa Hasty, Roland Stein, and Pampee Young for your constructive feedback and for always pushing me to improve. Neither my work nor my training would be as strong without your involvement. I also want to thank the faculty, administrators, and students of the Department of Molecular Physiology and Biophysics Department, and the organizers and staff of the Diabetes Research and Training Center and the Beta Cell Interest Group for providing such an enriching training environment. To my fellow medical, graduate, and MSTP students, thank you for the friendships, conversations, advice, and memories. It has been a privilege to be on this journey with you and to share our disappointments, struggles, victories, and achievements.

I have been blessed with a wonderfully supportive family and dear friends who have helped me make it through these last six years. Every opportunity I have had in life is due to my parents. Mom and dad, your encouragement and unquestioning love mean the world to me, and have opened up the world to me. Thank you for always being there and teaching me to reach for my dreams and beyond, and most importantly for showing me what is truly most important in life. To my sisters Heather, Danielle, Sharlene, Melanie, and my brother Robi, life would never be as entertaining or rewarding if I did not share it with you. I want to especially thank Heather and Andy for all of the meals, naps, and cathartic discussions over the years; it has been a blessing to live so close. To my nieces Evelyn and Olivia, I hope you never lose sight of how exciting the world is and how limitless your potential—keep giggling, questioning, and loving. Thank you to all my family for the love, prayers, memories, messages, laughter, and tears. I would not want to be in the forever club with any other group of people.

## **TABLE OF CONTENTS**

	Page
DEDICATION	ii
ACKNOWLEDGEMENTS	iii
LIST OF TABLES	ix
LIST OF FIGURES	жх
LIST OF ABBREVIATIONS	
Chapter	
I. BACKGROUND AND SIGNIFICANCE	1
The Pancreas Anatomy and physiology	
Pancreatic development and establishing β cell mass	3
Diabetes Mellitus	4
Epidemiology and pathophysiology	4
Pancreatic β cell replacement as a therapeutic goal	5
Pancreatic islet transplantation	
Differentiation of pluripotent stem cells  Transdifferentiation from mature endocrine cells and other lineages	
Expansion of adult β cells	
Pancreatic Islet Vascularization	
Pancreatic Islet Extracellular Matrix	11
Endocrine cell-cell interactions	12
Endocrine cell-matrix interactions	13
Integrin and non-integrin receptors	13
Collagen	14
Laminin	
Glycoproteins	
Proteoglycans	
Macrophages  Tissue homeostasis, inflammation, and repair	
·	
Functional roles in the pancreas	
Aims of Dissertation	16

II.	MATERIALS AND METHODS	18
	Mouse Models	18
	DNA extraction and genotyping	20
	Glucose measurements and glucose tolerance testing	20
	Bone marrow isolation, irradiation, and transplantation	20
	Compound preparation and administration	22
	Doxycycline (Dox)	22
	Diphtheria toxin (DT)	22
	Clodronate liposomes (Clod)	
	Tamoxifen (Tm)	
	Bromodeoxyuridine (BrdU)	
	Islet Isolation and In Vitro Analysis	
	Islet perifusion	23
	Islet VEGF-A secretion.	23
	Islet Transplantation	24
	Flow Cytometry and Cell Sorting	24
	RNA Isolation, Sequencing, and Analysis	25
	Tissue Collection, Fixation, and Analysis	26
	Intravital blood vessel labeling	26
	Pancreatic hormone content	26
	Immunohistochemistry, Imaging, and Analysis	27
	BrdU labeling in cryosections	27
	X-Gal enzymatic staining.	27
	Imaging and morphometry	29
	In Vitro Screening of Mitogenic Compounds on Primary Human Islet Cells	30
	Human islet dispersion, transduction, plating, and culture	30
	Compound preparation and islet cell treatment	30
	Immunocytochemistry, imaging, and analysis	30
	Statistical Analysis	32
III.	ISLET MICROENVIRONMENT, MODULATED BY VASCULAR ENDOTHELIAL	
	GROWTH FACTOR-A SIGNALING, PROMOTES β CELL REGENERATION	33
	Introduction	33
	Results	34
	Increased β cell VEGF-A production leads to islet endothelial cell expansion and	0.4
	β cell loss followed by β cell regeneration after VEGF-A normalizes	34

	Withdrawal of the VEGF-A stimulus results in increased proliferation of pre-existing β cells	40
	$\beta$ cell replication after VEGF-A normalization is independent of the pancreatic site and soluble circulating factors and is not limited to murine $\beta$ cells	44
	Recruited macrophages are crucial for the β cell proliferative response in βVEGF-A islets	47
	Both macrophages and endothelial cells in the βVEGF-A islet microenvironment produce factors that promote tissue repair and regeneration	56
	Discussion	59
IV.	INTERACTIONS BETWEEN PANCREATIC ISLET β CELLS, ENDOTHELIAL CELLS, MACROPHAGES, AND THE EXTRACELLULAR MATRIX PROMOTE β CELL PROLIFERATION	62
	Introduction	62
	Results  Genetic model of diphtheria toxin-mediated macrophage depletion fails to adequately remove macrophages or recreate the regenerative βVEGF-A islet microenvironment.	
	Chemical approach effectively depletes macrophages in $\beta$ VEGF-A islets and demonstrates that macrophages are required for $\beta$ cell proliferation	65
	Development of a model to evaluate the role of endothelial cells in the βVEGF-A microenvironment	65
	Identifying interactions between $\beta$ cells, endothelial cells, macrophages, and the extracellular matrix in the $\beta$ VEGF-A islet microenvironment	69
	Discussion	77
V.	EVALUATION OF ADULT HUMAN β CELL PROLIFERATION IN RESPONSE TO POTENTIAL MITOGENS <i>IN VITRO</i>	80
	Introduction	80
	Results	
	Developing a method for evaluating human β cell proliferation <i>in vitro</i>	
	Automated image analysis accurately measures human β cell proliferation	84
	Human β cells in purified islet preparations are functional and demonstrate proliferative potential	84
	Evaluation of potential adult human β cell mitogens	85
	Discussion	88
VI.	SIGNIFICANCE AND FUTURE DIRECTIONS	90
REF	FERENCES	96

## **LIST OF TABLES**

		Page
1.	Mouse models	18
2.	PCR primers and conditions for genotyping	21
3.	Antibodies for flow cytometry and sorting	25
4.	Primary antibodies for immunohistochemistry and immunocytochemistry	28
5.	Secondary antibodies for immunohistochemistry and immunocytochemistry	28
6.	Preparation of compounds tested on human islet cells	31
7.	Breeding scheme for mice with inducible endothelial cell-specific knockout of VEGFR2	68
8.	Function and reported effects of compounds tested on human islet cells	86

## **LIST OF FIGURES**

		Page
1.	Anatomy of the pancreas	1
2.	Islet morphology and composition varies between mice and humans	2
3.	Glucose-stimulated insulin secretion in β cells.	2
4.	Mouse and human β cell proliferation throughout life	4
5.	Proposed sources for replacing pancreatic β cells in patients with diabetes	5
6.	Activation of the PI3K/Akt and ERK/MAPK pathways by β cell mitogens	7
7.	Pancreatic islets are highly vascularized.	10
8.	Vascular niche of the pancreatic β cell	10
9.	Peripheral and internal extracellular matrix in the pancreatic islet	11
10.	Composition of the islet extracellular matrix differs between mice and humans	12
11.	Integrin and cadherin signaling in pancreatic β cells	13
12.	VEGF-A expression and endothelial cell proliferation in βVEGF-A mice after induction and withdrawal of the VEGF-A stimulus	34
13.	Increasing $\beta$ cell VEGF-A production increases intra-islet endothelial cells but leads to $\beta$ cell loss followed by $\beta$ cell regeneration after withdrawal of the VEGF-A stimulus	35
14.	Maintenance of α cells in βVEGF-A mice after induction and withdrawal of the VEGF-A stimulus	36
15.	Characterization of glucose homeostasis, body weight, pancreatic hormone content, and $\beta$ cell mass in $\beta$ VEGF-A mice after induction and withdrawal of the VEGF-A stimulus	36
16.	Transient expansion of intra-islet endothelial cells leads to increased $\beta$ cell apoptosis	37
17.	Prolonged VEGF-A induction exacerbates the phenotype of βVEGF-A mice	38
18.	Dox has no effect on monotransgenic controls	39
19.	Removal of the VEGF-A stimulus results in a transient burst in β cell proliferation	41
20.	Expression of Pdx1, MafA, and Bmi-1 in βVEGF-A pancreases following induction and withdrawal of the VEGF-A stimulus	42
21.	New $\beta$ cells in the $\beta$ VEGF-A model arise from replication of pre-existing $\beta$ cells	43
22.	Morphology of βVEGF-A islet grafts	45

23.	$\beta$ cell replication is independent of the pancreatic site and soluble circulating factors and is not limited to murine $\beta$ cells.	46
24.	CD45+ bone marrow-derived cells are recruited to the site of $\beta$ cell injury upon VEGF-A induction and persist in islet remnants during $\beta$ cell regeneration	48
25.	Macrophages are recruited to βVEGF-A islets upon VEGF-A induction	49
26.	Recruited macrophages infiltrate βVEGF-A islets upon VEGF-A induction, while T cells, B cells, and neutrophils are rare in the infiltrating bone marrow-derived cell population	50
27.	Low incidence of CD45+ cells and limited recovery of $\beta$ cells after STZ-mediated $\beta$ cell ablation.	51
28.	Recruited CD45+ and F4/80+ macrophages infiltrate βVEGF-A grafts upon VEGF-A induction.	53
29.	Low incidence of CD45+ and F4/80+ cell infiltration in wild-type islet grafts	54
30.	Recruitment of macrophages into $\beta$ VEGF-A islets upon VEGF-A induction is necessary for the $\beta$ cell proliferative response	55
31.	Gene expression profile of whole βVEGF-A islets and purified islet-derived macrophages and endothelial cells by RNA-sequencing	56
32.	Transcriptome analysis of βVEGF-A islets and purified islet-derived macrophages and endothelial cells	57
33.	New paradigm for the role of macrophage – endothelial cell interactions in β cell regeneration	58
34.	Genetic model of inducible monocyte depletion in βVEGF-A mice	63
35.	Genetic model of monocyte depletion in βVEGF-A mice does not adequately remove islet macrophages or recreate the islet regenerative microenvironment	64
36.	Macrophages are required for $\beta$ cell proliferation in $\beta$ VEGF-A mice	66
38.	EC-SCL-CreER mice have Cre activity in intra-islet endothelial cells	67
37.	Model of inducible endothelial cell-specific knockdown of VEGFR2 in βVEGF-A mice	67
39.	Workflow for sorting and analyzing islet $\beta$ cells, islet-derived endothelial cells, and islet-derived macrophages from $\beta$ VEGF-A mice	70
40.	Transcriptome analysis demonstrates a high degree of separation between sorted islet cell populations	71
41.	Changes in gene expression and biological processes in islet $\beta$ cells from $\beta$ VEGF-A mice during VEGF-A induction and normalization	72
42.	Changes in gene expression and biological processes in islet-derived endothelial cells from BVEGF-A mice during VEGF-A induction and normalization	73

43.	Changes in gene expression and biological processes in islet-derived macrophages from βVEGF-A mice during VEGF-A induction and normalization	74
44.	Gene expression profile of islet β cells by RNA-sequencing	75
45.	Gene expression profile of islet-derived endothelial cells and macrophages by RNA-sequencing	76
46.	Model of interactions between $\beta$ cells, macrophages, endothelial cells, and the extracellular matrix in $\beta$ cell regeneration	77
47.	Workflow for semi-automated evaluation of human β cell proliferation	82
48.	Validation of the Imaris analysis method for quantifying human $\beta$ cell proliferation	83
49.	Adenoviral expression of cyclin D3 and cdk6 induce human β cell proliferation	85
50.	Human β cell proliferation is induced by treatment with some, but not all, compounds tested.	87

#### LIST OF ABBREVIATIONS

Akt Akt-protein kinase B

ANOVA analysis of variance

AUC area under the curve

 $\beta$ -gal  $\beta$ -galactosidase

βVEGF-A RIP-rtTA; TetO-VEGF mouse model of Dox-inducible

 $\beta$  cell-specific overexpression of human VEGF-A<sub>165</sub>

BM bone marrow

BMC bone marrow-derived cell

BMI body mass index

BMT bone marrow transplant

bp base pairs

BrdU bromodeoxyuridine

BSA bovine serum albumin

Cav-1 caveolin-1

CDK cyclin-dependent kinase

Clod clodronate liposomes

Cre Cre recombinase

CreER<sup>™</sup> tamoxifen-dependent Cre recombinase

CSF colony-stimulating factor

CTGF connective tissue growth factor

Dapi 4'6-diamidino-2-phenylindole

DBA dolichos biflorus agglutinin, ductal marker

DDR discoidin domain receptor

DM diabetes mellitus

Dox doxycycline

DT diphtheria toxin

DTR diphtheria toxin receptor

E embryonic day

EC endothelial cell

ECM extracellular matrix

Eph ephrin

ERK extracellular-signal-regulated kinase

ES embryonic stem

FACS fluorescence-activated cell sorting

FBS fetal bovine serum

FGF fibroblast growth factor

fl flox, flanked by loxP sites

FN fibronectin

Gcg glucagon

GFP green fluorescent protein

GIP gastric inhibitory polypeptide

GLP-1 glucagon-like peptide 1

GPCR G protein-coupled receptor

GTT glucose tolerance test

HBSS Hank's balanced salt solution

hC-pep human C-peptide

HGF hepatocyte growth factors

HI human islet

HSA human serum albumin

Iba1 ionized calcium-binding adaptor molecule 1, macrophage marker

IBMX 3-isobutyl-1-methylxanthine

IGF-1 insulin-like growth factor 1

Ins insulin

iPS induced pluripotent stem

LM laminin

Lut Lutheran blood group glycoprotein

M-CSF macrophage colony-stimulating factor

MAPK mitogen-activated protein kinase

MΦ macrophage

N-CAM neural cell adhesion molecule

PCR polymerase chain reaction

PDGF platelet-derived growth factor

PDL poly-D-lysine

Pdx1 pancreatic and duodenal homeobox 1

Pdx1<sup>PB</sup> Pst-Bst fragment of *Pdx1* promoter enhancer

pH2AX gamma-phosphorylated histone H2AX

PI3K phosphoinositide 3-kinase

PRL prolactin

R26R<sup>LacZ</sup> ROSA26 LacZ reporter

RIP rat insulin promoter

RNA-Seq RNA-sequencing

RPKM reads per kilobase per million mapped reads

rpm rotations per minute

STZ streptozotocin

TGF $\beta$  transforming growth factor  $\beta$ 

TL endothelium-binding tomato lectin

Tm tamoxifen

VEGF-A vascular endothelial growth factor A

VEGFR1 vascular endothelial growth factor receptor 1

VEGFR2 vascular endothelial growth factor receptor 2

VN vitronectin

WD withdrawal, from doxycycline

WI whole islet

WT wild-type, C57BL/6

#### **CHAPTER I**

#### **BACKGROUND AND SIGNIFICANCE**

#### The Pancreas

#### Anatomy and physiology

The pancreas is a glandular organ composed of two distinct tissue types that perform different, but equally important functions (Figure 1):

Most of the pancreatic mass (>95%) is composed of exocrine tissue, which secretes digestive enzymes directly into the intestine via a branching ductal system<sup>1</sup>. Secretory acinar cells are organized in clusters at the ends of the ducts and produce enzymes such as proteases, amylases, lipases, and nucleases, most of which are secreted as inactive precursors<sup>2</sup>. Once secreted into the ductal system, these precursor enzymes combine with bicarbonate and mucin produced by ductal cells, and drain into the duodenum where the enzymes are activated<sup>3</sup>.

Conversely, pancreatic endocrine cells secrete hormones directly into the bloodstream. Endocrine tissue is organized into islets of Langerhans—discrete, spherical clusters of 100-1000 cells embedded within the acinar tissue, making up only 1-2% of pancreatic mass<sup>3,4</sup>. Islets contain five types of

hormone-secreting endocrine cells. The insulin-secreting  $\beta$  cell is the most abundant, followed by the glucagon-secreting  $\alpha$  cell, then the somatostatin-secreting  $\delta$  cell. Two rarer cell types produce pancreatic polypeptide (PP cells) and ghrelin ( $\epsilon$  cells).

The organization and relative abundance of the endocrine cell types in islets varies between species. In rodents,  $\beta$  cells are located in the center of the islet surrounded by a mantle of  $\alpha$  and  $\delta$  cells (Figure 2A). Human islets lack this clear core-mantle organization:  $\beta$  cells are found intermingled with  $\alpha$  and  $\delta$  cells in the center of the islet and on the periphery (Figure 2B)<sup>5,6</sup>. Endocrine cell composition is also much more heterogeneous in humans, with  $\beta$  cells ranging anywhere from 28-75% of islet endocrine cells as opposed to 61-81% in mice. Similarly, the abundance of human  $\alpha$  cells (10-65% versus 9-31% in mice) and  $\delta$  cells (1.2-22% versus 1-13% in mice) displays a much wider variability than in mice (Figure 2C-D)<sup>5</sup>.

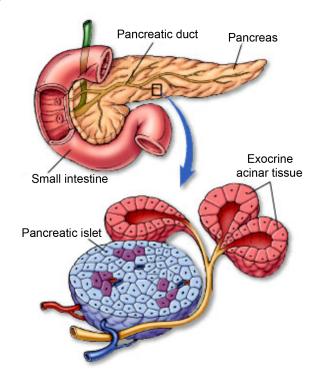


**Figure 1. Anatomy of the pancreas.** The pancreas is a bifunctional organ composed of exocrine tissue that secretes digestive enzymes into the duodenum, and endocrine tissue made up of islets of Langerhans that are dispersed throughout the pancreas and secrete hormones directly into the bloodstream. Image adapted from Saladin, 2001<sup>21</sup>.

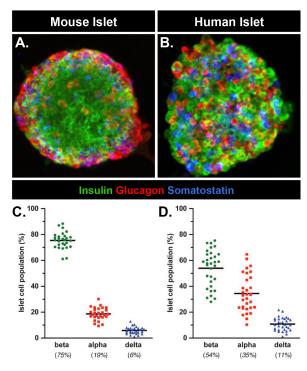


Figure 2. Islet morphology and composition varies between mice and humans. (A) Mouse and (B) human islets labeled for insulin (green), glucagon (red), and somatostatin (blue). Endocrine cell composition of (C) mouse islets, n=28, and (D) human islets, n=32, determined by analysis of optical sections taken throughout the entire islets. Human islet composition differed significantly (p<0.0001) across all endocrine cell populations examined. Horizontal bar represents the mean of each cell population. Image adapted from Brissova et al., 2005<sup>5</sup>.

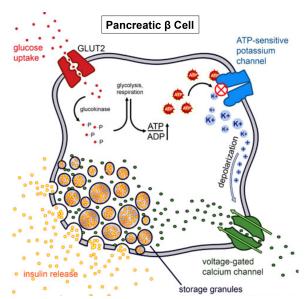


Figure 3. Glucose-stimulated insulin secretion in  $\beta$  cells. As blood glucose levels rise, it enters  $\beta$  cells through the GLUT-2 transporter and undergoes glycolysis, causing an increase in the intracellular ATP:ADP ratio. This increased ratio closes ATP-sensitive potassium channels, leading to membrane depolarization, which in turn opens voltage-gated calcium channels. The subsequent influx of calcium causes insulin granules to undergo exocytosis, releasing insulin into the bloodstream. Image adapted from Cartailler,  $2004^{22}$ .

The hormones released by the endocrine pancreas regulate nutrient metabolism, specifically glucose homeostasis. Before secreting hormones into the

bloodstream, islet endocrine cells sense and integrate a variety of signals including glucose, hormones, neurotransmitters, and other nutrients  $^{7-10}$ . Insulin, secreted by  $\beta$  cells, lowers blood glucose by increasing glucose uptake in liver, muscle, and adipose tissue and promoting glycolysis and glycogen storage. Conversely, glucagon is released from  $\alpha$  cells when glucose levels are low and causes the liver to break down glycogen, releasing glucose into the bloodstream  $^{7,11}$ . Tightly regulated insulin release by  $\beta$  cells is particularly important for maintaining normal blood glucose levels.

 $\beta$  cells synthesize and store insulin in preformed secretory granules, which allows them to rapidly respond to increases in blood glucose (Figure 3). Glucose enters the  $\beta$  cell through the GLUT-2 transporter in rodents, and subsequently undergoes glycolysis, followed by the citric acid cycle and oxidative phosphorylation. This process produces ATP, causing a rise in the intracellular ATP:ADP ratio which closes the ATP-sensitive potassium channel, leading to membrane depolarization. Upon membrane depolarization, voltage-gated calcium channels open, allowing an influx of calcium into the cell. The increased intracellular calcium concentration triggers the fusion of secretory granules with the cell membrane and granule exocytosis, releasing the preformed insulin. Intracellular calcium concentration in  $\beta$  cells is oscillatory, causing pulsatile insulin release, which is believed to be important in maintaining insulin sensitivity<sup>12-14</sup>.

These general principles and mechanisms of glucose homeostasis remain consistent between rodents and humans, despite the fact that humans have different nutritional and metabolic needs. Because of differences in islet composition and morphology between species discussed above (Figure 2),  $\beta$  cells are more likely to be in contact with  $\alpha$  cells in human versus mouse islets<sup>15</sup>. Although it is not entirely clear what effect these differences may have on nutrient sensing and hormone secretion, insulin secretion is increased when individual human  $\beta$  cells are in contact with  $\alpha$  cells, suggesting that islet morphology may influence endocrine cell function<sup>16</sup>. Humans also have only one insulin gene (*INS*) as opposed to two in rodents (*Ins1*, *Ins2*), and GLUT-1 is the major glucose transporter in human  $\beta$  cells rather than GLUT-2<sup>17-19</sup>. In the various forms of diabetes, loss of glucose homeostasis occurs through a combination of absolute or relative insulin deficiency and an excess of glucagon<sup>20</sup>.

## Pancreatic development and establishing $\beta$ cell mass

Both endocrine and exocrine cells are derived from embryonic foregut endoderm. Most of the mechanisms regulating pancreas development have been discovered through studies in mice, and are briefly summarized below:

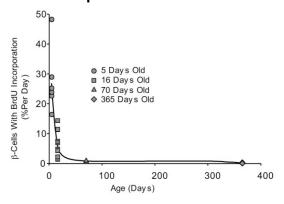
Development begins as the early monolayer epithelial cells actively proliferate, forming dorsal and ventral multilayered stratified epithelial buds that first become apparent around embryonic day 9.5 (E9.5). Throughout development these buds undergo dramatic morphogenic changes as the epithelium remodels into a branched, tubular tree starting around E12.5 when the two buds merge after rotation of the gut tube brings them together<sup>2</sup>. During this remodeling, the epithelium segregates into distinct tip and trunk domains<sup>2,23,24</sup>. The trunk domain harbors endocrine cell progenitors, while epithelial tips contain multipotent progenitor cells. Differentiation of endocrine cells occurs in two stages, or transitions. The primary transition (E9.5-12.5) begins after the formation of the initial dorsal and ventral pancreatic buds. These early endocrine cells are α cells that often co-express multiple hormones, and are thought to be eliminated without significantly contributing to mature islets<sup>25,26</sup>. At the onset of the secondary transition (E13.5), tip cells actively proliferate, become more pro-acinar, and start expressing digestive enzymes. At the same time, progenitor cells residing in the trunk domain of the pancreatic epithelium begin taking on an endocrine fate, and delaminate to form small islet-like cell clusters<sup>23</sup>. This secondary transition (E13.5-16.5) is characterized by a major endocrine cell expansion. During late embryogenesis (E16.5-18.5), the epithelium expands even further as endocrine cell clusters continue delaminating, remaining close to the pancreatic epithelium<sup>2,24</sup>. Delaminated endocrine cell clusters become progressively larger and form more structured islets during late gestation and early postnatal life<sup>2,27</sup>. Functional maturation of islets takes place after birth<sup>28</sup>.

The process of  $\beta$  cell differentiation described above is a complex series of cell specification events regulated by dynamically changing and successive expression of transcription factors as reviewed in Pan and Wright, 2011². Although not much is known about the morphological and regulatory differences in pancreatic development between mice and humans, studies conducted on human fetal tissue have demonstrated that (1) overall, human pancreas formation parallels that in the mouse, (2) transcriptional factors regulating mouse and human pancreas development are similar, (3) humans may only have a single transition, rather than two distinct transitions as observed in mice, and (4) differences in the

aggregation of islet cell clusters leads to the distinct morphology seen in human islets (Figure 2)<sup>2,29-33</sup>.

In addition to β cell differentiation from pancreatic progenitor cells, which continues through early postnatal life, β cell mass is established through a burst in proliferation of these mature β cells. This proliferation peaks neonatally, at about 10-20% in mice (Figure 4A), while human β cell proliferation only reaches 1-3% (Figure 4B)<sup>32,34-38</sup>. Shortly after birth, β cell proliferation declines to near negligible levels and the established β cells typically remain quiescent throughout adulthood in both mice and humans with very little turnover (Figure 4)<sup>34,39,40</sup>. However, in conditions of increased metabolic demand, such as pregnancy or obesity, new β cells are formed by duplication of pre-existing mature  $\beta$  cells<sup>40-44</sup>, and several studies have identified factors (e.g., growth factors, hormones, mitogenic agents) capable of driving adult  $\beta$  cell proliferation<sup>45-51</sup>. This adaptive expansion of adult β cells to increased metabolic load and response to mitogenic factors is much more extensive in mouse models than in humans, with most compounds that cause robust β cell proliferation in mice having limited to no effect on human β cells<sup>40,44-49,51</sup>. Once established through differentiation and proliferation, maintaining β cell mass throughout life is necessary to ensure continuing glucose regulation.

## A. Mouse β Cell Proliferation



## B. Human β Cell Proliferation

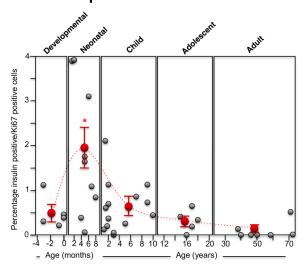


Figure 4. Mouse and human  $\beta$  cell proliferation throughout life. (A) Mouse  $\beta$  cell replication rate reported as % BrdU-positive  $\beta$  cells per day by age in normal mice; from Teta et al., 2005<sup>34</sup>. (B) Human  $\beta$  cell proliferation incidence reported as % Ki67-positive  $\beta$  cells by age in human autopsy samples; from Gregg et al., 2012<sup>32</sup>.

#### **Diabetes Mellitus**

## Epidemiology and pathophysiology

Diabetes mellitus (DM) refers to a group of metabolic disorders in which patients have abnormally high blood glucose levels, or hyperglycemia, due to the inability of  $\beta$  cells to produce enough insulin to meet the body's metabolic demand<sup>52</sup>. Diabetes affects an estimated 29.1 million people in the United States, which represents a staggering 9.3% of the population<sup>53</sup>. Global estimates are similar, with worldwide prevalence estimated to be 9%<sup>54</sup>. Approximately 5% of patients with diabetes have inadequate insulin production due to the autoimmune destruction of pancreatic  $\beta$  cells, and are diagnosed as having type 1 DM<sup>53,55</sup>. These patients are unable to lower their blood glucose levels without delivery of exogenous insulin by injection or a pump. Type 2 DM is the most common form, accounting for 90-95% of diagnosed patients. In these patients, insulin resistance in peripheral tissues (muscle, liver, fat) causes a need for increasing amounts of insulin production. When  $\beta$  cells are unable to meet this increased

demand due to deficiency and/or dysfunction, patients develop hyperglycemia<sup>56,57</sup>. Depending on the contribution of insulin resistance versus β cell dysfunction, these patients may be able to control their blood glucose levels with a combination of lifestyle changes, medications designed to enhance insulin secretion, and/or treatment with exogenous insulin. Pregnant women who develop gestational DM typically have increased blood glucose levels during their second or third trimester, which resolves in 90-95% of cases after pregnancy. These patients do have an increased risk of gestational DM recurring in future pregnancies and of developing type 2 DM<sup>53,58</sup>. Less common forms of diabetes (1-5% of patients) include those caused by rare genetic mutations that reduce insulin production (e.g., maturity-onset diabetes of the young, neonatal DM) or those secondary to or caused by other medical conditions (e.g., surgery, medication, infection, pancreatic disease)<sup>53,59,60</sup>.

In addition to the acute dangers of hyperglycemia (e.g., diabetic ketoacidosis), patients with DM face an increased risk of long-term complications including heart disease, stroke, blindness, kidney disease, and neuropathy, which present a major healthcare challenge<sup>53,61</sup>. The estimated direct medical cost of DM was \$176 billion in 2012, with an additional \$69 billion in indirect costs from lost productivity, disability, and premature death<sup>53</sup>. Advances in glucose monitoring, insulin delivery, and medications have allowed diabetic patients to more carefully regulate their glucose levels. However, concern about dangerous hypoglycemic episodes often prevents the tight glucose regulation required to avoid these long-term complications<sup>55,62-64</sup>. With the incidence of both type 1 and type 2 DM rising, and the age of newly diagnosed patients decreasing, the need for new strategies to prevent and treat DM is paramount<sup>53</sup>.

### Pancreatic β cell replacement as a therapeutic goal

Because loss and/or dysfunction of pancreatic  $\beta$  cells occurs in both type 1 and type 2 DM, major efforts are being made to develop effective approaches to restore  $\beta$  cell mass in these patients in

hopes of re-establishing homeostatic glucose regulation and preventing the short- and long-term consequences of hyperglycemia.

These efforts are focused primarily on (1) introducing new  $\beta$  cells from exogenous sources, such as cadaveric islets or pluripotent stem cells; or (2) generating  $\beta$  cells from endogenous sources, such as multipotent precursor cells, pre-existing  $\beta$  cells, or transdifferentiation of other adult endocrine or non-endocrine cells (Figure 5).

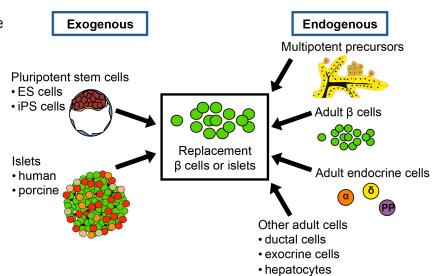


Figure 5. Proposed sources for replacing pancreatic  $\beta$  cells in patients with diabetes. Because  $\beta$  cells are lost in both type 1 and type 2 DM, strategies to replace these lost cells from exogenous sources (e.g., cadaveric islet transplants, differentiation of pluripotent stem cells) or endogenous sources (e.g., pancreatic stem cells, adult  $\beta$  cells, non- $\beta$  endocrine cells, adult cells from other lineages) are being developed.

#### Pancreatic islet transplantation

Replacing β cells by transplanting human islets isolated from donor organs can successfully reverse type 1 DM<sup>65,66</sup>. However, even with improvements in islet quality and immunosuppressive therapy introduced with the Edmonton protocol, which injects islets into the portal vein for engraftment into the liver, most of these patients do not remain insulin independent after five years; although many do remain free from dangerous hypoglycemic episodes<sup>65,66</sup>. Several challenges remain before islet transplantation can be more widely implemented to treat diabetes<sup>66-69</sup>. First, the extremely low survival rate of transplanted islets requires multiple donor organs to achieve a sufficient number of islets to restore glucose homeostasis in a single recipient<sup>65,70-72</sup>. A shortage of donor organs even further limits the number of patients who can benefit from this treatment. Efforts to improve the survival of transplanted islets have focused on enhancing revascularization and reinnervation of the islet grafts, and exploring less damaging sites for islet engraftment<sup>73-77</sup>. Some have proposed circumventing the supply shortage by using islets from pigs for xenotransplantation into human recipients, although enormous barriers to avoid immune rejection would need to be overcome before this approach could be seriously considered as a therapeutic option<sup>78,79</sup>. Major immunological challenges also need to be addressed to advance human islet transplantation including identifying strategies to dampen the autoimmune response responsible for β cell loss in type 1 DM, and improving immunosuppressive agents to both decrease graft rejection and minimize  $\beta$  cell damage from the agents themselves<sup>66-68,80-82</sup>.

#### Differentiation of pluripotent stem cells

While shortage of donor tissue will always be a limitation of cadaveric islet transplantation, generating β cells de novo from human embryonic stem (ES) cells or induced pluripotent stem (iPS) cells, could potentially provide an unlimited supply of cells available for transplantation. Efforts to generate functional  $\beta$  cells from ES cells have focused primarily on recreating the steps of  $\beta$  cell differentiation during pancreatic development in vitro. These efforts have been successful in differentiating ES cells into definitive endoderm and pancreatic progenitors, and when engrafted into mice, these human ES-derived pancreatic progenitors mature into β-like cells<sup>83-87</sup>. More recent attempts to reconstruct the final steps necessary to produce glucose-responsive, insulin-secreting cells have suggested that it may be possible to generate functional β cells in vitro<sup>88,89</sup>. However, challenges still remain with identifying effective immunosuppressive therapies, developing an immunoisolation device for ES cell-derived β cell transplantation, determining an ideal transplantation site, and ensuring transplants do not become tumorigenic86,87,90,91. Reprogramming somatic cells from individual patients to make iPS cells for the purpose of differentiating them into  $\beta$  cells is a promising alternative to human ES cells as a source for β cell replacement<sup>92</sup>. Recent studies have demonstrated the feasibility of making iPS cells from patients with diabetes, and differentiating insulin-producing cells from iPS cells<sup>85,93,94</sup>. While technical and safety issues still need to be addressed, this approach would remove ethical concerns of working with human ES cells and reduce immunological challenges associated with allotransplantation.

#### Transdifferentiation from mature endocrine cells and other lineages

Other strategies have focused on endogenous sources for  $\beta$  cell replacement. After  $\beta$  cell mass is established as described previously,  $\beta$  cell turnover is extremely limited in both mice and humans<sup>34,39,40</sup>. However, when new  $\beta$  cells are formed they are produced through replication of mature  $\beta$  cells rather than differentiation from stem cells<sup>42</sup>. In fact, evidence that multipotent pancreatic progenitor cells exist

in adult islets is scarce, though some are pursuing the possibility in hopes of harnessing this population to differentiate new  $\beta$  cells<sup>95,96</sup>. During development, all endocrine cells have a common progenitor, and studies in mice have found that in circumstances of extreme  $\beta$  cell loss, non- $\beta$  endocrine cells can reprogram to insulin-producing cells<sup>97,98</sup>. Before puberty, this process occurs through extensive dedifferentiation of  $\delta$  cells, which then proliferate and differentiate into  $\beta$  cells<sup>98</sup>. During puberty and throughout adulthood, if extensive  $\beta$  cell loss occurs,  $\alpha$  cells have the ability to transdifferentiate into  $\beta$  cells<sup>97,98</sup>. Reprogramming  $\alpha$  cells can also be achieved by forced expression of Pax4, a transcription factor that promotes  $\beta$  and  $\delta$  cell fates, or by inactivating Arx, a transcription factor that drives the  $\alpha$  cell fate<sup>99,100</sup>. Additional studies using genetic reprogramming have demonstrated the ability to transdifferentiate mature acinar cells, pancreatic duct cells, and hepatocytes into insulin-producing cells<sup>101-103</sup>. While these findings are promising, more work is needed to determine the feasibility and efficacy of reprogramming human endocrine cells or non-endocrine cells to replace  $\beta$  cells in patients with diabetes.

#### Expansion of adult β cells

Small numbers of functional  $\beta$  cells persist in pancreases of patients, even with longstanding diabetes 104-106. Identifying endogenous factors (e.g., growth factors, hormones, mitogenic agents) and/or exogenous compounds (e.g., small molecules) capable of inducing  $\beta$  cell proliferation in hopes of developing treatments that promote regeneration of lost  $\beta$  cells in diabetes has been the focus of numerous studies. Some of these are highlighted below:

Growth factors play important roles in pancreatic development and maintaining normal islet function, and loss of these protective factors can lead to decreased  $\beta$  cell survival and diabetes.

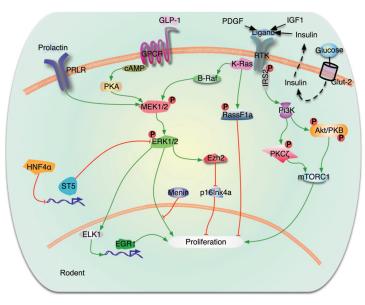


Figure 6. Activation of the PI3K/Akt and ERK/MAPK pathways by  $\beta$  cell mitogens. Growth factors (e.g., PDGF, IGF-1) bind tyrosine kinase receptors (RTK), activating the PI3K/Akt and ERK1/2 (also called MAPK) signaling pathways, which drive  $\beta$  cell proliferation. Activation of GPCRs by incretin hormones (e.g., GLP-1) and other receptors (e.g., PRL receptor) can also cause activation of these pathways. Image from Stewart et al.,  $2015^{47}$ .

Insulin-like growth factor (IGF-1) is a ubiquitous hormone that stimulates growth of most tissue types in conjunction with insulin and is critical for maintaining normal glucose homeostasis<sup>48,107</sup>. In β cells, IGF-1 works primarily through the IGF-1 receptor, although it is also able to bind and activate the insulin receptor. Downstream signaling through the PI3K/Akt and ERK/MAPK pathways promote cell survival and proliferation (Figure 6)47,48,107,108. Although IGF-1 is not required during early β cell development, increasing levels of IGF-1 in β cells leads to decreased β cell apoptosis and increased β cell proliferation following streptozotocin (STZ)-induced β cell damage<sup>107,109</sup>. While IGF-1 may play a role in regenerating β cell mass following injury, deletion of the IGF-1 receptor in  $\beta$  cells does not alter  $\beta$  cell mass,

suggesting that IGF-1 receptor signaling is not required to maintain  $\beta$  cell mass<sup>110</sup>. Human  $\beta$  cells express the IGF-1R and downstream signals, but it is unclear what role IGF-1 plays in human  $\beta$  cell function, mass regulation, and response to injury<sup>48,107</sup>.

Platelet-derived growth factor (PDGF) plays a role in development, cell proliferation and migration, angiogensis, fibrosis, and other disease processes. Although it is stored and released by platelets, PDGF is also made by a number of other cell types. Recently it was found that PDGF also regulates the age-dependent reduction in  $\beta$  cell proliferation that occurs in all islets<sup>51</sup>. PDGF signaling promotes  $\beta$  cell proliferation through ERK activation (Figure 6)<sup>47,51</sup>. Over time,  $\beta$  cells lose expression of PDGF receptors and this reduction in PDGF-mediated signaling results in decreased ERK activation, which in turn decreases  $\beta$  cell replication. Conversely, stimulation of PDGF signaling in quiescent mouse  $\beta$  cells triggers proliferation<sup>51</sup>. In humans, stimulation of juvenile  $\beta$  cells with PDGF causes increased  $\beta$  cell proliferation, but adult human  $\beta$  cells do not express the PDGF receptor, making them unresponsive<sup>51</sup>.

Connective tissue growth factor (CTGF) is highly expressed in islet vasculature and interacts with several signaling pathways including transforming growth factor  $\beta$  (TGF $\beta$ ) and Wnt<sup>111,112</sup>. CTGF is required for allocating endocrine progenitor cells into different lineages and promoting proliferation of developing  $\beta$  cells<sup>111,113</sup>. In adult  $\beta$  cells, increasing CTGF has no effect on  $\beta$  cell proliferation under normal conditions; however, CTGF does promote increased  $\beta$  cell proliferation following diphtheria toxin (DT)-mediated ablation of  $\beta$  cells expressing diphtheria toxin receptor (DTR)<sup>112</sup>. Enhanced  $\beta$  cell proliferation in this model occurs through CTGF upregulation of ERK/MAPK-dependent TGF $\beta$  signaling and other growth factors<sup>112</sup>. The role of CTGF in human  $\beta$  cell function and  $\beta$  cell mass regulation is unknown.

Fibroblast growth factors (FGFs) play important roles in wound healing, development, and disease. During pancreatic development, FGF-7 is required for trunk cell proliferation and  $\beta$  cell differentiation, and disrupting FGF signaling in  $\beta$  cells leads to decreased  $\beta$  cell number and diabetes 114,115. Although overexpressing FGF-7 in acinar tissue leads to islet hyperplasia and increased  $\beta$  cell mass, when overexpressed in  $\beta$  cells under the insulin promoter, islets become fibrotic, suggesting that tight control of islet FGF-7 levels is important for regulating  $\beta$  cell mass 116,117. While FGF receptors are known to work through PI3K/Akt and ERK/MAPK pathways, downstream signaling of FGF receptors in  $\beta$  cells has not been investigated. The feasibility of using FGFs to promote human adult  $\beta$  cell proliferation is unknown, but a study of engrafted human fetal tissue in rats demonstrated increased  $\beta$  cell number in response to elevated FGF-7118.

Several other growth factors and hormones are also known to play important roles in  $\beta$  cell development and proliferation. Hepatocyte growth factor (HGF) has been shown to promote fetal  $\beta$  cell proliferation and proliferation of mature  $\beta$  cells in pregnancy<sup>119</sup>. Prolactin (PRL) has been implicated in regulating  $\beta$  cell function and proliferation during pregnancy, when levels of circulating PRL and  $\beta$  cell PRL receptor expression are increased<sup>120-123</sup>. PRL receptor signaling activates the JAK/STAT pathway, which then activates other signaling cascades such as PI3K/Akt and ERK/MAPK (Figure 6)<sup>121</sup>. Interestingly, PRL can also work synergistically with other growth factors to activate ERK/MAPK<sup>124,125</sup>. The effect of PRL on human  $\beta$  cells during pregnancy is not fully understood. Incretin hormones

glucagon-like peptide 1 (GLP-1) and gastric inhibitory polypeptide (GIP) signal through G protein-coupled receptors (GPCRs), activating PI3K/Akt and ERK/MAPK signaling, and promoting survival and proliferation of  $\beta$  cells in rodents (Figure 6); however, their role in human  $\beta$  cell proliferation is not known<sup>126,127</sup>.

Mitogenic compounds and small molecules that induce  $\beta$  cell proliferation have also been discovered. Regulation of glucose metabolism by glucokinase has been shown to promote  $\beta$  cell replication in response to increased metabolic demand in mice, and enhancing glucokinase activity with pharmacologic activators also stimulates  $\beta$  cell proliferation<sup>50</sup>. Increasingly, high throughput screening mechanisms are being used to identify small molecules capable of activating  $\beta$  cell replication. A screen in zebrafish embryos identified small molecules that enhance adenosine signaling (e.g., NECA, A-134974) and are capable of inducing  $\beta$  cell proliferation in zebrafish and rodent  $\beta$  cells<sup>128</sup>. Adenosine kinase inhibitors 5-iodotubercidin and ABT-702, capable of promoting proliferation of rodent and pig  $\beta$  cells, were identified in a screen using dispersed rat islet cells<sup>129</sup>. DYRK inhibitor, harmine, was identified using a two-part screening system that first identified hits using a human hepatocyte cell line expressing a luciferase reporter driven by the human MYC promoter, and then screening those hits on dispersed rat islet cells to determine which molecules promoted rat  $\beta$  cell proliferation<sup>45</sup>. Once harmine was identified, further testing demonstrated that it is capable of promoting mouse  $\beta$  cell proliferation *in vivo*, and human  $\beta$  cell proliferation both *in vitro* and *in vivo* using a transplant model in immunodeficient mice<sup>45</sup>.

Although most endogenous  $\beta$  cell mitogens activate the ERK/MAPK pathway (Figure 6), this activation does not always lead to an increase in  $\beta$  cell replication<sup>47-49,130</sup>. Therefore, it has been proposed that  $\beta$  cell replication is the result of both sustained ERK/MAPK activation and cross talk with other signaling pathways, suggesting that coordinated signals from multiple sources may be required to activate cell cycle machinery in  $\beta$  cells<sup>47</sup>. Intersections between the ERK/MAPK pathway and both adenosine signaling and DYRK have been identified, suggesting that promoting  $\beta$  cell proliferation through these mechanisms may also be dependent on ERK/MAPK activation<sup>131-134</sup>.

Though several of these endogenous factors and exogenous compounds show promise in their potential to influence  $\beta$  cell regeneration, efforts to translate findings from rodent  $\beta$  cells into humans have been largely disappointing, with most compounds that cause robust  $\beta$  cell proliferation in rodents having minimal to no effect on human  $\beta$  cells<sup>40,44-49,51</sup>. Because proliferation in adult human  $\beta$  cells is so limited, an effort needs to be made to test all  $\beta$  cell mitogens identified in animal models in human  $\beta$  cells to determine their therapeutic potential. With an increasing number of these compounds being identified, new strategies need to be developed to enable effective and accurate screening in human  $\beta$  cells<sup>135</sup>. Moving forward, we need a greater understanding of (1) how growth factors, hormones, and mitogenic compounds regulate  $\beta$  cell proliferation, and (2) whether a single factor is sufficient to activate  $\beta$  cell proliferation or if combinations of coordinated signals are needed. In addition to endocrine cells, the islet contains a rich vascular network and extracellular matrix (ECM), which provide signals that can coordinate and support cellular differentiation, survival, and proliferation, and may contribute to and help regulate the pathways and signals involved in  $\beta$  cell regeneration<sup>4,136-139</sup>. Defining

these microenvironmental factors and the intrinsic and extrinsic signals that influence mature  $\beta$  cell replication will hopefully allow us to identify compounds or combinations of compounds that can be developed to successfully regenerate  $\beta$  cells in patients with diabetes.

#### **Pancreatic Islet Vascularization**

A characteristic feature of islets is their extensive vascularization (Figure 7). Although islets only represent 1-2% of pancreatic mass, they receive 6-20% of the direct arterial blood flow to the pancreas<sup>4</sup>. Intra-islet capillaries are fenestrated and are thicker, denser, and more tortuous than capillaries in exocrine tissue<sup>140,141</sup>.  $\beta$  cells directly communicate with these capillaries, suggesting that increased vascularization is important for  $\beta$  cells to rapidly respond to increases in blood glucose levels by secreting insulin into the bloodstream<sup>142</sup>. Intra-islet capillaries connect endocrine cells to the blood supply to ensure proper gas exchange, nutrition, and waste removal. However, blood vessels also play an important role in providing non-nutritional signals to islets, creating a vascular niche in which cross-talk between  $\beta$  cells and endothelial cells is necessary to ensure proper  $\beta$  cell development

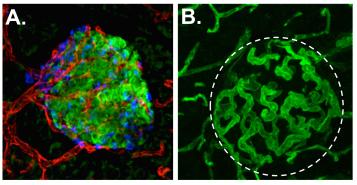


Figure 7. Pancreatic islets are highly vascularized. (A) Representative pancreatic islet from mouse immunolabeled for insulin (insulin), glucagon (blue), and endothelial cell marker, CD31 (red). (B) Mouse islet from an animal infused with FITC-conjugated tomato lectin (green) to label the functional vasculature. Islet capillaries (within dashed line) are thicker, denser, and more tortuous than vessels in the surrounding exocrine tissue. Images courtesy of Marcela Brissova.

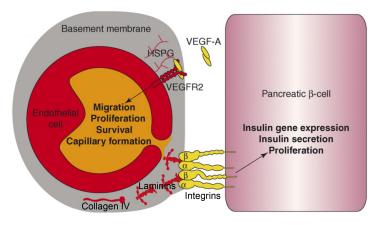


Figure 8. Vascular niche of the pancreatic  $\beta$  cell. VEGF-A produced by  $\beta$  cells signals endothelial cells by binding to VEGF-A receptors, and extracellular matrix components signal  $\beta$  cells by binding integrin and non-integrin receptors. Image adapted from Nikolova et al., 2007<sup>143</sup>.

Signaling between endothelial cells and the developing pancreatic epithelium throughout pancreatic development is critical to establish islet vasculature and β cell mass. During the specification of the pancreatic epithelium from the foregut, embryonic aortic endothelial cells are in direct contact with the dorsal pancreatic bud, and provide signals necessary for β cell differentiation; interrupting these signals prevents pancreatic differentiation<sup>138</sup>. These endothelial cell signals regulate expression of transcription factors in the developing pancreas that are required to maintain the multipotent progenitor population and induce lineage differentiation<sup>144</sup>. After the early pancreatic epithelium remodels, it produces vascular endothelial growth factor A (VEGF-A), which binds VEGF receptors on endothelial cells, promoting endothelial migration and proliferation<sup>145</sup>. Signals from these recruited blood vessels regulate acinar cell differentiation and pancreas branching, and the density and location of endothelial cells at the trunks and tips is critical to ensure proper exocrine differentiation<sup>146</sup>. Signals from these recruited blood vessels regulate pancreas

and function (Figure 8)143.

branching and differentiation of exocrine and endocrine cells, and disrupting VEGF-A signaling either in the early pancreas or newly formed  $\beta$  cells leads to excessive exocrine differentiation and failure of the intra-islet plexus to form, causing significant defects in  $\beta$  cell proliferation, insulin secretion and glucose homeostasis <sup>146-148</sup>. Conversely, overexpressing VEGF-A in developing  $\beta$  cells induces endothelial cell expansion and hypervascularization which disrupts islet formation and results in  $\beta$  cell loss <sup>149-151</sup>. Therefore, precise control of VEGF-A is required for normal development of both the exocrine and endocrine pancreas.

In addition to regulating development of the pancreatic epithelium, VEGF-A is also required to establish and maintain normal islet vascularization, innervation, and function  $^{137,138,144,150-155}$  After development, the endocrine pancreas continues expressing VEGF-A at much higher levels than the exocrine pancreas  $^{156}$ . This continued VEGF-A expression is important in maintaining the distinctive microvasculature of the islet  $^{4,137,140,141}$ . A decrease in  $\beta$  cell-specific VEGF-A expression not only reduces islet vascularity 10-fold, but also leads to decreased innervation, impaired insulin secretion and reduced glucose tolerance, which indicates an important role for VEGF-A in normal  $\beta$  cell function  $^{137,147,154}$ . The vasculature also contributes key components to the islet extracellular matrix (ECM), and these endothelial-derived matrix components are critical in  $\beta$  cell differentiation, function, and proliferation  $^{157}$ .

#### Pancreatic Islet Extracellular Matrix

Pancreatic islets are separated from exocrine tissue by an incomplete peripheral capsule. This capsule is made up of a single layer of fibroblasts and collagen fibers sandwiched between two basement membranes (Figure 9A)<sup>139</sup>. The first basement membrane is located beneath the exocrine epithelium, and the other beneath the endocrine epithelium (peri-islet). Occasional breaks in the capsule allow direct exocrine-endocrine cell contact, and extensive membrane interdigitation occurs between the cell types in these areas<sup>158</sup>.

Studies in mice have demonstrated that unlike on the periphery, within the islet interior pancreatic endocrine cells lack a basement membrane, and directly interact with the vascular basement membrane surrounding islet capillaries (Figure 9B)<sup>158-161</sup>. In addition to maintaining islet vasculature, this vascular basement membrane acts as a reservoir for the growth factors needed to maintain islet-specific phenotypes and promote

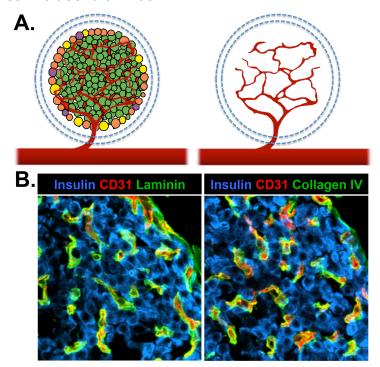


Figure 9. Peripheral and internal extracellular matrix in the pancreatic islet. (A) The peripherial extracellular matrix (ECM) is a discontinuous capsule composed of a layer of fibroblasts sandwiched between an exocrine cell-derived basement membrane and an endocrine cell-derived basement membrane (broken blue lines). (B) The internal ECM is made up of a perivascular basement membrane. Outline of the basement membrane components of the islet ECM include laminin (left; green) and collagen IV (right; green), which co-localize with endothelial cell marker CD31 (red). Adapted from Reinert et al., 2014<sup>154</sup>.

β cell proliferation<sup>115,137,162,163</sup>. Human islets were originally thought to have the same internal matrix architecture, but a recent study demonstrated that unlike mice, humans have two distinct layers of basement membrane surrounding islet capillaries (Figure 10)<sup>164</sup>. The vascular basement membrane is still present, but there is also a distinctive peri-islet basement membrane which invaginates into islets along vascular channels and expresses different laminin isoforms than the vascular basement membrane<sup>165</sup>.

#### Endocrine cell-cell interactions

Because of the paucity of extracellular matrix (ECM) within the islet, connections between endocrine cells have been characterized much more extensively than cell-matrix interactions. These interendocrine cell interactions rely on cell adhesion molecules (e.g., N-CAM, cadherins), gap junctions, and ephrin (Eph) receptors and ligands. Cell adhesion molecules are important in the development of islet architecture, contributing to the characteristic distribution of endocrine cells within islets and normal islet function. Blocking neural cell adhesion molecule (N-CAM) prevents endocrine cell types from segregating properly and leads to abnormalities in both insulin and glucagon secretion<sup>166-168</sup>. During development, E-cadherin is required for β cell aggregation and islet formation, and is important

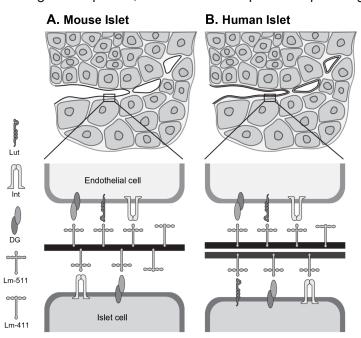


Figure 10. Composition of the islet extracellular matrix differs between mice and humans. Differences in the internal islet extracellular matrix in mouse (A) and human (B) islets. In humans the perivascular area contains two basement membranes, versus one in mice. Image from Otonkoski et al., 2008<sup>165</sup>.

for glucose sensing and insulin secretion in mature islets<sup>169-171</sup>. E-cadherin also mediates β cell survival and proliferation in mice by activating  $\alpha$ - and  $\beta$ -catenins (Figure 11)<sup>172</sup>. Gap junctions connect the cytoplasm of cells together, and in β cells they allow exchange of ions and metabolites, including cytoplasmic calcium. This exchange of calcium is necessary to synchronize calcium oscillations across β cells and to maintain normal biosynthesis, storage, and insulin release; loss of gap junction proteins disrupts pulsatile glucose-stimulated insulin release<sup>173-177</sup>. Ephs are receptor tyrosine kinases which initiate signaling upon binding their Eph ligands<sup>178</sup>. Pancreatic β cells express both classes of Ephs (A and B), and EphA signaling plays an important role in regulating insulin secretion at both high and low glucose<sup>137,179</sup>.

#### Endocrine cell-matrix interactions

#### Integrin and non-integrin receptors

Integrins are heterodimeric cell surface receptors made up of both  $\alpha$  and  $\beta$  subunits that can participate in both cell-cell and cell-matrix attachments. They enable cells to sense and respond to their surroundings using both outside-in and inside-out signaling. Many types of integrins can be formed by combining different  $\alpha$  and  $\beta$  subunits. Depending on their specificity, integrins can bind various ECM ligands such as collagen, laminin, fibronectin, and vitronectin<sup>180</sup>. Several integrin receptors are expressed in islets and have been found to influence islet development,  $\beta$  cell survival and function, and islet vascular remodeling<sup>181-183</sup>. However, the exact composition of these islet integrins remains controversial<sup>184</sup>. This controversy is partially due to the fact that expression of integrin receptors on islet cells is developmentally regulated, with the composition of integrins changing throughout development<sup>185,186</sup>. During the secondary transition,  $\alpha V \beta 3$  and  $\alpha V \beta 5$  integrins are expressed in both the pancreatic ductal epithelium and the clusters of endocrine cells, and help regulate the delamination of these cells from the ducal epithelium<sup>182,186</sup>. Integrins also promote the motility of these delaminated endocrine cells, which is necessary for the development of normal islet architecture and insulin secretion<sup>183</sup>. During development,  $\beta 1$  integrin plays a crucial role in establishing  $\beta$  cell mass by regulating expansion of newly formed  $\beta$  cells,

and mice without \( \beta 1 \) integrin on β cells demonstrate a significant reduction in  $\beta$  cell mass and impaired  $\beta$  cell function<sup>187,188</sup>. Furthermore, blocking β1 integrin signaling in human fetal islet epithelial cell cultures causes decreased differentiation and survival of islet cells<sup>189</sup>. These integrins signal through Akt/β-catenin and ERK/MAPK pathways to promote β cell survival and proliferation (Figure 11)47,189-191. While expression of some of these developmentally important integrins is retained on adult islet cells, others are downregulated. However, treatment with CTGF following DT-mediated ablation of β cells caused an increase in β1 integrin corresponding with improved β cell regeneration, suggesting that changes in β cell integrin expression may contribute to β cell regeneration in adult islets<sup>112</sup>.

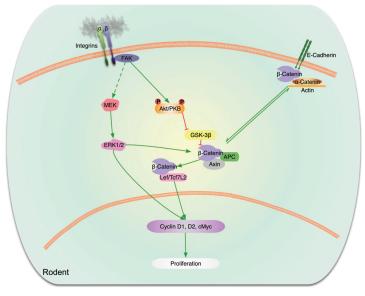


Figure 11. Integrin and cadherin signaling in pancreatic β cells. Activation of β integrin receptors on β cells leads to (1) Akt phosphorylation, which drives β-catenin signaling, and potentially (2) activation of the ERK/MAPK pathway. Both of these pathways promote β cell proliferation. Cadherin activation leads to β-catenin signaling and cell proliferation though interactions with the  $\alpha$ - and  $\beta$ -catenin complex. Image from Stewart et al.,  $2015^{47}$ .

Although integrins appear to be the primary receptors involved in cell-matrix interactions in the islet, a few non-integrin receptors also play a role in these interactions. Discoidin domain receptors (DDRs) are receptor tyrosine kinases that bind collagens I-V and regulate ECM production, and cell adhesion, migration, and differentiation<sup>192</sup>. Expression of DDR1 has been found in islet cells, but not in the surrounding exocrine tissue, suggesting that it may play a role in regulating endocrine cell development

and/or function<sup>193</sup>. Laminins can also bind several non-integrin receptors that are expressed in islets including, laminin receptor-1, dystroglycan protein complex, and Lutheran blood group glycoprotein (Lut), which is exclusively expressed on human islet cell membranes facing the basement membrane<sup>164,165,193</sup>.

Interactions between endocrine cells and the matrix are critical for normal development and continuing β cell survival and function and appear to be mediated by both integrin and non-integrin receptors. However, further work is still needed to determine which specific receptor-ligand interactions and signaling pathways are involved in these developmental and functional processes.

### Collagen

The fibroblasts in the peripheral capsule produce some fibrillar collagens (I, III, and V) and collagen VI, which forms beaded filaments<sup>158,160,194,195</sup>. While these collagens may contribute to maintaining the architecture of the capsule, it is not know whether they play additional roles in islet development or function. The capsule is disrupted by collagenase during isolation of islets for transplantation, and some have speculated that disruption of these capsular collagens may contribute to the low survival rate of transplanted islets<sup>184</sup>.

Because both the peripheral and internal ECM of islets is primarily composed of basement membrane molecules, collagen IV (Col-IV) is the collagen most often associated with islets  $^{194}$ . Cell-matrix interactions typically occur by Col-IV binding to integrins located on the cell surface. There is evidence that Col-IV binds  $\alpha1\beta1$  integrin on  $\beta$  cells  $^{183}$ . This interaction is important during human islet development where it enables fetal  $\beta$  cells to attach and migrate to form normal islet architecture, and enhances insulin secretion  $^{183}$ . However, in adult islets there is no clear Col-IV/integrin binding pathway, and Col-IV interactions with endocrine cells appear to be limited  $^{183}$ . The influence of Col-IV on  $\beta$  cell survival and function is also unclear. Culturing islets on Col-IV improves islet survival compared to culture with Col-I, but also appears to decrease insulin secretion  $^{159,196}$ . This conflicting evidence has caused some to conclude that cell-matrix interactions with laminin may be more significant than interactions with collagens.

#### Laminin

Laminins (LMs) are cross-shaped trimeric glycoproteins that contain an  $\alpha$ -chain,  $\beta$ -chain, and  $\gamma$ -chain connected by disulfide bonds<sup>197</sup>. Along with Col-IV, laminins are a major component of basement membranes, and are therefore abundant in both the peripheral capsule and within islets<sup>158,160,164,195,198</sup>. The specific expression and distribution of laminin isoforms in islets, and which cells produce the different isoforms is still unclear. However, some studies have found temporal and spatial differences in expression. LM-111 is the primary isoform expressed in the developing pancreas, and promotes  $\beta$  cell differentiation<sup>199</sup>. Laminin binding to either dystroglycan or  $\alpha$ 6 integrin may play a role in this laminin-mediated  $\beta$  cell differentiation<sup>185,200</sup>. As islets mature, LM-511 completely replaces LM-111, and other isoforms found in islets include LM-411 which is primarily located in the vascular basement membrane, and LM-332 which is associated with  $\alpha$  cells<sup>198,201,202</sup>. The internal ECM in human islets also contains the laminin  $\beta$ 2 chain, a component of both LM-421 and LM-521, which is typically only found in specialized tissue such as kidney glomeruli<sup>164</sup>. Laminins work through several different integrin

and non-integrin receptors on  $\beta$  cells including  $\beta$ 1 integrins, aV integrins,  $\alpha$ 6 $\beta$ 4, Lut, dystroglycan, and laminin receptor 1<sup>139,164,193</sup>. These interactions are important for enhancing insulin secretion and gene expression, and for promoting  $\beta$  cell survival and proliferation 1<sup>39,196,203</sup>.

#### **Glycoproteins**

Fibronectin is a large dimeric glycoprotein that plays an important role in binding matrix components together as well as binding cells to the matrix by interacting with several integrins and non-integrin receptors. Vitronectin, another matrix glycoprotein, has a similar function and is only expressed during pancreas development. Both fibronectin and vitronectin are necessary for normal islet development, and are thought to play a role in endocrine cell motility during islet formation  $^{185,186,195}$ . Blocking these fibronectin or vitronectin-integrin interactions in the fetal pancreas results in a significant decrease in the number of  $\beta$  cells  $^{186}$ . In adult islets, fibronectin is located in the peripheral capsule and perivascular areas within the islets, and is often associated with collagens and laminins  $^{160,195,198,204}$ . It is unclear what contributions fibronectin makes to the function and survival of adult islets  $^{184}$ .

## **Proteoglycans**

Proteoglycans are composed of a core protein covalently bound to one or more negatively charged glycosaminoglycan (GAG) chains. These GAG chains include heparan sulfate (HS), chondroitin sulfate (CS), dermatan sulfate, and keratan sulfate. Proteoglycans typically form large complexes by binding to hyaluronan and other matrix proteins. They can also bind and sequester cations, water, and growth factors, which allows them to regulate the movement, stability, and availability of molecules in the matrix<sup>205</sup>. Not much is known about the composition of proteoglycans in islet ECM and whether they play a role in islet development and function. However, HS and CS proteoglycans have been detected in islets<sup>193</sup>. HS proteoglycans are known to bind and regulate the bioavailability of growth factors such as FGFs, VEGFs, and HGF which are important for islet development, function, and regeneration<sup>115,137,206-208</sup>. Spatiotemporal differences in expression of HS proteoglycans in islets suggest that they may play a role in regulating processes during pancreas development<sup>193,209-211</sup>.

## **Macrophages**

#### Tissue homeostasis, inflammation, and repair

Macrophages belong to the mononuclear phagocytic system and represent a phenotypically and functionally heterogeneous cell population. During development, macrophages originating from the yolk sac or hematopoietic tissues (i.e., fetal liver or bone marrow) seed tissues throughout the body where they establish self-renewing resident populations<sup>212</sup>. In addition to providing immune surveillance, these tissue-resident macrophages are highly specialized to perform tissue- and niche-specific functions, with their phenotype being dictated by signals they receive from their widely variable microenvironments<sup>212</sup>. In response to signals from infected or damaged tissue, circulating monocytes leave the bloodstream and infiltrate tissues, differentiating into macrophages, where they can function to phagocytize cell debris, recruit additional inflammatory cells, resolve inflammation, and restore tissue homeostasis, among other things<sup>213</sup>. Macrophages are often broadly classified into classically activated (M1) and alternatively activated (M2) phenotypic subtypes, corresponding to exposure to inflammatory signals (i.e., INFY, LPS) and subsequent inflammatory phenotype (M1 macrophages) or exposure to

anti-inflammatory signals (e.g., IL-4, IL-13, CSF-1, TGFβ) leading to a tissue reparative/regenerative phenotype (M2 macrophages)<sup>214</sup>. However, these oversimplified categories poorly reflect the broad spectrum of functions macrophages can perform. Instead, macrophage phenotype is extremely plastic, with gene expression and resulting function being continuously dictated by the type, concentration, and duration of signals from their immediate surroundings<sup>214</sup>.

#### Functional roles in the pancreas

Macrophage precursors are present in the pancreatic buds by E12.5 and mature by E14.5, when they are in close association with developing insulin-expressing endocrine progenitors<sup>215</sup>. Expansion of these macrophage precursors with colony-stimulating factor (M-CSF) in cultured E12.5 fetal pancreas explants leads to an increased number of insulin-producing cells<sup>215</sup>. Signaling between macrophages and developing E14.5-15.5 pancreatic epithelium *in vitro* regulates migration and cell cycle progression, and increasing macrophages at this stage leads to both increased delamination of endocrine cells from developing ducts and decreased proliferative capacity in these differentiated endocrine cells<sup>216</sup>. Mice homozygous for a null mutation in the colony-stimulating factor 1 (CSF-1) gene are deficient in the entire mononuclear lineage, have decreased  $\beta$  cell mass from E18.5 throughout adulthood, and exhibit abnormal islet morphogenesis and impaired postnatal  $\beta$  cell proliferation<sup>217</sup>. These studies suggest that macrophages may function to regulate  $\beta$  cell differentiation, survival, and/or proliferation during pancreatic development.

Tissue-resident macrophages are present in the adult pancreas, but have not been well characterized  $^{215,217}$ . Moreover, because no distinction has been made between resident macrophages in acinar versus islet tissues it is unclear what homeostatic functions these macrophages may have in adult islets. However, inflammatory macrophages recruited to islets do play a role in the pathogenesis of diabetes where they contribute to islet damage and  $\beta$  cell loss  $^{104,218,219}$ . Before conducting the research included in this Dissertation, not much was known about whether macrophages contribute to  $\beta$  cell regeneration  $^{220}$ . Our findings establish a new role for macrophages in  $\beta$  cell regeneration, and two additional studies published last year independently reported the involvement of macrophages in  $\beta$  regeneration using different models of  $\beta$  cell loss—surgically-induced pancreatitis and DT-mediated ablation of the whole pancreas or  $\beta$  cells  $^{153,221,222}$ .

#### Aims of Dissertation

The primary goal of the research included in this Dissertation is to advance understanding of how non-endocrine components of the islet microenvironment—including endothelial cells, macrophages, and the extracellular matrix—contribute to the regulation of  $\beta$  cell mass in adult pancreatic islets.

Reciprocal signaling between endothelial cells and developing endocrine cells is crucial for the establishment of  $\beta$  cell mass and islet vascularization during pancreas development<sup>147</sup>. VEGF-A produced by islet cells is the principle regulator of islet vascularization, and several recent studies have demonstrated that precise control of VEGF-A production in developing and adult  $\beta$  cells is essential for normal islet vascularization, which in turn regulates several important aspects of islet biology including islet innervation,  $\beta$  cell mass, function, and regeneration<sup>137,138,144,150-155</sup>. When VEGF-A is inactivated

either in the early pancreas or newly formed  $\beta$  cells, the intra-islet capillary plexus fails to fully mature, resulting in substantial defects in  $\beta$  cell proliferation, insulin secretion, and glucose homeostasis <sup>148,207</sup>. In contrast, overexpression of VEGF-A in developing  $\beta$  cells induces endothelial cell expansion and hypervascularization that are detrimental to islet formation and result in  $\beta$  cell loss <sup>149-151</sup>. Although VEGF-A production by endocrine cells is required to maintain islet vascularization and function in adults, it is unclear whether intra-islet endothelial cells continue to provide other signals that regulate  $\beta$  cell mass and proliferation throughout life <sup>137</sup>.

In Chapter III, to test the hypothesis that endothelial cells in adult islets provide signals that positively regulate  $\beta$  cell mass and proliferation, we generated a model of inducible VEGF-A overexpression in  $\beta$  cells, and expected that this increase in VEGF-A would lead to both endothelial cell and  $\beta$  cell expansion. We found that increased VEGF-A signaling in adult islets did lead to endothelial cell expansion. Surprisingly,  $\beta$  cells mass was reduced rather than increased, and withdrawal of the VEGF-A stimulus was followed by robust  $\beta$  cell proliferation, leading to islet regeneration, normalization of  $\beta$  cell mass, and re-establishment of the intra-islet capillary network. The source of the stimulus for  $\beta$  cell proliferation in this model was localized to the islet microenvironment, consisting of endothelial cells and recruited macrophages. Macrophages in islet biology have historically been perceived as damaging to islets, contributing to  $\beta$  cell loss in diabetes 104,218,219. To unravel the mechanisms behind  $\beta$  cell regeneration in our model of VEGF-A overexpression, the interactions between these recruited macrophages, endothelial cells,  $\beta$  cells and extracellular matrix components of the microenvironment were investigated in Chapter IV.

Another exciting aspect of this model of  $\beta$  cell regeneration is that the regenerative islet microenvironment in these mice promotes human  $\beta$  cell proliferation. It has become increasingly evident over the last several years that regulation of human  $\beta$  cell proliferation differs from rodents, and most interventions that cause robust proliferation in rodent  $\beta$  cells have no effect on human  $\beta$  cells<sup>46</sup>. Therefore, testing whether compounds or signals that lead to  $\beta$  cell proliferation in animal models also have an effect on human  $\beta$  cells is critical. In Chapter V, we addressed the need for better methods of testing potential human  $\beta$  cell mitogens on human  $\beta$  cells *in vitro*.

The materials and methods used to conduct these studies are described in Chapter II, and the significance of these findings and future directions are presented in Chapter VI.

#### **CHAPTER II**

#### MATERIALS AND METHODS

Some methods in this chapter have been published in Brissova, Aamodt, Brahmachary et al., 2014<sup>153</sup>

#### **Mouse Models**

All animal studies described in this Dissertation were approved by the Institutional Animal Care and Use Committee at Vanderbilt University Medical Center, and animals were kept in facilities monitored by the Vanderbilt University Division of Animal Care on a 12 hour light/12 hour dark schedule with unrestricted access to standard chow and water except where noted below. Mouse models and abbreviations used to describe them below are summarized in Table 1.

Bitransgenic mice with doxycycline (Dox)-inducible  $\beta$  cell-specific overexpression of human VEGF-A<sub>165</sub> (abbreviated  $\beta$ VEGF-A) were generated by crossing RIP-rtTA male mice and TetO-VEGF female mice, both on a C57BL/6 background<sup>137,223-226</sup>. These mice were generously provided by Dr. Shimon Efrat of Tel Aviv University and Dr. Peter Campochiaro of Johns Hopkins University, respectively. In this  $\beta$ VEGF-A model the rat *Ins2* promoter drives expression of the tetracycline-responsive rtTA transactivator specifically in pancreatic  $\beta$  cells. This rtTA transactivator binds the tetracycline operator (*TetO*) upon exposure to Dox, driving expression of human VEGF-A<sub>165</sub> in  $\beta$  cells. Details of Dox preparation and administration are included below.

Mice for lineage tracing analysis were generated by crosses of the Pdx1<sup>PB</sup>-CreER<sup>Tm</sup> line<sup>227,228</sup> and R26R<sup>lacZ</sup> reporter strain<sup>229</sup> with RIP-rtTA and TetO-VEGF transgenic mice. Pdx1<sup>PB</sup>-CreER<sup>Tm</sup> mice on a mixed background were provided by Drs. Maureen Gannon and Chris Wright of Vanderbilt University, and R26R<sup>lacZ</sup> reporter mice on a C57BL/6 background were obtained from Jackson Laboratories (stock #003474). In this lineage tracing model, the  $Pdx1^{PB}$  enhancer drives expression of a tamoxifen (Tm)-inducible Cre recombinase in pancreatic  $\beta$  cells of  $\beta$ VEGF-A mice. The ROSA26 locus causes ubiquitous expression of the R26R<sup>lacZ</sup> reporter, which contains a stop codon flanked by loxP sites

preventing expression of  $\beta$ -galactosidase ( $\beta$ -gal). Upon exposure to Tm, Cre recombinase translocates to the nucleus, removing the stop codon through CreloxP recombination and driving expression of  $\beta$ -gal in  $\beta$  cells. Details of Tm preparation and administration are included below.

Table 1. Mouse models		
MGI Nomenclature or Strain Name	Abbreviation	Reference
Tg(Ins2-rtTA)2Efr	RIP-rtTA	Milo-Landesman et al., 2001
unlisted	TetO-VEGF	Ohno-Matsui et al., 2002 Efrat et al., 1995
Tg(Pdx1-cre/Esr1)1Mga	Pdx1 <sup>PB</sup> -CreER <sup>Tm</sup>	Gannon et al., 2001 Zhang et al., 2005
Gt(ROSA)26Sor <sup>tm1Sor</sup>	R26RlacZ	Soriano et al., 1999
NOD.Cg- <i>Prkdc</i> <sup>scid</sup> <i>II2rg</i> <sup>tm1Wjl</sup> /SzJ	NOD-scid-IL2ry <sup>null</sup>	Shultz et al., 2005
Tg(Tal1-cre/ERT)1Jrg	EC-SCL-CreER	Gothert et al., 2004
C57BL/6-Tg(CAG-EGFP)1Osb/J	GFP	Okabe et al., 1997
B6.FVB-Tg(ITGAM-DTR/EGFP)34Lan/J	CD11b-DTR	Duffield et al., 2005
STOCK Kdr <sup>tm2Sato</sup> /J	VEGFR2fl/fl	Hooper et al., 2009
B6.Cg-Tg(Ins1-EGFP)1Hara/J	MIP-GFP	Hara et al., 2003

To enable fluorescence-activated cell sorting (FACS) of pancreatic  $\beta$  cells from  $\beta$ VEGF-A mice, an additional transgene was introduced into the  $\beta$ VEGF-A mouse model by crossing MIP-GFP mice on a C57BL/6 background<sup>230</sup> with RIP-rtTA and TetO-VEGF mice (abbreviated  $\beta$ VEGF-A+MIP-GFP). These MIP-GFP mice were obtained from Jackson Laboratories (stock #006864). In these mice, the mouse *Ins1* promoter drives green fluorescent protein (GFP) expression in  $\beta$  cells. Details of islet cell dispersion and FACS are included below.

To create an inducible model of endothelial cell (EC)-specific knockdown of VEGFR2 in βVEGF-A mice, EC-SCL-CreER and VEGFR2<sup>fl/fl</sup> mice<sup>231,232</sup> were crossed with RIP-rtTA and TetO-VEGF transgenic mice as described in Chapter IV (see Table 7). EC-SCL-CreER; R26R<sup>lacZ</sup> were generously provided by Dr. Antonis Hatzopoulos of Vanderbilt University on a C57BL/6 background, and used to test Cre activity in intra-islet endothelial cells (Chapter IV). The R26R<sup>lacZ</sup> was removed from these mice by backcrossing them with wild-type C57BL/6 mice (abbreviated WT) obtained from Jackson Laboratories (stock #000664) and EC-SCL-CreER offspring were used in the crosses described above. Heterozygous VEGFR2<sup>fl/wt</sup> mice on a C57BL/6 background from Jackson Laboratories (stock #018977) were bred to create a homozygous VEGFR2<sup>fl/fl</sup> line also used in the crosses described. In this model, a Tm-inducible Cre recombinase is specifically expressed in endothelial cells of βVEGF-A mice and upon exposure to Tm, it translocates to the nucleus where floxed VEGFR2 alleles are excised by Cre-loxP recombination, preventing expression of VEGFR2 in endothelial cells. Details of Tm preparation and administration are included below.

GFP mice (stock #003291) $^{233}$ , WT mice (stock #000664), and CD11b-DTR mice (stock #006000) $^{234}$ , all on a C57BL/6 background and obtained from Jackson Laboratories were used as bone marrow donors for  $\beta$ VEGF-A transplant recipients. Bone marrow from GFP mice was used to determine whether bone marrow-derived cells (BMCs) are recruited to  $\beta$ VEGF-A islets upon VEGF-A induction (Chapter III). In CD11b-DTR mice, the CD11b promoter drives diphtheria toxin receptor (DTR) expression in monocytes and macrophages. Bone marrow from these mice was transplanted into  $\beta$ VEGF-A mice to establish a model of diphtheria toxin (DT)-inducible macrophage depletion to evaluate whether macrophages are required for  $\beta$  cell proliferation in  $\beta$ VEGF-A islets (Chapter IV). Details of bone marrow transplantation and DT preparation and administration are included below.

WT mice from Jackson Laboratories (stock #000664) as well as  $\beta$ VEGF-A mice were used as islet donors for  $\beta$ VEGF-A recipients (Chapter III). Human islets combined with either WT or  $\beta$ VEGF-A islets in these experiments were transplanted into immunodeficient NOD-scid- $IL2r\gamma^{null}$  mice<sup>235,236</sup> obtained in collaboration with Dr. Leonard Shultz from Jackson Laboratories (stock #005557). These mice lack mature T cells, B cells, natural killer cells and exhibit deficient cytokine signaling, making them ideal recipients for xenotransplantation.

#### DNA extraction and genotyping

Mouse models used for breeding were maintained by genotyping using the primers and PCR conditions listed in Table 2. DNA was extracted and PCR reactions were performed with tail snips from mice using the Red Extract N-Amp Tissue PCR kit (XNAT; Sigma, St. Louis, MO), except in VEGFR2<sup>fl/fl</sup> mice, where the Kapa Hot Start PCR kit (KK5621; Kapa Biosystems, Wilmington, MA) was used instead. Both DNA extraction and preparation of PCR reaction mixtures were performed according to the manufacturer's instructions. Primers were obtained from Sigma Genosys and reconstituted in RNase/DNase-free water to 100 µM and further diluted 1:20 and stored at -20°C for use in PCR reactions. Thermal cycler conditions listed in Table 2 were used to amplify DNA before resolving on agarose gels with 100 ng/mL ethidium bromide in 1x TBE buffer as indicated (Table 2).

### Glucose measurements and glucose tolerance testing

Glucose tolerance testing was performed after a 14-16 hour fast by administering 2 g/kg of filter-sterilized 10% D-glucose prepared in 10 mM PBS by intraperitoneal injection<sup>137</sup>. Plasma glucose was measured in whole blood from nicked tail veins before glucose injection and at 15, 30, 60, 90, and 120 minutes after injection using an Accu-chek glucose meter (Roche Diagnostics, Indianapolis, IN) calibrated according to the manufacturer's instructions. Random blood glucose levels were measured at 3:00 pm.

#### Bone marrow isolation, irradiation, and transplantation

Bone marrow was harvested in collaboration with the Vanderbilt Cardiovascular Pathophysiology and Complications Core from cleaned femurs and tibias of 6-8 week old GFP, CD11b-DTR, or WT donor mice by flushing them with RPMI-1640 medium containing 2% fetal bovine serum plus heparin (5 U/mL). Six to eight week old  $\beta$ VEGF-A recipients received a single dose of lethal irradiation (9 Gy) followed by injection of  $5x10^6$ - $10x10^6$  bone marrow cells delivered in 100- $200~\mu$ L RPMI-1640 media via the retro-orbital sinus. Recipients were treated with 100~mg/L neomycin and 10~mg/L polymyxin B sulphate (X-Gen Pharm) in drinking water beginning 3 days prior to irradiation and continuing for 2-3 weeks after bone marrow transplantation (BMT). Hematopoietic engraftment of GFP+ bone marrow was assayed 8 weeks after transplantation as well as at 1 week Dox, and 2 weeks after Dox withdrawal by flow cytometry analysis. All animals achieved high hematopoietic chimerism (>80 %). Partial bone marrow ablation to prevent recruitment of bone marrow-derived cells to  $\beta$ VEGF-A islets was achieved with 5 Gy irradiation (Chapter III) $^{237}$ .

	Table 2. PCR primers and conditions	for genotyping	
Mouse Model	Genotyping Primers	PCR Conditions	Expected Products
RIP-rtTA	5' - GTG AAG TGG GTC CGC GTA CAG - 3' (forward) 5' - GTA CTC GTC AAT TCC AAG GGC ATC - 3' (reverse)	92°C2' 94°C30" 57°C30" 30 cycles 72°C30" 72°C10' 4°Chold	400 bp for transgene (1.5% agarose)
TetO-VEGF	5' - TCG AGT AGG CGT GTA CGG - 3' (forward) 5' - GCA GCA GCC CCC GCA TCG - 3' (reverse)	95°C4' 95°C1' 57°C30" 29 cycles 72°C1' 72°C10' 4°Chold	420 bp for transgene (1.0% agarose)
Pdx1 <sup>PB</sup> -CreER <sup>Tm</sup>	5' - TGC CAC GAC CAA GTG ACA GC - 3' (forward) 5' - CCA GGT TAC GGA TAT AGT TCA TG - 3' (reverse)	93°C3' 93°C20" 60°C20" 30 cycles 65°C45" 72°C5' 4°Chold	675 bp for <i>Cre</i> (1% agarose gel)
R26R <sup>lacZ</sup>	5' - AAA GTC GCT CTG AGT TGT TAT - 3' (common forward) 5' - GGA GCG GGA GAA ATG GAT ATG - 3' (WT reverse) 5' - GCG AAG AGT TTG TCC TCA ACC - 3' (mutant reverse)	93°C2' 93°C30" 58°C30" 40 cycles 65°C1' 65°C5' 6°Chold	500 bp for wild-type 250 bp for <i>R26R</i> <sup>lacZ</sup> (1% agarose gel)
EC-SCL-CreER	5' - TCC CGC AGA ACC TGA AGA TGT TCG C - 3' (forward) 5' - ACC AGA GAC GGA AAT CCA TCG CTC - 3' (reverse)	93°C3' 93°C20" 60°C20" 30 cycles 72°C45" 72°C5' 4°Chold	750 bp for <i>SCL</i> (1.5% agarose gel)
VEGFR2 <sup>fl/fl</sup>	5' - CCA CAG AAC AAC TCA GGG CTA - 3' (forward) 5' - GGG AGC AAA GTC TCT GGA AA - 3' (reverse)	94°C2' 94°C20" 65°C15" 10 cycles 68°C10" 94°C15" 28 cycles 72°C10" 72°C11' 4°Chold	179 bp for wild-type 230 bp for <i>VEGFR2</i> <sup>loxP</sup> (3.0% agarose gel)
MIP-GFP	5' - AAG TTC ATC TGC ACC ACC G - 3' (tg primer 1) 5' - TCC TTG AAG AAG ATG GTG CG - 3' (tg primer 2) 5' - CTA GGC CAC AGA ATT GAA AGA TCT- 3' (IC forward) 5' - GTA GGT GGA AAT TCT AGC ATC ATC C - 3' (IC reverse)	94°C1.5′ 94°C30′ 60°C1′ 35 cycles 72°C1′ 72°C2′ 4°Chold	173 bp for <i>GFP</i> 324 bp for internal control (2.0% agarose gel)

#### Compound preparation and administration

#### **Doxycycline (Dox)**

VEGF-A transgene expression was activated in βVEGF-A mice by Dox administration (5 mg/mL) in light-protected drinking water containing 1% Splenda® for a period of 1-3 weeks. Mice used in genetic macrophage knockdown experiments (Chapter IV, Figure 35) were administered Dox prepared in sterile water (10 ng/mL) by daily oral gavage (200 μL/day) for a period of 1 week.

#### Diphtheria toxin (DT)

Macrophage depletion in  $\beta VEGF$ -A mice transplanted with bone marrow from CD11b-DTR mice was achieved by daily retro-orbital injections of DT (2  $\mu g/\mu L$  in saline; 10 ng/g of body weight) 8-10 weeks after transplantation for a period of 8 days. DT injections continued for one day longer than simultaneous Dox administration. Control  $\beta VEGF$ -A mice transplanted with WT bone marrow received the same treatment. Mice receiving DT injections were supplemented with Transgenic Dough Diet (21.2% protein, 12.4% fat, 46.5% carbohydrate; BioServ, Flemington, NJ) throughout the course of the experiment.

#### **Clodronate liposomes (Clod)**

Clodronate-mediated macrophage depletion in  $\beta VEGF$ -A mice was accomplished by injecting clodronate liposomes (5 mg/mL clodronate; Clodrosome, Brentwood, TN) retro-orbitally (150-200  $\mu$ L) every other day over a 1-2 week period for a total of 4-8 injections. Liposome injections began one day before Dox administration, and continued for 1 week after in mice harvested at later time points. Control liposomes with the same lipid composition (Clodrosome, Brentwood, TN) were administered to  $\beta VEGF$ -A mice using the same route, volume, and schedule. Mice receiving liposome injections were supplemented with Transgenic Dough Diet (21.2% protein, 12.4% fat, 46.5% carbohydrate; BioServ, Flemington, NJ) throughout the course of the experiment.

#### Tamoxifen (Tm)

Tm was prepared fresh in filter-sterilized corn oil the day before each injection at 10-20 mg/mL and allowed to dissolve overnight on a nurator at room temperature, protected from light<sup>238</sup>. For lineage tracing analysis,  $\beta$  cells were genetically marked with  $\beta$ -gal by administering 1 mg Tm by subcutaneous injection (10 mg/mL; 100  $\mu$ L) every 48 hours for a total of 3 doses over 5 days, starting 2 weeks before Dox administration. To test the EC-SCL-CreER transgene, EC-SCL-CreER; R26R<sup>lacZ</sup> mice were given 4 mg Tm subcutaneously (20 mg/mL; 200  $\mu$ L) every 48 hours for a total of 3 doses over 5 days. Pancreata were harvested 3 days after the last injection. Vetbond tissue adhesive (3M) was used to seal injection sites to prevent oil leakage.

## **Bromodeoxyuridine (BrdU)**

BrdU (Sigma, St. Louis, MO) was administered at 0.8 mg/mL in drinking water for 7 days prior to tissue collection.

#### Islet Isolation and In Vitro Analysis

Mouse islets were isolated in collaboration with the Vanderbilt Islet Procurement and Isolation Core by intra-ductal infusion of 3 mL collagenase P (0.6 mg/mL; Roche Molecular Biochemicals, Indianapolis, IN) prepared in Hank's balanced salt solution (HBSS) as described<sup>239,240</sup>. Following injection, the inflated pancreas was removed and digested in 6.7 mL collagenase P (0.6 mg/mL in HBSS) for an additional 4-8 minutes on a wrist-action shaker at 37°C and 1-2 minutes by manual shaking at room temperature. Collagenase was inactivated by adding 7-8 mL cold 10% fetal bovine serum (FBS) in HBSS, then pancreata were washed three times with 14 mL of 10% FBS/HBSS, centrifuging at 1000 rpm for 2 minutes at 4°C between washes to pellet the tissue. After the last wash, pancreatic tissue was resuspended in 10% FBS/HBSS and plated in petri dishes on ice. Islets were handpicked to near 100% purity in 10% FBS/HBSS with RNase-free pipette tips using an inverted microscope. Islets from  $\beta$ VEGF-A mice and  $\beta$ VEGF-A+MIP-GFP used for dispersion and sorting were isolated using Clonetics EGM MV Microvascular Endothelial Cell Growth Medium (Lonza, Basel, Switzerland) in place of 10% FBS/HBSS to wash and plate pancreatic tissue, and to handpick islets.

#### Islet perifusion

Mouse and human islet function was studied in a dynamic cell perifusion system in collaboration with the Vanderbilt Islet Procurement and Isolation Core as described<sup>137,241,242</sup>. Base perifusion medium was prepared fresh in 1 L deionized water by combining 1 g Dulbecco's modified Eagle's medium powder, 3.2 g NaHCO<sub>3</sub>, 0.58 g L-glutamine, 0.11 g sodium pyruvate, 1.11 g HEPES, 1 g RIA-grade bovine serum albumin (BSA), and 3 mL 0.5% phenol red. Following vacuum filtration, D-glucose and 3-isobutyl-1-methylxanthine (IBMX) were added to this base medium to create solutions of (1) 5.6 mM glucose to measure basal insulin secretion, (2) 16.7 mM glucose to measure glucose-stimulated insulin secretion, and (3) 16.7 mM glucose + 100 μM IBMX to enhance glucose stimulated insulin secretion. All reagents used to create these solutions were obtained from Sigma-Aldrich (St. Louis, MO). Purified, size-matched islets were placed in the perifusion chamber at 37°C and sequentially perifused with 5 mM glucose, 16.7 mM glucose, and 16.7 mM glucose + IBMX media at a perifusate flow rate of 1 mL/min. Effluent was collected at 3-minute intervals using an automatic fraction collector. Insulin concentration in each fraction was measured by radioimmunoassay (RI-13K; Millipore, Billerica, MA).

#### Islet VEGF-A secretion

Size-matched islets were cultured in eight-well chamber slides containing 50–70 islets/well in 470  $\mu$ L RPMI-1640 media containing 10% fetal bovine serum and 5.6 mM glucose for 48 hours at 37°C. VEGF-A production by isolated islets was measured by a species–specific VEGF-A enzyme-linked immunosorbent assay (R&D Systems, Minneapolis, MN) according to the manufacturer's protocol as described<sup>137</sup>.

#### **Islet Transplantation**

WT C57BL/6 and  $\beta$ VEGF-A islets were transplanted under contralateral kidney capsules into  $\beta$ VEGF-A recipients (200 islets/graft) as described<sup>240</sup>. Islets from donor mice were isolated and purified by handpicking as described above, then washed three times in sterile 10 mM PBS with 1% mouse serum (collected from donor mice) before being loaded into P10 tubing for transplantation. Mice were anesthetized and their kidneys exposed by dissecting through flank skin and muscle layers. The capsule was separated from the kidney parenchyma using a 23-gauge butterfly needle and the P10 tubing containing donor islets was inserted into the channel created by the needle. Muscle and skin layers were closed and mice were observed daily for 2 weeks after surgery.

Human islets from three donors with an average age of 23 years (range 20-28) and average BMI of 28.7 (range 19.0-33.8) were obtained through the Integrated Islet Distribution Program (iidp.coh.org). Mixtures with equal amounts of purified human and WT or βVEGF-A islets (100 islet equivalents per group) were transplanted beneath contralateral kidney capsules of immunodeficient NOD-*scid-IL2ry*<sup>null</sup> mice using the same protocol described above.

## Flow Cytometry and Cell Sorting

Flow analysis and sorting was performed in collaboration with the Vanderbilt Flow Cytometry Core. Peripheral blood and islet cells used for flow analysis or sorting were prepared as described below:

Peripheral blood (50-100  $\mu$ L) was collected from the retro-orbital sinus of  $\beta$ VEGF-A mice using heparinized capillary tubes 24 hours after beginning liposome or DT injections to evaluate depletion of circulating monocytes. Blood was incubated for 3-5 minutes at 37°C with 1 mL warmed, filter-sterilized erythrocyte lysis buffer (8.26 g ammonium chloride, 1 g potassium bicarbonate, and 0.38 g EDTA in 1 L Milli-Q water). Cells were pelleted by centrifuging at 1800 rpm for 2-3 minutes at 4°C and supernatant discarded. Incubation with erythrocyte lysis buffer was repeated, and then cells were washed with 1 mL FACS buffer (2 mM EDTA and 2% FBS in 10 mM PBS) prior to antibody incubation. Blood from WT mice was collected for antibody compensation controls.

Isolated islets from  $\beta VEGF$ -A mice and  $\beta VEGF$ -A+MIP-GFP mice handpicked in Clonetics EGM MV Microvascular Endothelial Cell Growth Medium (Lonza, Basel, Switzerland) were washed 3 times with 2 mM EDTA in 10 mM PBS and then dispersed by incubating with Accutase (Innovative Cell Technologies, San Diego, CA) at 37°C for 10 minutes with constant pipetting. Accutase was quenched with EGM MV media, and then islet cells were washed twice with the same media and counted using a hemocytometer prior to antibody incubation. Anti-rat Ig,  $\kappa$  CompBead Plus Compensation Particles (BD Biosciences, San Jose, CA) and EasyComp Fluorescent Particles, GFP (Spherotech, Lake Forest, IL) were used as single color compensation controls for islet cell sorts.

Peripheral blood and islet cells prepared as described above, and anti-rat Ig compensation particles were incubated for 15-20 minutes at 4°C with fluorophore-conjugated antibodies in FACS buffer followed by one wash with FACS buffer. All antibodies for flow cytometry and their working dilutions are listed in Table 3. Prior to analysis or sorting, either propidium iodide (0.05 µg/100,000 cells; Invitrogen

Molecular Probes, Eugene, OR) or Dapi (0.25 μg/1,000,000 cells; Invitrogen Molecular Probes, Eugene, OR) was added to samples for non-viable cell exclusion. Flow analysis was performed using an LSRFortessa cell analyzer (BD Biosciences, San Jose, CA), and a FACSAria III cell sorter (BD Biosciences, San Jose, CA) was used for FACS. Analysis of flow cytometry data was completed using FlowJo 7.6.5 (Tree Star, Ashland, OR).

	Table 3. A	Antibodies fo	or flow cytometry an	d sorting	
Antigen	Conjugate	Species	Source	Catalog #	Dilution
CD45	APC-Cy7	Rat	BD Pharmingen	561037	1:500
CD45	PE	Rat	BD Pharmingen	561087	1:500
CD11b	APC	Rat	BD Pharmingen	561690	1:100, 1:500
Gr1 (Ly6G/Ly6C)	FITC	Rat	BD Pharmingen	553126	1:500
Ly6G	FITC	Rat	BD Pharmingen	551460	1:500
F4/80	Pacific Blue	Rat	Invitrogen Molecular Probes	MF48028	1:500
CD31	PE	Rat	BD Pharmingen	561073	1:500, 1:1000

## RNA Isolation, Sequencing, and Analysis

Isolated whole islets (100-300) or sorted islet-derived cells (8,000-400,000) were added to 200-400 µL lysis/binding solution in the RNAqueous small scale or micro scale phenol-free total RNA isolation kits (Ambion, Austin, TX). Trace contaminating DNA was removed with TURBO DNA-free or DNA-free (Ambion, Austin, TX). RNA quality control quantification was performed using a Qubit Fluorometer (Invitrogen, Carlsbad, CA) and an Agilent 2100 Bioanalyzer. All RNA samples had an RNA integrity number (RIN) ≥5.0. RNA was amplified using the NUGEN Technologies Ovation RNA amplification kit optimized for RNA sequencing. Following amplification, the resulting cDNA was sheared to an average insert size of 300 bp and used for library preparation. Sequencing was performed using standard Illumina methods as described<sup>243,244</sup>. Following RNA sequencing, raw reads were mapped to reference mouse genome mm9 using TopHat v2.0<sup>245</sup>. Aligned reads were imported onto the Avadis NGS data analysis platform (Strand Scientific Intelligence, Bengalor). Reads were first filtered on their quality metrics, and then duplicate reads were removed. Normalized gene expression was quantified using the TMM (Trimmed Mean of M-values) algorithm<sup>246,247</sup>. The transcriptional profile from sample groups (whole islets, sorted islet β cells, islet-derived macrophages and endothelial cells at all time points) was compared by principle component analysis (PCA) and hierarchal clustering analysis to determine the layout and spread of the samples. A minimum expression cutoff (normalized expression ≥20 at one or more time points) was applied before determining differential expression between conditions, which was calculated on the basis of fold change (cutoff ≥2.0) and the p-value was estimated by z-score calculations (cutoff 0.05) as determined by the Benjamini Hochberg false discovery rate (FDR) method<sup>248</sup>. Differentially expressed genes underwent gene set enrichment analysis (GSEA), gene ontology (GO) analysis, and pathway analysis using DAVID, and Ingenuity Pathway Analysis. The top 350 GO Biological Processes terms (by p-value) for each fold-change comparison were summarized and visualized using REVIGO (revigo.irb.hr)<sup>249</sup>. RNA quality control, amplification, sequencing, and analysis were performed in collaboration with the Genomic Services Laboratory at HudsonAlpha Institute for Biotechnology.

#### Tissue Collection, Fixation, and Analysis

Pancreata and kidneys bearing islet grafts were collected from anesthetized mice prior to cervical dislocation. Pancreata and kidneys were washed in ice-cold 10 mM PBS and fat and other excess tissue was removed before pancreata were weighed and tissues fixed with 4% paraformaldehyde in 100 mM PBS on ice for 90 minutes. Following fixation, tissues were washed 4 times for 30 minutes in 100 mM PBS on ice then transferred to a 30% sucrose solution to equilibrate at 4°C overnight.

Tissues were prepared for cryosectioning by blotting to remove excess sucrose before mounting them in Tissue Tek cryomolds filled with Optimal Cutting Temperature (OTC) compound (VWR Scientific Products, Radnor, PA). Kidneys were cut in half along the transverse plane near the graft tissue before mounting to simplify visualization of islet grafts in cross-sections. Tissue molds were placed on dry ice until the OTC was set, then stored at -80°C. Tissues were sectioned from 5-10 µm thick on a Leica CM1950 cryostat (Leica, Wetzlar, Germany) and these cryosections were attached to Superfrost Plus Gold slides (ThermoFischer Scientific, Waltham, MA).

#### Intravital blood vessel labeling

The function of the islet vasculature was assessed by infusing 100  $\mu$ L fluorescein isothiocynate-conjugated tomato lectin (*Lycopersicon Esculentum*, 1 mg/mL; Vector Laboratories, Burlingame, CA) into the jugular vein to circulate for 5 minutes before sacrificing the animal and removing and fixing the pancreas as described above<sup>137</sup>.

#### Pancreatic hormone content

Pancreata collected to evaluate hormone content were removed and washed as described above. After washing with 10 mM PBS, pancreata were blotted to remove excess liquid before being weighed. Tissues were then placed on ice and homogenized in 2 mL acid alcohol (1 mL 10N HCl + 110 mL 95% ethanol) using a Polytron PT 10/35 homogenizer (Brinkmann Instruments, Riverview, FL). Following homogenization, another 3 mL acid alcohol was added and homogenates were placed on a rotator for 48 hours at 4°C. Supernatant was collected by centrifuging at 2500 rpm for 30 minutes and stored at -20°C. Insulin and glucagon content in these pancreatic extracts were determined by radioimmunoassay (insulin, RI-13K; glucagon, GL-32K; Millipore, Billerica, MA) in collaboration with the Vanderbilt University Hormone Assay and Analytical Services Core.

#### Immunohistochemistry, Imaging, and Analysis

Immunohistochemistry was performed as described previously<sup>240</sup> using primary and secondary antibodies listed in Tables 4-5.

Cryosections (5-10 µm thick) were allowed to air dry then either post-fixed with 1% paraformaldehyde in 10 mM PBS for 10 minutes before permeabilization, or immediately permeabilized in 0.2% Triton-X in 10 mM PBS. Following permeabilization, sections were washed three times with 10 mM PBS for 3-5 minutes each, then blocked in 5% normal donkey serum in 10 mM PBS for 60-90 minutes in a humidified chamber at room temperature. Sections incubated overnight with primary antibodies diluted in antibody buffer (0.1% Triton-X and 1% BSA in 10 mM PBS) in a humidified chamber at 4°C, and then were washed three times with 0.1% Triton-X in 10 mM PBS for 10 minutes each. Secondary antibodies prepared in antibody buffer were then added to sections and incubated for 60-90 minutes in a humidified chamber protected from light at room temperature. Sections were treated with Dapi (5 mg/mL stock diluted 1:50,000 in 10 mM PBS) for 10 minutes, and then washed three times with 0.1% Triton-X in 10 mM PBS for 15 minutes each, followed by three successive washes with 10 mM PBS. Slides were mounted using SlowFade Gold antifade reagent (Invitrogen Molecular Probes, Eugene, OR) and sealed with fingernail polish prior to imaging.

#### BrdU labeling in cryosections

Following permeabilization, BrdU incorporated into DNA was exposed for immunofluorescence labeling by treatment with DNase (100 Kunitz/mL; Promega, Madison, WI) in a humidified chamber for 45 minutes at 37°C. Sections were then blocked and stained as described above.

#### X-Gal enzymatic staining

X-gal enzymatic staining was used to detect β-galactoside activity in EC-SCL-CreER; R26R<sup>lacZ</sup> mice following Tm treatment to determine whether Cre recombinase was active in intra-islet endothelial cells. Cryosections (10 μm thick) were allowed to air dry, and then post-fixed with 1% paraformaldehyde/ 0.2% glutaraldehyde for 15 minutes at room temperature. Sections were washed 3 times with 10 mM PBS for 5 minutes each then permeabilized with permeabilizing solution (2 mM MgCl<sub>2</sub>, 0.01% sodium deoxycholate, and 0.02% Nonidet P-40 in 10 mM PBS) for 10 minutes at room temperature before incubating with X-gal enzymatic staining solution (2 mM MgCl<sub>2</sub>, 0.01% sodium deoxycholate, 0.02% Nonidet P-40, 5 mM potassium ferricyanide, and 5 mM potassium ferrocyanide) overnight in a humidified chamber at 37°C. Following staining, sections were washed 3 times with 10 mM PBS for 10 minutes each and mounted using Aqua-Poly/Mount mounting medium (Polysciences Inc., Warrington, PA)<sup>240</sup>.

Table 4. Primary antibod	lies for immu	unohistocher	mistry and immunocy	/tochemistry
Antigen	Species	Dilution	Source	Catalog #
Insulin	Guinea pig	1:500	Dako	A0564
Glucagon	Rabbit	1:100	Cell Signaling	2760s
MafA	Rabbit	1:25000	gift from Dr. Stein	BL1225
Pdx1	Rabbit	1:10000	gift from Dr. Wright	N/A
Amylase	Rabbit	1:1000	Sigma	A8273
BrdU	Rat	1:500	Abcam	ab6326
CD31	Rat	1:100	BD Pharmingen	550389
Ki67	Rabbit	1:500	Abcam	ab15580
DBA-biotinylated	N/A	1:1000	Vector	B-1035
CD45	Rat	1:100, 1:500	BD Pharmingen	550539
B220	Rat	1:100	BD Pharmingen	550286
CD3	Rat	1:100	BD Pharmingen	555273
F4/80	Rat	1:100	Invitrogen	MF48000
GFP	Rabbit	1:10000	Invitrogen	A11122
VEGF-A	Goat	1:200	R&D Systems	AF564
Bmi-1	Mouse	1:200	Millipore	05-637
β-galactosidase	Chicken	1:5000	Abcam	ab9361
Caveolin-1 (N-20)	Rabbit	1:1000	Santa Cruz BT	sc-894
Caveolin-1	Rabbit	1:2000	Abcam	ab2910
C-peptide	Mouse	1:500	Developmental Studies Hybridoma Bank	GN-ID4-c
Phospho-histone H2AX (Ser139)	Rabbit	1:500	Abcam	ab2893
lba1	Rabbit	1:500	Wako	019-19741

Table 5. Se	condary antibodies	for immuno	histochem	nistry and immunocyto	chemistry
Host Species	Primary Ab Species	Fluorophore	Dilution	Source	Catalog #
Donkey		Cy2	1:200	Jackson Immunoresearch	711-225-152
Donkey	Dobbit	Alexa488	1:200	Jackson Immunoresearch	711-545-152
Donkey	Rabbit	Су3	1:500	Jackson Immunoresearch	711-165-152
Donkey		Cy5	1:200	Jackson Immunoresearch	711-175-152
Donkey	Goat	Су3	1:500	Jackson Immunoresearch	705-165-147
Donkey		Cy2	1:200	Jackson Immunoresearch	712-225-153
Donkey	Rat	Alexa488	1:200	Jackson Immunoresearch	712-545-153
Donkey	Ral	Су3	1:500	Jackson Immunoresearch	712-165-153
Donkey		Cy5	1:500	Jackson Immunoresearch	712-175-153
Donkey	Chicken	Cy2	1:200	Jackson Immunoresearch	703-225-155
Donkey	Chicken	Cy3	1:500	Jackson Immunoresearch	703-165-155
Donkey		Cy2	1:200	Jackson Immunoresearch	706-225-148
Donkey		Alexa488	1:200	Jackson Immunoresearch	706-545-148
Donkey	Guinea Pig	СуЗ	1:500	Jackson Immunoresearch	706-165-148
Donkey		Cy5	1:200	Jackson Immunoresearch	706-175-148
Donkey		Alexa647	1:200	Jackson Immunoresearch	706-605-148

#### Imaging and morphometry

Digital images were acquired with an Olympus BX-41 fluorescence microscope (Olympus, Tokyo, Japan) equipped with a Spot Flex digital camera (Diagnostic Instruments, Inc., Sterling Heights, MI), a Zeiss LSM510 META laser scanning confocal microscope (Carl Zeiss, Jena, Germany), a Leica DMI6000B fluorescence microscope equipped with a Leica DFC360FX digital camera (Leica, Wetzlar, Germany), a ScanScope FL or a ScanScope CS (Aperio, Vista, CA). Image analysis was performed using MetaMorph 7.7 software (Molecular Devices, Downingtown, PA), ImageScope software (Aperio, Vista, CA), or HALO software (Indica Labs, Corrales, NM); 15-25 islets were analyzed/mouse/ treatment. A β cell was deemed positive for a nuclear marker only when at least 75% of the nucleus was surrounded by insulin+ cytoplasm; 500-2000 β cells were assessed/assay/mouse.

For  $\beta$  cell mass measurements, the pancreas was removed, weighed, and fixed as described above and then pancreatic cryosections were labeled for insulin and  $\alpha$ -amylase. To systematically examine  $\beta$  cell mass in the pancreas, 8- $\mu$ m thick pancreatic sections spaced by 200  $\mu$ m from seven consecutive levels of the pancreatic tissue block were examined (4 pancreata/time point; total of 28 sections/time point). Images of entire pancreatic sections were captured at 20x magnification using a ScanScope FL system (Aperio, Vista, CA) and archived using a web-based Spectrum digital slide database (Aperio, Vista, CA). Image analysis of whole pancreatic sections was performed with an Aperio area quantification algorithm.  $\beta$  cell mass was calculated by expressing the  $\beta$  cell area (sum of insulin+ area) as a percentage of pancreatic area (combined  $\alpha$ -amylase+ and insulin+ area) of the section and then multiplying by the pancreatic weight.

## In Vitro Screening of Mitogenic Compounds on Primary Human Islet Cells

#### Human islet dispersion, transduction, plating, and culture

Human islets from 11 donors (8 male, 3 female) with an average age of 43 years (range 29-57) and average BMI of 31.5 (range 23.8-37.9) were obtained through the Integrated Islet Distribution Program (IIDP; iidp.coh.org). Upon arrival islets were handpicked to near 100% purity in CMRL islet media (CMRL media with 25% human serum albumin, 4.8 µM Vitamin E, and 8.2 mM Vitamin B3) or Standard Prodo Islet Media (Prodo Laboratories Inc.; Irvine, CA). Sixty purified islets were taken and assessed for β cell function using a dynamic cell perifusion system as previously described<sup>242</sup>. The remaining islets were washed 3 times with 2 mM EDTA in 10 mM PBS and dispersed by incubating with 0.025% trypsin in 10 mM PBS at room temperature for 12-15 minutes with constant gentle pipetting. Trypsin was guenched with RPMI culture medium (RPMI medium with 10% FBS and 1% penicillin/ streptomyocin) at basal glucose (5 mM) and then islet cells were washed twice with the same media. Cells were counted using a hemocytometer, then resuspended in RPMI culture medium at basal (5 mM) or high (11 mM) glucose and plated on collagen I-coated 384-well plates (BD Biosciences; San Jose, CA) at 20,000-30,000 cells/well. Prior to plating, an aliquot of cells at each glucose level was taken and co-transfected with adenoviruses encoding cyclin D3 and cdk6 (100-250 multiplicity of infection, MOI) in RPMI culture medium without FBS for 1 hour at 37°C. Adenoviruses were prepared as described previously<sup>250</sup>. After 1 hour, the transduction was terminated by adding RPMI culture medium and cells were plated as described above. All plated cells were cultured at 37°C and allowed to adhere for 24 hours prior to compound treatment.

## Compound preparation and islet cell treatment

Compounds were prepared in RPMI culture medium at basal (5 mM) and high (11 mM) glucose from stock concentrations as described in Table 6. After dispersed islet cells adhered for 24 hours, the culture medium was replaced with medium containing compounds and cells remained in culture for another 72 hours before fixation and staining.

#### Immunocytochemistry, imaging, and analysis

Following treatment, the culture medium was removed and wells were rinsed once with 10 mM PBS before cells were fixed and immunolabeled directly in the wells. Cells were fixed with fresh 4% paraformaldehyde in 10 mM PBS for 30 minutes at 4°C, then washed with 10 mM PBS for 20 minutes at room temperature before permeabilization with 0.2% Triton X-100 in 10 mM PBS for 15 minutes at room temperature. Wells were then blocked with 5% normal donkey serum for 30 minutes at room temperature prior to labeling with primary antibodies against insulin or C-peptide, Pdx1, and Ki67 prepared in fresh antibody buffer (10 mM PBS with 1% BSA and 0.1% Triton X-100) overnight at 4°C. Cells were washed with 0.1% Triton X-100 in 10 mM PBS for 30 minutes then labeled with appropriate secondary antibodies prepared in fresh antibody buffer for 1 hour at room temperature. Information and dilutions for primary and secondary antibodies are listed in Tables 4-5.

7	Table 6. Preparatio	n of compounds te	Preparation of compounds tested on human islet cells	slle	
COMPOUND	STOCK CONCENTRATION	SOLVENT	CONCENTRATIONS TESTED	SOURCE	CATALOG NUMBER
DYRK Family					
Harmine	100 mM	DMSO	1, 10 µM	Sigma	286044
Neurotransmitters					
y-Aminobutyric acid (GABA)	100 mM	PBS	100, 1000, 2500 µM	Sigma	A2129
Serotonin (5HT)	10 mM	water	10, 100, 250 µM	Sigma	L510041
TGF-β Superfamily					
Myostatin (GDF-8)	100 µg/mL	4mM HCI / 0.1% BSA	500, 1000, 2500 ng/mL	R&D Systems	788-G8-010
Activin A	50 µg/mL	PBS / 0.1% BSA	10, 100, 1000 ng/mL	R&D Systems	338-AC-010
Follistatin-like 3 (FSTL3)	100 µg/mL	PBS / 0.1% BSA	50, 100, 500 ng/mL	R&D Systems	1288-F3-025
Adenosine Signaling/Metabolism					
NECA	40 mM	DMSO	1, 10, 100 µM	Tocaris	1691
UK-432097	1 mM	DMSO	0.1, 1, 10 µM	Axon Medchem	1193
A-134974	10 mM	water	0.1, 1, 10 μM	Sigma	A2846
Hormones/Growth Factors					
Human prolactin (PRL)	0.1 mg/mL	4mM HCI / 0.1% BSA	100, 1000, 2500 ng/mL	R&D Systems	682-PL-050
Platelet-derived growth factor (PDGF)	0.025 mg/mL	PBS	50, 500, 1250 ng/mL	Sigma	P3076
Erythropoietin (EPO)	500 units/mL	PBS / 0.1% BSA	1, 10, 20 units/mL	R&D Systems	287-TC-500
Exendin-4 (Ex-4)	10 µM	PBS	10 nM	California Peptide	207-77

Cells were labeled with Dapi (1:50,000) for 10 minutes, washed with 0.1% Triton X-100 in 10 mM PBS for 15 minutes followed by a 15 minute wash in 10 mM PBS all at room temperature. Fluoroshield Mounting Medium (Abcam; Cambridge, England) was added to each well and the plates were either immediately imaged or stored at 4°C protected from light and dehydration. Images were acquired with a Leica DMI 6000B fluorescence microscope equipped with a Leica DFC360FX digital camera, XY scanning stage and Z autofocus function (Leica Microsystems; Wetzlar, Germany). The Multiple Mosaics application in the LAS AF MATRIX M3 Developer Suite (Leica Microsystems; Wetzlar, Germany) was used to automate plate imaging. One mosaic was set up per well encompassing the entire area of the well, and imaged at 20x magnification using autofocus to find the focal plane in every field. Images were analyzed for  $\beta$  cell proliferation with Imaris 7.6 software (Bitplane; Zurich, Switzerland) using Surfaces and Spots functions to identify  $\beta$  cells by both cytoplasmic insulin or C-peptide and nuclear Pdx1, and proliferating cells by nuclear Ki67.  $\beta$  cell proliferation was reported as  $\beta$  proliferating  $\beta$  cells (insulin or C-peptide+Pdx1+). An average of 3500 total  $\beta$  cells (range 1000-16,100) were counted per donor for each treatment condition.

#### **Statistical Analysis**

Prism software (GraphPad, La Jolla, CA) was used to perform statistical analysis comparing two groups using unpaired t tests and one-way analysis of variance with Newman-Keuls multiple comparison test to compare three or more groups to evaluate outcomes in mice of different genotypes. Data were expressed as mean ± standard error of mean. Statistical analysis of RNA-sequencing data is described above (see RNA Isolation, Sequencing, and Analysis).

#### **CHAPTER III**

# ISLET MICROENVIRONMENT, MODULATED BY VASCULAR ENDOTHELIAL GROWTH FACTOR-A SIGNALING, PROMOTES β CELL REGENERATION

The text and data in this chapter have been published in Brissova, Aamodt, Brahmachary et al., 2014<sup>153</sup>

#### Introduction

Pancreatic islets are highly vascularized and contain a structurally and functionally unique capillary network where each  $\beta$  cell is in cellular proximity to endothelial cells (ECs)<sup>137,225</sup>. Endothelial cells produce instructive signals necessary for early pancreatic endoderm specification and endocrine cell differentiation<sup>138,144</sup>, but several recent studies proposed that requirements for blood vessel-derived signals may differ between early and later stages of pancreas development<sup>149-151</sup>. Vascular endothelial growth factor-A (VEGF-A) produced by islet endocrine cells is a principal regulator of islet vascular development and vascular homeostasis<sup>137,207</sup>. Inactivation of VEGF-A, either in endocrine progenitors or differentiated  $\beta$  cells, leads to a profound loss of intra-islet capillary density, vascular permeability and islet function. Though it is clear that altering islet microvasculature affects insulin delivery into peripheral circulation, the role of intra-islet endothelial cells and the VEGF-A signaling pathway in regulating adult  $\beta$  cell mass is not fully understood. Work by Lammert and colleagues suggests that continuous pancreas-wide overexpression of VEGF-A from early development to adulthood results in pancreatic hypervascularization,  $\beta$  cell mass expansion and islet hyperplasia<sup>138</sup>. However, a more recent report by Agudo et al. reveals that VEGF-A-stimulated intra-islet endothelial cell expansion in adult islets is associated with reduced  $\beta$  cell mass<sup>155</sup>.

 $\beta$  cells of the pancreatic islet have an extremely limited regenerative potential, so there are major efforts to foster  $\beta$  cell regeneration in type 1 and type 2 diabetes. Recent studies have identified several systemic factors and signaling pathways implicated in  $\beta$  cell replication during increased metabolic demand and following injury<sup>50,251</sup>, but the role of local islet molecular and cellular factors in  $\beta$  cell regeneration, and in particular human  $\beta$  cell regeneration, is unknown.

Increasing evidence suggests that local organ-specific vascular niches are determinant in organ repair and tumorigenesis where endothelial cells produce tissue-specific paracrine growth factors, defined as angiocrine factors<sup>252</sup>. VEGF-A signaling through its obligatory VEGFR2 receptor plays a critical role in this process. In addition to this emerging role for the VEGF-A signaling pathway in organ regeneration via angiocrine signaling, local increases in VEGF-A production during tissue injury and tumorigenesis leads to homing of bone marrow-derived cells (BMCs), especially monocytes which express the VEGFR1 receptor<sup>253</sup>. While these cells may enhance VEGF-induced neovascularization, they also actively participate in tissue repair.

To investigate how VEGF-A signaling modulates intra-islet vasculature, islet microenvironment, and  $\beta$  cell mass, we transiently increased  $\beta$  cell VEGF-A production in mature mouse islets ( $\beta$ VEGF-A model). This increased production of VEGF-A in  $\beta$  cells dramatically increases intra-islet endothelial cell

proliferation, but surprisingly leads to a rapid loss of  $\beta$  cells. Remarkably, 6 weeks after removing the VEGF-A stimulus, islet morphology, vascularization, mass, and function normalize due to replication of pre-existing  $\beta$  cells. Using an islet transplantation model with wild type (WT) and  $\beta$ VEGF-A islets transplanted under contralateral kidney capsules with or without human islets, we demonstrate that this  $\beta$  cell replication is independent of the pancreatic site and circulating factors, and not limited to murine  $\beta$  cells. Our studies indicate that the local islet microenvironment modulated by VEGF-A signaling can play an integral role in  $\beta$  cell regeneration. This process depends on VEGF-A-mediated recruitment of macrophages (M $\Phi$ s) which either directly, or cooperatively with quiescent intra-islet endothelial cells, induce  $\beta$  cell proliferation.

#### Results

# Increased $\beta$ cell VEGF-A production leads to islet endothelial cell expansion and $\beta$ cell loss followed by $\beta$ cell regeneration after VEGF-A normalizes

To dissect the role of the VEGF-A signaling pathway in regulating adult  $\beta$  cell mass, we used a mouse model of doxycycline (Dox)-inducible  $\beta$  cell-specific overexpression of human VEGF-A<sub>165</sub> ( $\beta$ VEGF-A)<sup>223,226</sup>. Islet VEGF-A production increased rapidly within 24 hours of Dox treatment (Figure 12) and robust proliferation of intra-islet endothelial cells was observed 72 hours after VEGF-A induction (Figure 12B). We found that a transient increase in  $\beta$  cell VEGF-A production for 1 week dramatically increased the number of intra-islet endothelial cells and led to a substantial loss of  $\beta$  cells (Figures 13A-B). One week after Dox withdrawal, VEGF-A expression returned to baseline (Figure 13C), and remarkably, islet morphology and vascularization normalized over 6 weeks after removal of the VEGF-A stimulus (Figures 13D-F and 14). The inverse relationship between  $\beta$  cells and intra-islet endothelial cells during the induction and withdrawal of the VEGF-A stimulus is shown in Figures 13G and 13H.

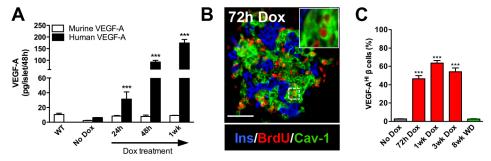


Figure 12. VEGF-A expression and endothelial cell proliferation in βVEGF-A mice after induction and withdrawal of the VEGF-A stimulus. (A) Islet VEGF-A levels increase rapidly after doxycycline (Dox) administration. Levels of murine and human VEGF-A were measured in culture supernatants from isolated WT and βVEGF-A islets prior to and after Dox administration. \*\*\*, p<0.001, human VEGF-A in βVEGF-A islets at 24h Dox, 48h Dox, and 1wk Dox compared with murine VEGF-A in WT and βVEGF-A islets at No Dox, 24h Dox, 48h Dox, and 1wk Dox. (B) Intra-islet endothelial cells (ECs) undergo extensive proliferation. After 72-hour Dox and BrdU administration, βVEGF-A cryosections were labeled with antibodies to insulin (Ins, blue), BrdU (red), and EC marker caveolin-1 (Cav-1, green). Scale bar in panel B represents 50 μm. Inset shows proliferating endothelial cells in the area denoted by the dashed box. (C) Assessment of β cells with induced VEGF-A<sup>HI</sup> expression. \*\*\*, p<0.001; n=3 mice/time point.

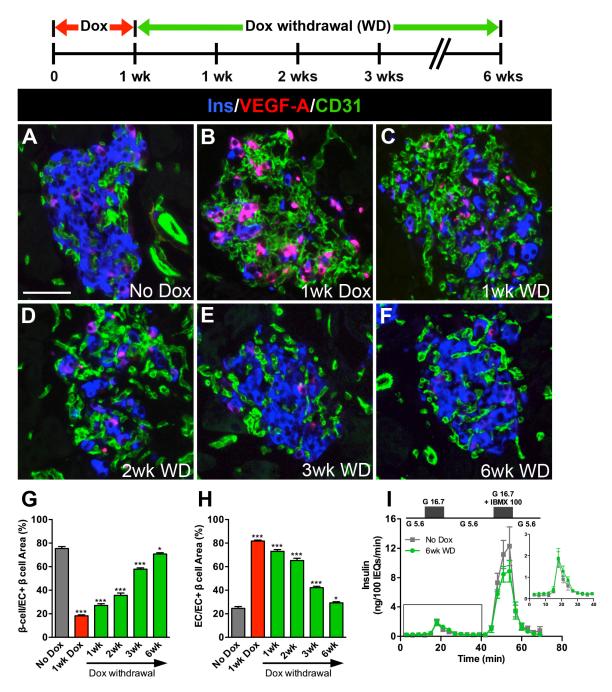


Figure 13. Increasing β cell VEGF-A production increases intra-islet endothelial cells but leads to β cell loss followed by β cell regeneration after withdrawal of the VEGF-A stimulus. VEGF-A was induced for 1 week by Dox administration followed by 6 weeks of Dox withdrawal (WD). (A-F) Labeling for insulin (Ins, blue), VEGF-A (red), and endothelial cell (EC) marker CD31 (green). Scale bar is 50 μm and applies to A-F. (G, H) Relationship between β cells (G) and intra-islet endothelial cells (H) upon induction and withdrawal of the VEGF-A stimulus. \*\*\*, p<0.001, 1wk Dox, 1wk WD, 2wk WD, or 3wk WD vs. No Dox control; \*, p<0.05, 6wk WD vs. No Dox control; n=4 mice/time point. Islet size measured by pixel area increased slightly but not significantly with intra-islet endothelial cell expansion; No Dox, 6545±1687 pixels; 1wk Dox, 10705±1712 pixels, p=0.1939. (I) Islets isolated from No Dox controls and at 6wk WD (n=4 mice/group) were examined in a cell perifusion system. Both groups had normal basal insulin secretion at 5.6 mM glucose (G 5.6) and the magnitude of the insulin secretory response was similar when stimulated with either 16.7 mM glucose (G 16.7; 9.6±2.1 vs. 11.3±2.5 ng/100 IEQ, p=0.63) or 16.7 mM glucose + 100 μM IBMX (G 16.7 + IBMX 100; 111±22 vs. 84±13 ng/100 IEQ, p=0.34). Inset shows enlarged boxed portion of insulin secretory profile.

Six weeks after Dox withdrawal, the regenerated BVEGF-A islets were functionally indistinguishable from No Dox controls (Figure 13I). βVEGF-A mice maintained normal glucose clearance, random blood glucose levels, and body weight during the brief 1-week Dox treatment and subsequent 6-week period of Dox withdrawal (Figures 15A-B and 15E-F). This was expected, since 1-week Dox treatment resulted in a partial (approximately 45%) β cell loss, as indicated by total pancreatic insulin content (Figure 15C) and β cell mass measurements (Figure 15D)<sup>254</sup>. This β cell loss occurred through upregulation of the apoptotic pathway (Figure 16) with an increased number of β cells positive for gamma-phosphorylated histone H2AX (pH2AX), an apoptotic marker of double-stranded DNA breaks, 1 week

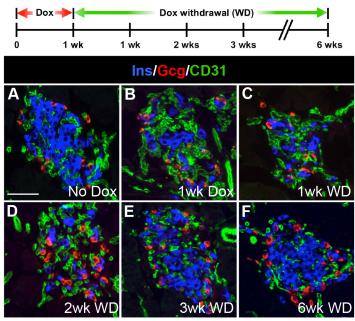


Figure 14. Maintenance of  $\alpha$  cells in  $\beta$ VEGF-A mice after induction and withdrawal of the VEGF-A stimulus. VEGF-A was induced for 1 week by Dox administration followed by 6 weeks of Dox withdrawal (WD). (A-F) Labeling for insulin (Ins, blue), glucagon (Gcg, red), and endothelial cell (EC) marker CD31 (green). Scale bar in panel A represents 50  $\mu$ m and applies to A-F.

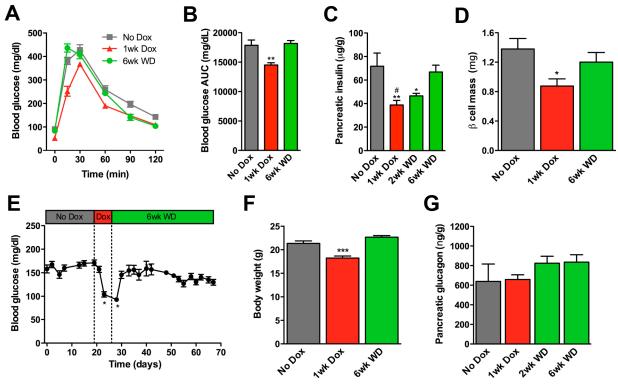


Figure 15. Characterization of glucose homeostasis, body weight, pancreatic hormone content, and β cell mass in βVEGF-A mice after induction and withdrawal of the VEGF-A stimulus. VEGF-A was induced for 1 week by Dox administration followed by 6 weeks of Dox withdrawal (WD). (A, B) Glucose clearance in βVEGF-A mice.

\*\*\*, p<0.01, 1wk Dox (n=10) vs. No Dox (n=14) or 6wk WD (n=5). (C) Loss in pancreatic insulin content 1 week after VEGF-A induction was restored over the 6 weeks following Dox withdrawal. \*\*\*, p<0.01, 1wk Dox vs. No Dox; \*, p<0.05, 2wk WD vs. No Dox; #, p<0.05, 1wk Dox vs. 6wk WD; No Dox vs. 6wk WD was not statistically significant; n=6-7 mice/time point. (D) Pancreatic β cell mass; n=4 mice/time point; \*, p<0.05, No Dox vs. 1wk Dox. (E) Random blood glucose levels; \*, p<0.05 compared with other time points. (F) Body weight measurements; \*\*\*\*, p<0.001, 1wk Dox vs. No Dox or 6wk WD. (G) Pancreatic glucagon content, p=0.3462; n=5-6 mice/time point.

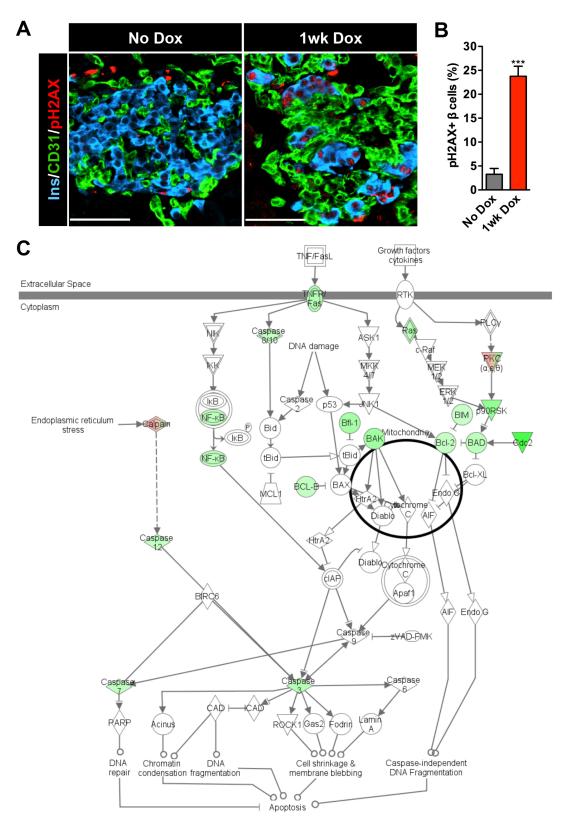


Figure 16. Transient expansion of intra-islet endothelial cells leads to increased β cell apoptosis. (A, B) Apoptosis in βVEGF-A islets was examined 1 week after VEGF-A induction using a marker of DNA double-stranded breaks, gamma-phosphorylated histone H2AX (pH2AX) $^{256-258}$ . β cells with nuclear pH2AX labeling were readily detectable after 1 week Dox, while pH2AX+ β cells were rare prior to VEGF-A induction. Scale bars in A represent 50 μm; n=4 mice/time point; 100-500 β cells analyzed/mouse. \*\*\*, p<0.001, 1wk Dox vs. No Dox. (C) Transcriptome analysis of whole βVEGF-A islets showed increased expression of multiple components of the apoptosis signaling pathway at 1wk Dox compared to No Dox with fold changes ≥2 (green). See Chapter 2 Materials and Methods and Figure 33 for transcriptome analysis details.

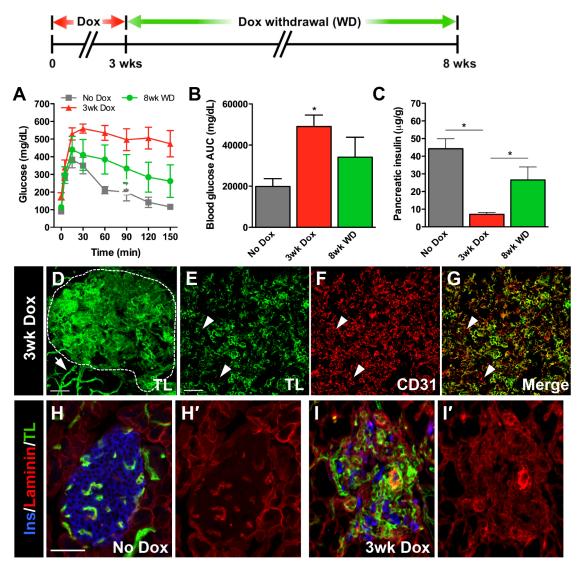
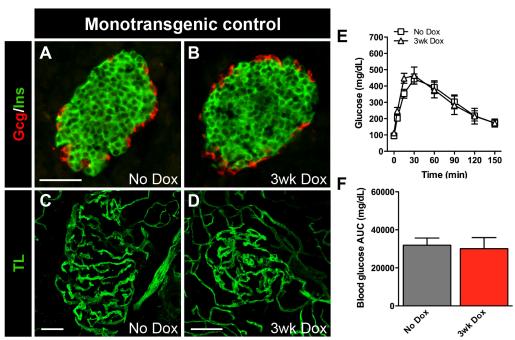


Figure 17. Prolonged VEGF-A induction exacerbates the phenotype of βVEGF-A mice. VEGF-A was induced for 3 weeks by Dox administration followed by 8 weeks of Dox withdrawal (WD). (A, B) Glucose tolerance test in βVEGF-A mice at No Dox (n=7), 3wk Dox (n=7), and 8wk WD (n=6) time points; \*, p<0.05, 3wk Dox vs. No Dox or 8wk WD. (C) Loss in pancreatic insulin content 3 weeks after VEGF-A induction was nearly restored over 8 weeks following Dox withdrawal. \*, p<0.05; \*\*, p<0.01; n=3 mice/time point. (D-G) Blood vessels in βVEGF-A islets remain functional after prolonged βVEGF-A induction. Pancreatic vasculature in βVEGF-A mice was assessed by intravital infusion of endotheliumbinding lectin-FITC (TL, green) after a 3-week Dox treatment. (D) Sixty-um thick pancreatic sections were optically sectioned and 3-D reconstructed. Islet is within the area marked by the dashed line. Arrow points to normal blood vessels in the adjacent exocrine tissue. Scale bar in panel D represents 50 μm. (E-G) Ten-μm thick sections of pancreatic tissue labeled intravitally with lectin-FITC (TL, green) were subsequently co-labeled with endothelial cell marker CD31 (red). Arrowheads point to CD31+ and TL- endothelial cell structures. Scale bar in panel E represents 50 µm and applies to E-G. (H, I) Capillaries in βVEGF-A islets were assessed at No Dox and 3wk Dox for the basement membrane component laminin; insulin (Ins, blue), laminin (red), and endothelium-binding lectin-FITC (TL, green). Panels H' and I' show laminin labeling alone. Scale bar in panel H represents 50 µm and applies to I.

after Dox (Figures 16A-B)<sup>255,256</sup>. Pancreatic glucagon was unchanged 1 week after Dox and during the 6-week period of Dox withdrawal (Figure 15G). The phenotype of βVEGF-A islets was exacerbated with prolonged VEGF-A induction (Figure 17). Dox treatment for 3 weeks in βVEGF-A mice led to glucose intolerance, increased fasting glucose levels, and an 80% reduction in total pancreatic insulin content, with approximately 60% recovery 8 weeks after Dox withdrawal (Figures 17A-C). Prolonged Dox administration (3 weeks) alone was not detrimental to glucose homeostasis, islet or endothelial cell morphology (Figure 18).

Dox treatment for 1 up to 3 weeks resulted in VEGF-A overexpression in approximately 65% of  $\beta$  cells (Figures 12C and 13B). We did note a very slight elevation in basal VEGF-A expression in  $\beta$ VEGF-A mice (Figures 12A and 13A), which caused a modest increase in endothelial cells adjacent to  $\beta$  cells with elevated VEGF-A expression (2-5%  $\beta$  cells). However, glucose clearance in  $\beta$ VEGF-A mice before Dox administration was identical to both monotransgenic and WT mice (Figures 15A-B, 17A-B, 18E-F and data not shown). Although islet vasculature became greatly disorganized with prolonged VEGF-A induction, blood vessels in adjacent exocrine tissue remained normal (Figure 17D-G), which is consistent with the short-range effect of heparin-bound VEGF-A<sub>165</sub> observed in other vascular beds<sup>259</sup>. Intravital labeling with endothelium-binding lectin-FITC revealed that even after 3 weeks of persistent VEGF-A overexpression, the majority of intra-islet capillaries were still perfused and functional (Figures 17D-G) and lined by a thin layer of laminin+ vascular basement membrane (Figures 17H-I). We conducted the remainder of our studies on  $\beta$  cell loss and regeneration using a 1-week Dox administration and 6-week Dox withdrawal paradigm to avoid any influence of hyperglycemia.



**Figure 18.** Dox has no effect on monotransgenic controls. Mice were treated with Dox for 3 weeks. (A, B) Cryosections from monotransgenic TetO-VEGF mice at No Dox and 3wk Dox were labeled with antibodies to insulin (Ins, green) and glucagon (Gcg, red). Scale bar in panel A represents 50 µm and also applies to B. (C, D) Pancreatic vasculature in TetO-VEGF islets was assessed by intravital infusion of endothelium-binding lectin-FITC (TL, green) at No Dox and 3wk Dox. Scale bars in C and D represent 50 µm. (E, F) Monotransgenic TetO-VEGF mice treated with Dox for 3 weeks maintained normal glucose clearance and fasting glucose levels.

#### Withdrawal of the VEGF-A stimulus results in increased proliferation of pre-existing $\beta$ cells

To define the time course of  $\beta$  cell regeneration in this model, we followed  $\beta$  cell proliferation in the  $\beta$ VEGF-A pancreas during the course of induction and withdrawal of the VEGF-A stimulus. One week after Dox treatment, intra-islet endothelial cells were highly proliferative, while  $\beta$  cell proliferation decreased below basal level (Figures 19A-B and 19G). This Ki67 labeling pattern was reversed 1 week after Dox withdrawal when endothelial cells begin to subside and  $\beta$  cells proliferate (Figures 19C and 19G). The burst in  $\beta$  cell proliferation was transient and peaked within 2 weeks after Dox withdrawal (Figures 19D-G). The same temporal profile of  $\beta$  cell replication was seen using BrdU (Figure 19H). Additionally, during 1-week Dox and 6-week recovery phases, the expression pattern of transcription factor Pdx1, known to be expressed in progenitor cells of the developing pancreas, did not differ from the No Dox control (Figure 20A), monotransgenic, or WT mice (data not shown). The number of  $\beta$  cells expressing the maturation marker MafA decreased at 1 week Dox, but gradually recovered during 6 weeks of Dox withdrawal (Figures 20B-C).

Previous reports indicated that  $\beta$  cell proliferation in the regenerative phase after STZ-mediated injury is dependent on re-expression of polycomb group proteins Bmi-1 and Ezh2 that modify chromatin structure at the *Ink4a/Arf* locus and control  $\beta$  cell growth<sup>260,261</sup>. To determine if a similar mechanism was responsible for  $\beta$  cell proliferation in  $\beta$ VEGF-A islets, we labeled pancreatic sections for Bmi-1 (Figures 20D-G). Although nearly all  $\beta$  cells were Bmi-1+ in No Dox controls at postnatal day 21 (Figure 20D), we did not detect Bmi-1 in  $\beta$  cells of adult  $\beta$ VEGF-A mice 1 or 2 weeks after Dox withdrawal when  $\beta$  cell proliferation reached a maximum (Figures 20F-G). This data suggests that the mechanism of  $\beta$  cell proliferation in regenerating  $\beta$ VEGF-A islets differs from the STZ injury model.

To further examine the cellular origin of regenerating  $\beta$  cells in this model, we utilized genetic lineage tracing by introducing Pdx1<sup>PB</sup>-CreER<sup>Tm</sup> and R26R<sup>IacZ</sup> components into the  $\beta$ VEGF-A system.  $\beta$  cells were genetically labeled with a  $\beta$ -galactosidase ( $\beta$ -gal) reporter using 3 x 1mg tamoxifen (Tm) prior to the onset of Dox treatment. We showed previously that this Tm dose effectively induces Cre-loxP recombination in 30% of  $\beta$  cells without undesirable long-lasting residual recombination effects following Tm administration<sup>238</sup>. A similar  $\beta$  cell recombination rate was achieved when the Pdx1<sup>PB</sup>-CreER<sup>Tm</sup>;R26R<sup>IacZ</sup> lineage tracing system was incorporated into the  $\beta$ VEGF-A background and was sustained after induction and withdrawal of the VEGF-A stimulus (Figures 21A-E). As previously reported,  $\beta$ -gal+lns- cells were very rare using the Pdx1<sup>PB</sup>-CreER<sup>Tm</sup> transgenic line (<1-3% islet non- $\beta$  cells)<sup>227,238</sup>. Consistent with the  $\beta$  cell recombination rate, approximately 30% of Ki67+  $\beta$  cells carried the  $\beta$ -gal reporter 2 weeks after Dox withdrawal (Figures 21F-G). Maintaining this steady proportion of  $\beta$ -gal+  $\beta$  cells throughout the time course indicates that new  $\beta$  cells in  $\beta$ VEGF-A mice arise by replication from pre-existing  $\beta$  cells and that the loss of insulin+ cells 1 week after Dox (Figures 13B and 21B) is the result of  $\beta$  cell death and not the loss of insulin labeling or  $\beta$  cell dedifferentiation.

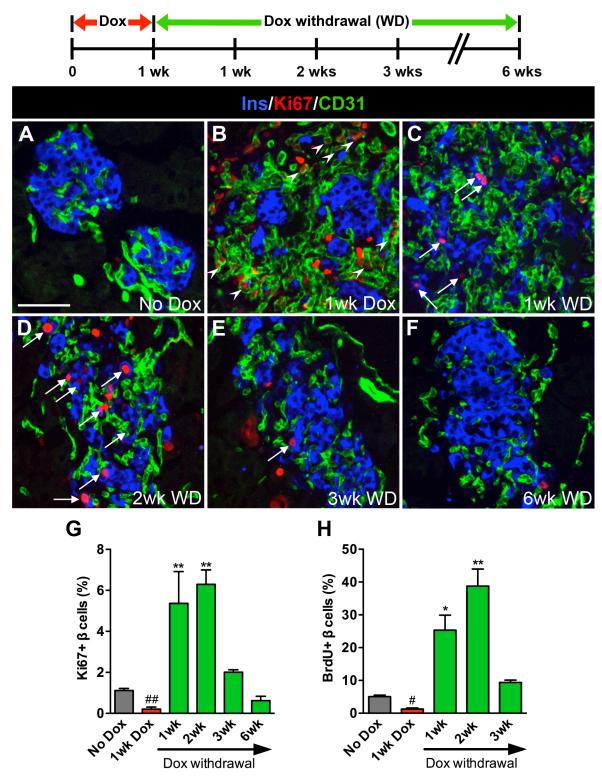


Figure 19. Removal of the VEGF-A stimulus results in a transient burst in β cell proliferation. (A-G) β cell proliferation was monitored during the experimental period outlined; n=4 mice/time point. (A-F) Labeling for insulin (Ins, blue), Ki67 (red), and CD31 (green). Scale bar is 50 μm and applies to A-F. (G) Quantification of β cell proliferation. ##, p<0.01, 1wk Dox vs. No Dox, 1wk WD, 2wk WD, or 3wk WD. \*\*, p<0.01, 1wk WD or 2wk WD vs. No Dox, 1wk Dox, 3wk WD, or 6wk WD. No Dox, 1wk Dox, 3wk WD, and 6wk WD comparisons were not statistically significant. (H) BrdU was administered in drinking water for 1 week prior to tissue collection. β cell proliferation was assessed in pancreatic cryosections using double immunolabeling with antibodies to insulin and BrdU; n=2 mice/time point. \*, p<0.05, 1wk WD vs. No Dox, 1wk Dox, or 3wk WD. \*\*, p<0.01, 2wk WD vs. No Dox, 1wk Dox, or 3wk WD.

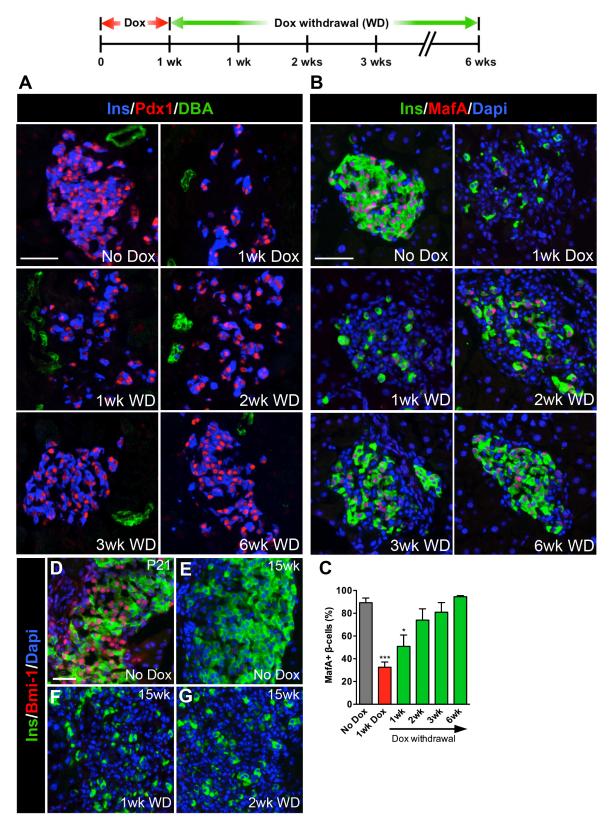


Figure 20. Expression of Pdx1, MafA, and Bmi-1 in βVEGF-A pancreases following induction and withdrawal of the VEGF-A stimulus. VEGF-A was induced for 1 week by Dox administration followed by 6 weeks of Dox withdrawal (WD). (A) Pancreatic sections from βVEGF-A mice were labeled with antibodies to insulin (Ins, blue), Pdx1 (red), and ductal marker DBA (green). (B) Pancreatic sections from βVEGF-A mice were labeled with antibodies to insulin (Ins, green), MafA (red), and counterstained with Dapi (blue). Scale bars in panels A and B represent 50 μm. (C) Quantification of MafA expression; \*\*\*, p<0.001, 1wk Dox vs. No Dox, 2wk WD, 3wk WD, or 6wk WD. \*, p<0.05, 1wk WD vs. No Dox, 2wk WD, 3wk WD, or 6wk WD. (D-G) Increased β cell proliferation in βVEGF-A mice was not associated with increased Bmi-1; insulin (Ins, green), Bmi-1 (red), Dapi (blue). Scale bar is 25 μm and applies to D-G.

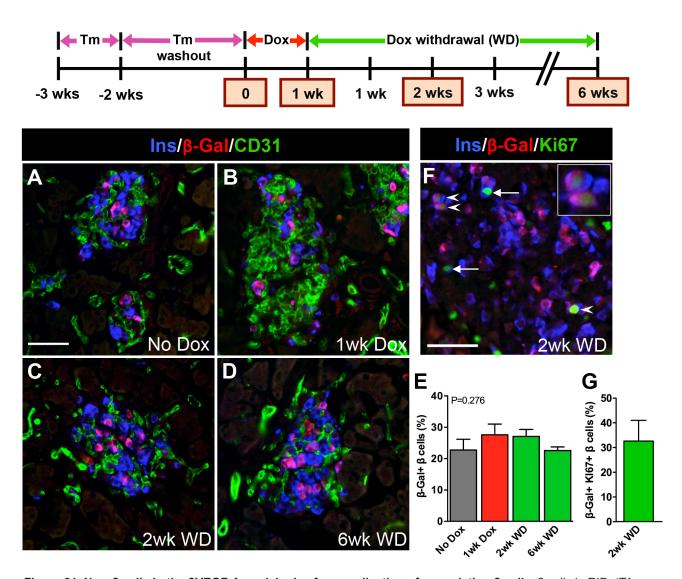
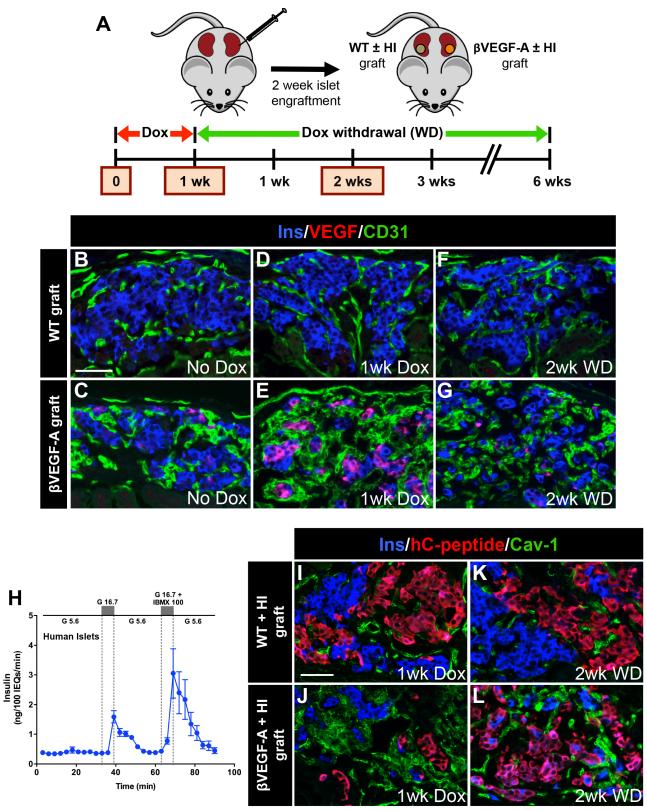


Figure 21. New β cells in the βVEGF-A model arise from replication of pre-existing β cells. β cells in RIP-rtTA; TetO-VEGF;Pdx1<sup>PB</sup>-CreER<sup>Tm</sup>;R26R<sup>wt/lacZ</sup> transgenic mice were genetically labeled by Tm injection 2 weeks prior to inducing VEGF-A for 1 week by Dox administration followed by 6 weeks of Dox withdrawal. Expression of β-gal in β cells was analyzed in 3-4 mice/time point. (A-D) Labeling for insulin (Ins, blue), β-galactosidase (β-Gal, red), and CD31 (green). Scale bar is 50 μm and applies to A-D. (E) β-Gal labeling index in β cells was not statistically different at any time point, p=0.2760. (F) Genetically labeled β cells proliferate. Arrowheads denote β-gal+Ki67+ β cells, progeny of surviving and proliferating β cells (enlargement in inset). Arrows point to β-gal-Ki67+ β cells. Scale bar is 50 μm. (G) One-third of all proliferation β cells expressed the β-gal genetic mark, which is consistent with genetic labeling in panel E. The β cell proliferation index at 2wk WD was 6.1±1.0%, consistent with Figure 19G.

# $\beta$ cell replication after VEGF-A normalization is independent of the pancreatic site and soluble circulating factors and is not limited to murine $\beta$ cells

We next sought to determine whether β cell proliferation in regenerating βVEGF-A islets required the pancreatic location and/or was dependent on soluble circulating factor(s). We also wanted to know whether the factor(s) responsible for this murine β cell proliferation were capable of inducing proliferation in human β cells. To address these questions we used an islet transplantation model where handpicked WT and βVEGF-A islets were transplanted beneath contralateral kidney capsules of βVEGF-A mice or alternatively, mixtures with equal amounts of human and WT or βVEGF-A islets were transplanted beneath contralateral kidney capsules of immunodeficient NOD-scid-IL2ry<sup>null</sup> mice (Figure 22A). All human islets (HI) used in these experiments demonstrated a robust insulin secretory response to glucose and this response was further augmented by cAMP potentiation (Figure 22H)<sup>262</sup>. Transplanted islets were allowed to engraft for 2 weeks and then the tissues were analyzed at baseline without Dox, 1 week after Dox treatment, and 2 weeks after Dox withdrawal (Figure 22A). After 1 week of Dox treatment VEGF-A was induced as effectively in βVEGF-A islet grafts (Figure 22E and 22J) as in native βVEGF-A islets (Figure 13B), with both showing an extensive increase in endothelial cell mass and β cell loss (Figures 13B, 22E and 22J). We noted that 1 week after VEGF-A induction, endothelial cells were assembled into multiple layers (Figures 13B, 22E and 22J). This was followed by a gradual rearrangement in endothelial and islet cells as endothelial cells transitioned to a more single-layered organization 2 weeks after Dox withdrawal (Figures 13D, 22G and 22L). Similar changes in graft morphology were observed in βVEGF-A grafts both with and without human islets (Figures 22E, 22G, 22J and 22L). Increased VEGF-A production in βVEGF-A islet grafts and native βVEGF-A islets had no effect on the vascularization of WT islet grafts in contralateral kidneys (Figures 22D, 22F, 22I and 22K), or the kidney cortex adjacent to βVEGF-A islet grafts (data not shown), pointing again to the localized effect of VEGF-A<sub>165</sub>.

We next measured  $\beta$  cell proliferation in WT and  $\beta$ VEGF-A islet grafts at No Dox, 1 week after Dox treatment, and 2 weeks after Dox withdrawal (Figures 23A-C) when  $\beta$  cell proliferation was maximal in native  $\beta$ VEGF-A islets (Figure 19G). As expected,  $\beta$  cell proliferation was similar in WT and  $\beta$ VEGF-A islet grafts at No Dox and 1 week after Dox treatment (Figure 23C). This low proliferation continued in WT islet grafts 2 weeks after Dox withdrawal (1.3±0.2%), but the  $\beta$  cell replication index in  $\beta$ VEGF-A islet grafts increased approximately 4 fold (4.20.8%) and was comparable to that in native  $\beta$ VEGF-A islets (6.2±0.7%). Similarly, 2 weeks after Dox withdrawal, the proliferation of human  $\beta$  cells in  $\beta$ VEGF-A+HI grafts was 3 fold higher (0.95±0.18%) than in WT+HI grafts (0.35±0.07%) (Figures 23D-F). Collectively, these data indicate that  $\beta$  cell replication in regenerating  $\beta$ VEGF-A islets is modulated by the local microenvironment independently of the pancreatic site and systemic soluble factors. Furthermore, the factor(s) responsible for  $\beta$  cell proliferation in  $\beta$ VEGF-A islets also promote significant proliferation of human  $\beta$  cells.



**Figure 22. Morphology of βVEGF-A islet grafts.** (A) Islets from βVEGF-A mice and WT controls were transplanted into  $\beta$ VEGF-A recipients or mixed with human islets (HI) and transplanted into  $\beta$ VEGF-A mice. Islets were allowed to engraft for 2 weeks then grafts were harvested and analyzed at No Dox, 1wk Dox, and 2wk WD time points; n=3-4 mice/time point (B-G) Cryosections from WT and  $\beta$ VEGF-A grafts were labeled with antibodies to insulin (Ins, blue), VEGF-A (red) and endothelial cell (EC) marker CD31 (green). Scale bar in panel B is 50 μm and also applies to C-G. (H) Human islets (HI) used in grafts have a robust glucose stimulated insulin secretory response; n=3 donors. (I-L) Cryosections from WT+HI and  $\beta$ VEGF-A+HI grafts were labeled with antibodies to insulin (Ins, blue), human C-peptide (hC-peptide, red) and EC marker caveolin-1 (Cav-1, green). Human  $\beta$  cells co-label with Ins and hC-peptide (purple). Scale bar in panel I is 50 μm and also applies to J-L.

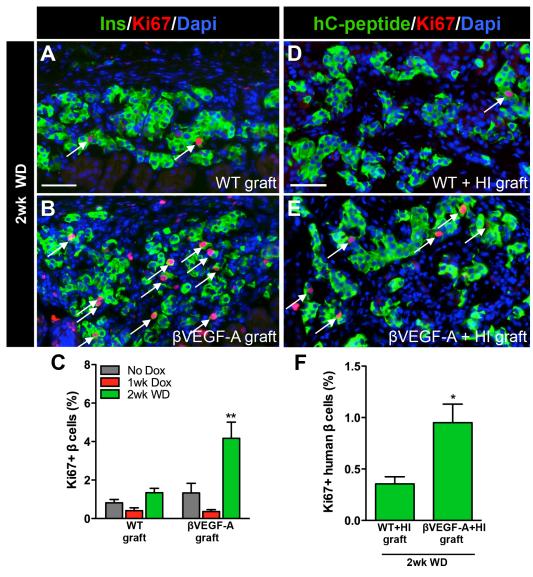


Figure 23. β cell replication is independent of the pancreatic site and soluble circulating factors and is not limited to murine β cells. Islets from βVEGF-A mice and WT controls were transplanted into βVEGF-A recipients or mixed with human islets (HI) and transplanted into NOD-scid- $IL2r\gamma^{null}$  mice. Islets engrafted for 2 weeks then grafts were harvested and analyzed at No Dox, 1wk Dox, and 2wk WD time points; n=3-4 mice/time point. (A-B) β cell proliferation at 2wk WD in WT and βVEGF-A islet grafts; insulin (Ins, green), Ki67 (red), and Dapi (blue). Scale bar is 50 μm and applies to A-B. (C) Quantification of β cell proliferation in WT and βVEGF-A islet grafts. \*\*, p<0.01, 2wk WD vs. No Dox and 1wk Dox across graft types. (D-E) β cell proliferation at 2wk WD in WT+HI and βVEGF-A+HI grafts; human C-peptide (hC-peptide, green), Ki67 (red), and Dapi (blue). Scale bar is 50 μm and applies to D-E. (F) Quantification of β cell proliferation in WT+HI and βVEGF-A+HI grafts at 2wk WD. \*, p<0.05.

#### Recruited macrophages are crucial for the $\beta$ cell proliferative response in $\beta$ VEGF-A islets

Since VEGF-A is known to stimulate the migration of circulating monocytes  $^{253}$ , and  $\beta$  cell proliferation was modulated by the local microenvironment created by increased VEGF-A expression, we sought to determine whether circulating monocytes homed to  $\beta$ VEGF-A islets upon VEGF-A induction and contributed to the  $\beta$  cell proliferative response.

βVEGF-A mice were transplanted with GFP-labeled bone marrow. After bone marrow reconstitution, VEGF-A induction stimulated a marked infiltration of BMCs to the site of β cell injury, and they persisted in islet remnants during the β cell regeneration phase (2 weeks after Dox withdrawal) (Figures 24A-D). Although GFP+ recruited BMCs were adjacent to β cells and endothelial cells, we did not detect any GFP+Ins+ cells or GFP+CD31+ cells. Occasional GFP+ cells were noted around βVEGF-A islets at No Dox (Figures 24A and 24E), but 1 week VEGF-A induction increased their infiltration nearly 6 fold (Figure 24D). This high level of BMC infiltration into βVEGF-A islets was sustained even 2 weeks after withdrawing the VEGF-A stimulus (Figure 24D), the time point when β cell proliferation is at a maximum. Nearly all GFP+ recruited BMCs expressed the pan-hematopoietic marker CD45 (Figures 24E-G), and BMC infiltration monitored by CD45 labeling was consistent in mice with or without bone marrow transplantation (data not shown), indicating that the bone marrow transplantation alone did not enhance the incidence of recruited BMCs in the pancreas and islets. This finding allowed us to use CD45 as a surrogate marker to follow the BMC infiltration.

Flow cytometry analysis of cells from βVEGF-A islets dispersed after 1 week VEGF-A induction revealed that the vast majority (90%) of CD45+ recruited BMCs are CD11b+Gr1- macrophages (Figure 25A). As monocytes develop into mature macrophages, they lose Gr1 expression and increase expression of mature macrophage markers CD11b and F4/80<sup>263</sup>. This maturation process is evident in the CD45+ BMC population recruited to βVEGF-A islets where only a few less-mature macrophages (CD11b+LO) express F4/80 (3%), while more-mature macrophages (CD11b+HO) are much more likely to express F4/80 (60%) (Figure 3.14B). Labeling tissue sections from mice that received GFP bone marrow transplants with F4/80 confirmed that nearly all GFP+ recruited BMCs in βVEGF-A islets were macrophages (Figures 26A-C). GFP+ cells expressing the T cell marker CD3 or the B cell marker B220 were very rare (Figures 26D-I), and chloroacetate esterase staining demonstrated that VEGF-A induction does not lead to neutrophil accumulation (Figures 26J-K).

Together, these data indicate that upon VEGF-A induction, circulating monocytes migrate to  $\beta$ VEGF-A islets and differentiate into a mature population of recruited macrophages that remain in the islets 2 weeks after the VEGF-A stimulus is withdrawn. In contrast, CD45+ cells were extremely rare in islet remnants after STZ-mediated  $\beta$  cell ablation, and  $\beta$  cell recovery was limited, as indicated by persistent hyperglycemia 6 weeks after STZ treatment (Figure 27).

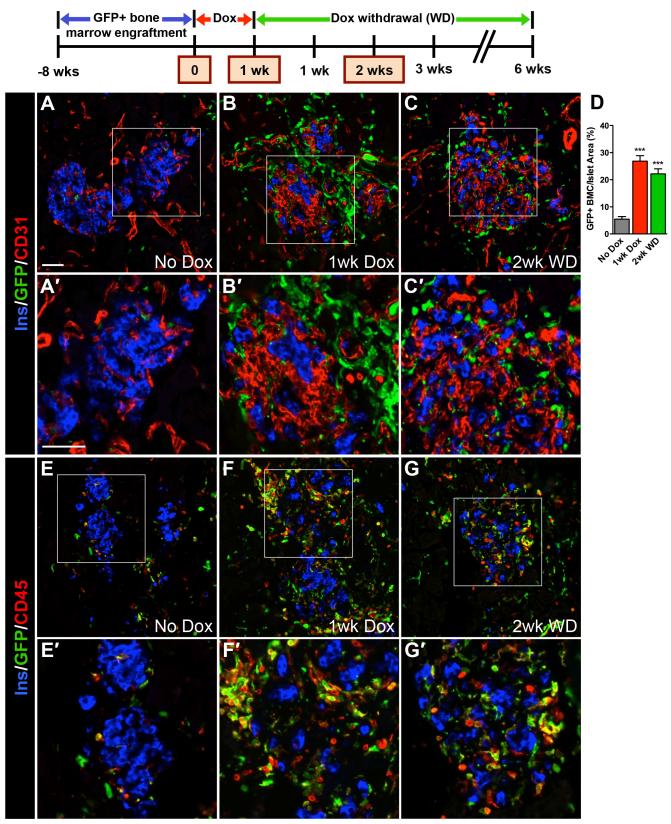
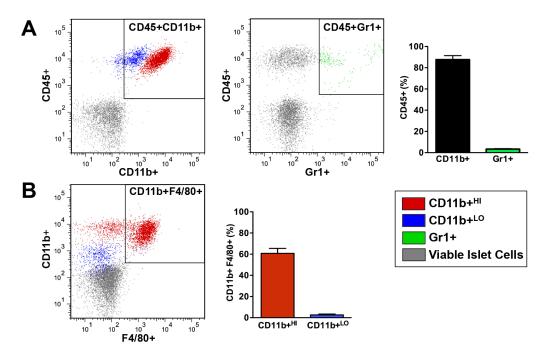


Figure 24. CD45+ bone marrow-derived cells are recruited to the site of  $\beta$  cell injury upon VEGF-A induction and persist in islet remnants during  $\beta$  cell regeneration.  $\beta$ VEGF-A mice were transplanted with GFP+ bone marrow, and 8 weeks later VEGF-A was induced for 1 week by Dox administration followed by 2 weeks of Dox withdrawal; n=4-6 mice/ time point. (A-C) Labeling for insulin (Ins, blue), CD31 (red) and GFP (green). (D) Quantification of BMC infiltration into  $\beta$ VEGF-A islets at No Dox, 1wk Dox, and 2wk WD time points. \*\*\*, p<0.001, 1wk Dox and 2wk WD vs. No Dox. (E-G) Labeling for insulin (Ins, blue), pan-hematopoietic marker CD45 (red) and GFP (green). Boxes in A-C and E-G denote enlargements in A'-C' and E'-G'. Scale bar in A is 50 µm and applies to A-C and E-G. Scale bar in A' is 50 µm and applies to A'-C' and E'-G'.



**Figure 25. Macrophages are recruited to βVEGF-A islets upon VEGF-A induction.** (A-B) Flow cytometry analysis of βVEGF-A islets after a 1-week Dox treatment. (A) The CD45+ bone marrow-derived cell (BMC) population recruited to βVEGF-A islets was composed of 90% CD11b+ macrophages (MΦs) and 3% Gr1+ cells. (B) F4/80 expression in subsets of more mature CD11b+ $^{\text{HI}}$  (60%) and less mature CD11b+ $^{\text{LO}}$  (3%) macrophages; n=5 islet preparations (1-2 mice/preparation).

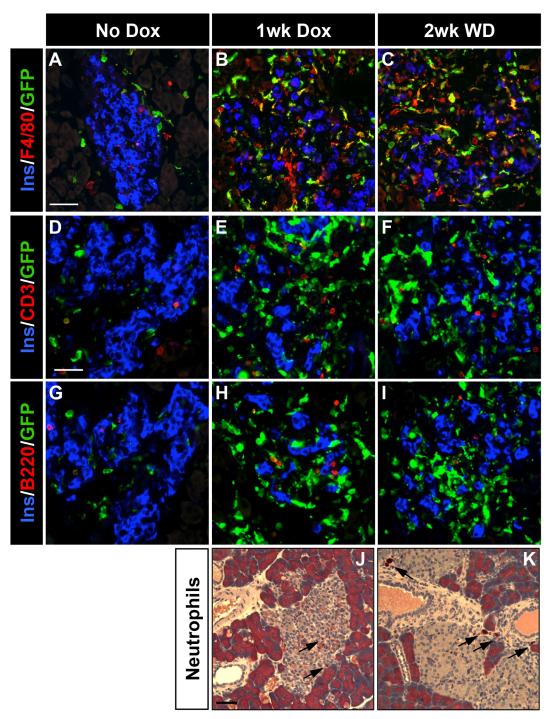


Figure 26. Recruited macrophages infiltrate  $\beta$ VEGF-A islets upon VEGF-A induction, while T cells, B cells, and neutrophils are rare in the infiltrating bone marrow-derived cell population.  $\beta$ VEGF-A mice were transplanted with GFP+ bone marrow and 8 weeks after bone marrow engraftment VEGF-A was induced transiently by 1-week Dox administration followed by 2 weeks of Dox withdrawal; n=3-4 mice/time point. Pancreatic cryosections from  $\beta$ VEGF-A mice transplanted with GFP+ bone marrow were analyzed for (A-C) Macrophages (M $\Phi$ s) with antibodies to insulin (Ins, blue), M $\Phi$  marker F4/80 (red) and GFP (green); (D-F) T cells with antibodies to insulin (Ins, blue), T cell marker CD3 (red) and GFP (green); and (G-I) B cells with antibodies to insulin (Ins, blue), B cell marker B220 (red) and GFP (green). Scale bar in A is 50  $\mu$ m and applies to A-C and scale bar in panel D represents 50  $\mu$ m and applies to panels D-I. (J, K) Paraffin-embedded pancreatic sections from  $\beta$ VEGF mice at 1wk Dox (J) and 2wk WD (K) were analyzed for neutrophils by staining for chloroacetate esterase. Scale bar in panel J represents 50  $\mu$ m and also applies to panel K.

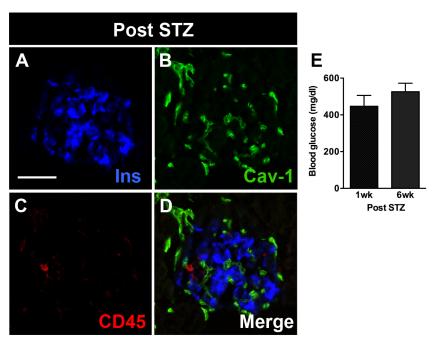


Figure 27. Low incidence of CD45+ cells and limited recovery of  $\beta$  cells after STZ-mediated  $\beta$  cell ablation. (A-D) Cryosections from mice 2 weeks after STZ treatment were labeled with antibodies to insulin (Ins, blue), endothelial cell (EC) marker caveolin-1 (Cav-1, green), and pan-hematopoietic marker CD45 (red). Scale bar in panel A represents 50  $\mu m$  and also applies to panels B-D. (E) Glucose levels in STZ-treated mice; n=3 mice/time point.

The pattern of CD45 labeling in  $\beta$ VEGF-A islet grafts was similar to native  $\beta$ VEGF-A islets. VEGF-A induction led to the infiltration of CD45+ cells into  $\beta$ VEGF-A islet grafts and they persisted within the grafts 2 weeks after VEGF-A stimulus withdrawal, while the population of CD3+ and B220+ cells remained extremely low (Figure 28 and data not shown). The incidence of CD45+ cells within WT islet grafts remained low at all three time points with the rare presence of T and B cells (Figure 29 and data not shown). Some CD45+ cells were detected around the periphery of islet grafts regardless of the islet genotype and VEGF-A induction, which could be due to the islet transplantation procedure and engraftment process being incompletely resolved. Also, VEGF-A production is increased in isolated islets as a result of hypoxia<sup>264</sup>, which alone could stimulate some recruitment of CD45+ cells even in WT islet grafts. Importantly, the infiltration of CD45+ cells was consistently observed only in  $\beta$ VEGF-A islets and  $\beta$ VEGF-A islet grafts after VEGF-A induction (Figures 24, 28, and 29). Similar to native  $\beta$ VEGF-A islets, the majority of CD45+ cells in  $\beta$ VEGF-A grafts were F4/80+ macrophages (Figure 28). In contrast, F4/80+ cells were rare within WT islet grafts (Figure 29).

To determine whether these recruited macrophages contribute to the  $\beta$  cell proliferative response during regeneration, we blocked recruitment of macrophages to  $\beta$ VEGF-A islets by partial bone marrow ablation (5 Gy irradiation). This methodology has been widely used for macrophage inactivation<sup>237,265,266</sup> and prior studies have shown that 5 Gy irradiation alone neither inhibits nor promotes  $\beta$  cell proliferation<sup>267,268</sup>. Immediately after receiving 5 Gy irradiation,  $\beta$ VEGF-A mice began 1-week Dox treatment. The partial bone marrow ablation significantly reduced infiltration of CD45+ macrophages into  $\beta$ VEGF-A overexpressing islets (Figures 30A-E). In spite of the greatly reduced macrophage population, intra-islet endothelial cells continued to expand, resulting in  $\beta$  cell loss (Figure 30D). However, subsequent measurement of the Ki67 labeling index in  $\beta$  cells 2 weeks after Dox withdrawal showed reduced macrophage infiltration into  $\beta$ VEGF-A islets resulting in an approximately 3-fold decrease in  $\beta$  cell proliferation (Figure 30E). These results suggest that recruited macrophages support  $\beta$  cell proliferation following islet injury.

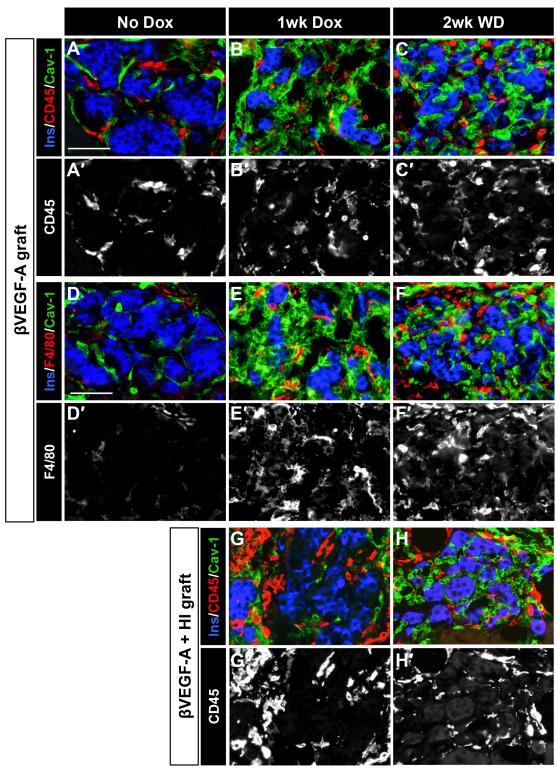


Figure 28. Recruited CD45+ and F4/80+ macrophages infiltrate βVEGF-A grafts upon VEGF-A induction. Islets from βVEGF-A mice and WT controls were transplanted into βVEGF-A recipients or mixed with human islets (HI) and transplanted into NOD-scid- $IL2r\gamma^{null}$  mice. Islets were allowed to engraft for 2 weeks then grafts were harvested and analyzed at No Dox, 1wk Dox, and 2wk WD time points; n=3-4 mice/time point. (A-C) Sections of βVEGF-A islet grafts were labeled with antibodies to insulin (Ins, blue), pan-hematopoietic marker CD45 (red) and endothelial cell (EC) marker caveolin-1 (Cav-1, green). Panels A'-C' display monochrome images of CD45 labeling in A-C. (D-F) Sections of βVEGF-A islet grafts were labeled with antibodies to insulin (Ins, blue), MΦ marker F4/80 (red) and EC marker caveolin-1 (Cav-1, green). Panels D'-F' show monochrome images of F4/80 labeling. (G-H) Sections of βVEGF-A+HI grafts were labeled with antibodies to insulin (Ins, blue), pan-hematopoietic marker CD45 (red) and EC marker caveolin-1 (Cav-1, green). Panels G'-H' display monochrome images of CD45 labeling in G-H. Scale bar in A is 50 μm and also applies to B-H.

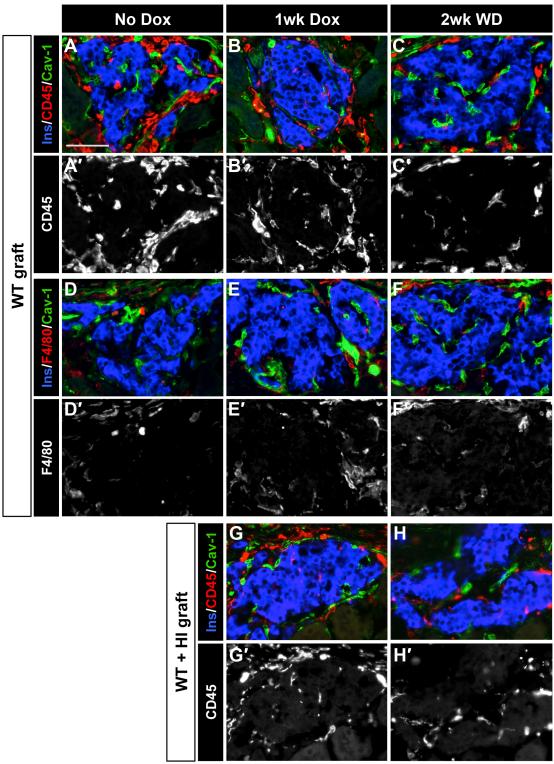


Figure 29. Low incidence of CD45+ and F4/80+ cell infiltration in wild-type islet grafts. Islets from βVEGF-A mice and wild-type (WT) controls were transplanted into βVEGF-A recipients or mixed with human islets (HI) and transplanted into NOD-scid-IL2rγ<sup>null</sup> mice. Islets were allowed to engraft for 2 weeks then grafts were harvested and analyzed at No Dox, 1wk Dox, and 2wk WD time points; n=3-4 mice/ time point. (A-C) Sections of WT islet grafts were labeled with antibodies to insulin (Ins, blue), panhematopoietic marker CD45 (red) and endothelial cell (EC) marker caveolin-1 (Cav-1, green). Panels A'-C' display monochrome images of CD45 labeling in A-C. (D-F) Sections of WT islet grafts were labeled with antibodies to insulin (Ins, blue), macrophage (MΦ) marker F4/80 (red) and EC marker caveolin-1 (Cav-1, green). Panels D'-F' display monochrome images of F4/80 labeling in D-F. (G-H) Sections of WT+HI grafts were labeled with antibodies to insulin (Ins, blue), pan-hematopoietic marker CD45 (red) and EC marker caveolin-1 (Cav-1, green). Panels G'-H' display monochrome images of CD45 labeling in G-H. Scale bar in A is 50 μm and also applies to B-H.

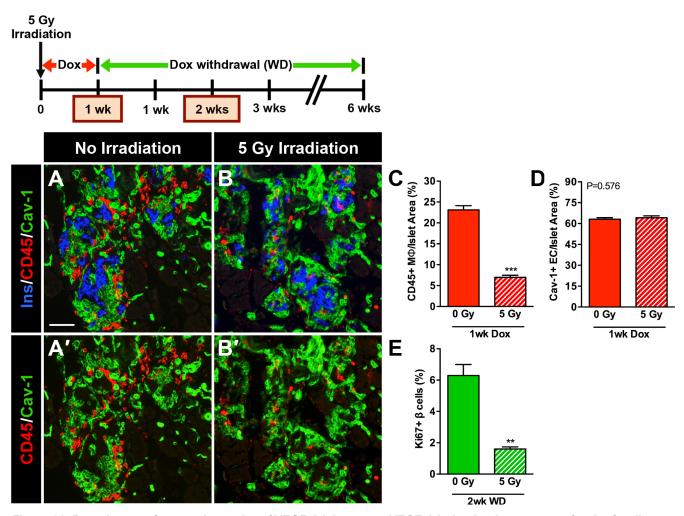


Figure 30. Recruitment of macrophages into βVEGF-A islets upon VEGF-A induction is necessary for the β cell proliferative response. Partial bone marrow ablation prior to VEGF-A induction blocks macrophage (MΦ) recruitment and prevents β cell proliferation. (A, B) Immediately after sublethal irradiation, VEGF-A expression in βVEGF-A mice was induced for 1 week by Dox administration and tissues were examined for the presence of CD45+ macrophages at 1wk Dox and compared with non-irradiated controls; n=4 mice/group; insulin (Ins, blue), CD45 (red) and endothelial cell (EC) marker caveolin-1 (Cav-1, green). Panel A' and B' show CD45 (red) and caveolin-1 (green) labeling. Scale bar is 50 μm and applies to A-B'. (C) Sublethal irradiation reduced infiltration of CD45+ macrophages, \*\*\*, p<0.001, 0 Gy vs. 5 Gy. (D) Sublethal irradiation did not affect intra-islet endothelial cell expansion, p=0.5760, 0 Gy vs. 5 Gy. (E) Two weeks after Dox withdrawal, β cell proliferation was significantly reduced in sublethally irradiated βVEGF-A mice vs. non-irradiated controls, \*\*, p<0.01; n=4 mice/group.

# Both macrophages and endothelial cells in the βVEGF-A islet microenvironment produce factors that promote tissue repair and regeneration

Tissue regeneration is a multi-step process mediated by complex interactions between multiple cell types  $^{269}$ . Because recruited macrophages and intra-islet endothelial cells are two major components of the  $\beta$ VEGF-A islet microenvironment at the onset of  $\beta$  cell regeneration, we postulated that macrophages produce effector molecules that induce  $\beta$  cell proliferation/regeneration either directly or in concert with intra-islet endothelial cells. To identify the components and cellular sources of intra-islet signaling at the onset of  $\beta$  cell proliferation, we performed transcriptome analysis of whole  $\beta$ VEGF-A islets isolated at No Dox and 1 week after VEGF-A induction, when both endothelial cells and macrophages are most abundant in islets, and compared their transcriptional profiles to purified islet-derived macrophages and endothelial cells (Figures 31A-C and 32). Our data revealed that some factors are unique to individual cell types and some are shared by macrophages and endothelial cells. For example, after 1-week VEGF-A induction, recruited macrophages were highly enriched

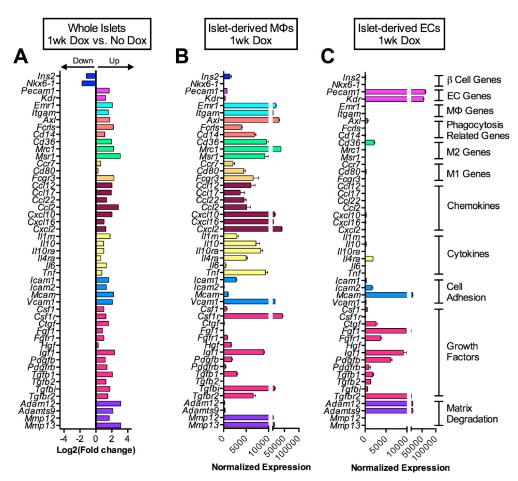


Figure 31. Gene expression profile of whole βVEGF-A islets and purified islet-derived macrophages and endothelial cells by RNA-sequencing. n=3 replicates/each sample set. (A) Differential expression of β cell-, endothelial cell (EC)-, and macrophage (MΦ)-specific genes, phagocytosis-related genes, macrophage phenotype markers (M1, classical; M2, alternative), chemokines, cytokines, cell adhesion molecules, growth factors, and matrix degrading enzymes between islets at 1wk Dox vs. No Dox, p<0.05 for fold change  $\geq$ 2. (B) At 1wk Dox, recruited macrophages are highly enriched for transcripts of phagocytosis-related genes, M2 markers, chemokines, cytokines, cell adhesion molecules, and metalloproteinases involved in tissue repair. (C) Intra-islet endothelial cells mainly express growth factors and matrix degrading enzymes that facilitate growth factor release from the extracellular matrix. Data in B and C are plotted as mean  $\pm$  SEM.

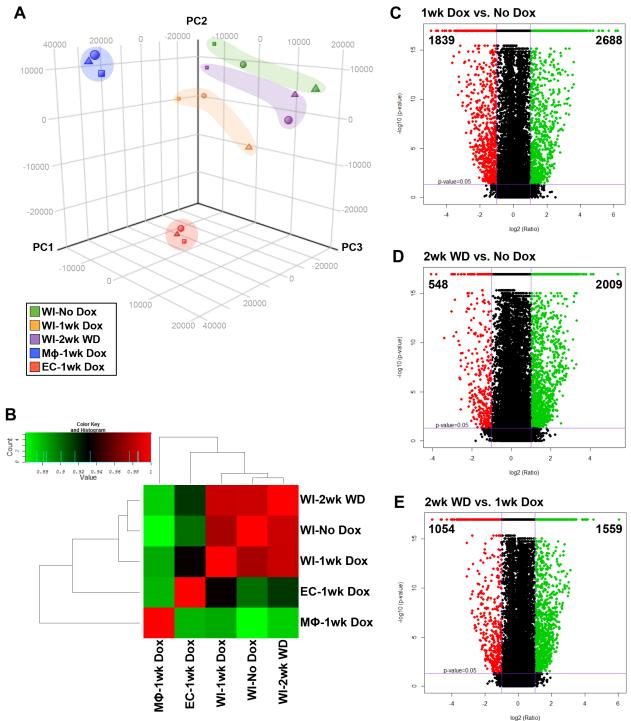


Figure 32. Transcriptome analysis of βVEGF-A islets and purified islet-derived macrophages and endothelial cells. (A) Principal component analysis (PCA) plot shows the clustering of samples prepared from whole islets (WI, n=3 sets/time point) at No Dox (green), 1wk Dox (orange) and 2wk WD (purple), and purified macrophages (MΦs) (blue, n=3) and endothelial cells (ECs) (red, n=3) isolated from βVEGF-A islets at 1wk Dox based on their transcriptional profiles. (B) The heat map of the pairwise correlation between all samples based on the Spearman correlation coefficient, which ranks and quantifies the degree of similarity between each pair of samples (perfect correlation=1; red). The highest correlation is between WIs prior to VEGF-A induction (WI-No Dox) and 2 weeks after withdrawal of the VEGF-A stimulus (WI-2wk WD), followed by WIs after VEGF-A induction (WI-1wk Dox). Endothelial cells and macrophages after VEGF-A induction (EC- and MΦ-1wk Dox) are most similar to WIs after VEGF-A induction (WI-1wk Dox) and 2 weeks after withdrawal of the VEGF-A stimulus (WI-2wk WD), when endothelial cell and macrophage numbers are highest in islets. (C-E) Volcano plots display the differential expression of the statistically significant transcripts between βVEGF-A islet samples at No Dox, 1wk Dox, and 2wk WD. Differential expression between conditions was calculated on the basis of fold change (cutoff ≥2.0) and the p-value was estimated by z-score calculations (cutoff 0.05). (C) 1wk Dox vs. No Dox (D) 2wk WD vs. No Dox and (E) 2wk WD vs. 1wk Dox pairwise comparisons. Each volcano plot shows the total number of upregulated (green) and downregulated transcripts (red) in the upper right and left corner, respectively.

for transcripts of phagocytosis-related genes (*Axl*, *Fcrls*, *Cd14*), markers of alternatively activated macrophages (M2) (*Cd36*, *Mrc1*, *Msr1*), some markers of classically activated macrophages (M1) (*Ccr7*, *Cd80*, *Fcgr3*), chemokines (*Ccl12*, *Ccl2*, *Cxcl10*, *Cxcl2*), cytokines (*Il10*, *Il10ra*, *Il4ra*, *Tnf*), cell adhesion molecules (*Icam1*, *Vcam1*), metalloproteinases (MMPs) involved in tissue repair (*Mmp12*, *Mmp13*), and some growth factors (*Hgf*, *Igf1*, *Pdgfb*, *Tgfb1*, *Tgfbi*) (Figure 31B). In contrast, intraislet endothelial cells mainly expressed growth factors (*Ctgf*, *Fgf1*, *Igf1*, *Pdgfb*) and matrix-degrading enzymes (*Adam12*, *Adamts9*) that facilitate growth factor release from the extracellular matrix (Figure 31C) <sup>270,271</sup>. Additionally, our data indicates that intra-islet endothelial cells produce factors (*Tgfb* family; including *Tgfb1*, *Tgfb2*) and cell adhesion molecules (*Icam2*, *Mcam*) directly involved in monocyte recruitment and M2 macrophage activation<sup>266,272,273</sup>. These data provide strong evidence for a model of β cell regeneration where factors produced by both recruited macrophages and intra-islet endothelial cells create a microenvironment that promotes β cell proliferation (Figure 33).

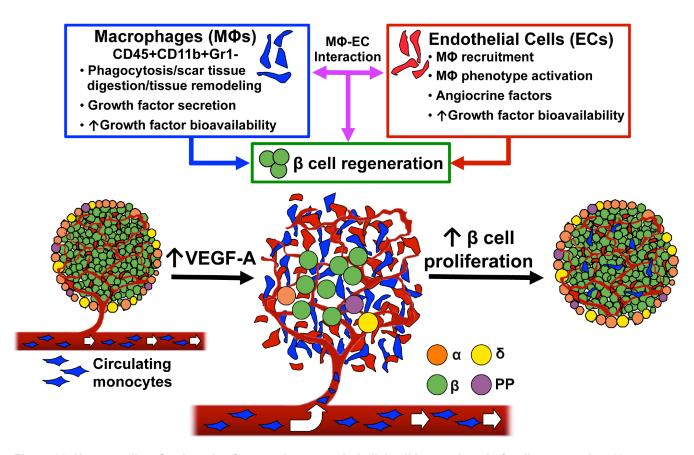


Figure 33. New paradigm for the role of macrophage – endothelial cell interactions in  $\beta$  cell regeneration. Upon VEGF-A induction intra-islet endothelial cells proliferate and circulating monocytes recruited to islets differentiate into macrophages. These CD45+CD11b+Gr1- recruited macrophages and endothelial cells produce effector molecules that either directly or cooperatively induce  $\beta$  cell proliferation and regeneration.

### **Discussion**

VEGF-A is a master regulator of islet vascular patterning, microvascular permeability, and function, but the role of the VEGF-A signaling pathway and intra-islet endothelial cells in regulating  $\beta$  cell mass is incompletely understood. Here we used a model of inducible and reversible  $\beta$  cell-specific VEGF-A overexpression to investigate how VEGF-A signaling modulates intra-islet vasculature, islet microenvironment, and  $\beta$  cell mass. Increasing intra-islet endothelial cells by transient VEGF-A induction surprisingly led to reduced, not increased,  $\beta$  cell mass. However, withdrawal of the VEGF-A stimulus created a local microenvironment that promoted robust  $\beta$  cell proliferation, with restoration of  $\beta$  cell mass, islet architecture, and vascularization. This proliferation, which was independent of the pancreatic environment or systemic factors, required recruitment of macrophages to the site of islet regeneration. Based on these findings, we propose a mechanism to induce  $\beta$  cell regeneration, involving recruited macrophages and intra-islet endothelial cells (discussed below).

Transiently increased VEGF-A production in adult  $\beta$  cells in our model resembled recently described restrictive effects of hypervascularization on pancreatic epithelial branching, endocrine cell differentiation and  $\beta$  cell mass<sup>149-151,155</sup>, and contrasted with previously reported islet hyperplasia in a Pdx1-VEGF-A transgenic model<sup>138</sup>. Similar deleterious effects of VEGF-A-induced neovascularization were observed previously in liver and heart<sup>274</sup>. In our study, a significant decrease in  $\beta$  cell proliferation and mass and increased apoptosis were observed when intra-islet endothelial cells became proliferative. It is possible that activated endothelial cells produce factors causing  $\beta$  cell loss, or  $\beta$  cells regress due to space constraints and perturbed cell-cell contacts within the islet caused by rapid endothelial cell outgrowth. Although the expanding islet endothelium became disorganized, it is unlikely that the loss of  $\beta$  cells was caused by lack of blood flow or hemorrhage, since islet vasculature was perfused as shown by labeling with endothelium-binding lectin<sup>137</sup>. Determining the exact cause(s) of  $\beta$  cell death will require additional investigation. Taken together, we show that precise control of VEGF-A production in adult  $\beta$  cells is crucial for islet vascular homeostasis and maintenance of normal  $\beta$  cell mass. This is important for efforts to utilize endothelial cells in embryonic stem cell-differentiation protocols or to promote islet survival after islet transplantation.

Withdrawal of the VEGF-A stimulus in  $\beta$ VEGF-A islets led to a remarkably rapid recovery of  $\beta$  cells by a transient increase in proliferation. Lineage tracing analysis showed that  $\beta$  cell proliferation from pre-existing  $\beta$  cells was the main mechanism of  $\beta$  cell recovery in the  $\beta$ VEGF-A model. Furthermore, using a transplantation model with WT and  $\beta$ VEGF-A islets transplanted under contralateral kidney capsules, we were able to exclude systemic effects of soluble factors, namely glucose<sup>50</sup>, and demonstrate conclusively that  $\beta$  cell proliferation following injury was stimulated by signals derived from the local islet milieu. Remarkably, these localized signals were also able to significantly increase human  $\beta$  cell proliferation.

Although  $\beta$  cell proliferation in the  $\beta$ VEGF-A model is independent of systemic soluble factors, we found that islet vascular expansion and  $\beta$  cell loss were accompanied by a dramatic infiltration of CD45+CD11b+Gr1- macrophages. In addition, our data demonstrates that recruited macrophages infiltrating  $\beta$ VEGF-A islets and islet grafts neither incorporate into islet vasculature nor differentiate into insulin-producing cells, but instead remain in close association with  $\beta$  cells and intra-islet endothelial

cells. This robust recruitment of macrophages is, for example, very distinct from the STZ-mediated model of β cell injury where transplantation of BMCs has an extremely limited effect on β cell recovery and BMCs were mostly found around pancreatic ducts<sup>275,276</sup>. Moreover, when the recruitment of CD45+CD11b+Gr1- macrophages in our model was blocked by partial bone marrow ablation, \( \beta \) cell proliferation was greatly reduced, suggesting that infiltration of these macrophages are crucial for the β cell proliferative response in regenerating βVEGF-A islets. Depending on the microenvironment, macrophages can acquire distinct functional phenotypes. Two well-established macrophage phenotypes are often referred to as classically activated pro-inflammatory macrophages (M1) and alternatively activated macrophages (M2) that promote tissue repair/regeneration through phagocytosis, scar tissue digestion, and growth factor secretion and release from the extracellular matrix<sup>277</sup>. Transcriptome analysis showed that macrophages recruited to βVEGF-A islets express high levels of M2 markers along with MMPs associated with tissue restoration and remodeling, and lower levels of M1 markers, indicating that these macrophages likely have a unique regenerative phenotype<sup>266,277</sup>. Very little is known about the role of macrophages in adult β cell maintenance, but during late stages of pancreatic development, mice with severe macrophage deficiency had reduced  $\beta$  cell proliferation, β cell mass, and impaired islet morphogenesis<sup>217</sup>.

While recruited macrophages are present in  $\beta$ VEGF-A islets during VEGF-A induction,  $\beta$  cell proliferation does not begin until 1 week after Dox withdrawal when intra-islet endothelial cells switch from proliferative angiogenesis to quiescence, suggesting that quiescent intra-islet endothelial cells provide permissive or instructive signals for the  $\beta$  cell regenerative process. These islet-derived endothelial cells produce several modulators of cell proliferation and also secreted factors that direct M2 macrophage activation<sup>272,278</sup>. Recent work from several groups suggests that organ-specific vascular niches and VEGF-A-VEGFR2 signaling are major determinants in organ repair and tumorigenesis where endothelial cells produce tissue-specific paracrine growth factors, termed angiocrine factors<sup>252</sup>. For example, during liver regeneration sinusoidal endothelial cells provide the vascular niche required to initiate hepatic proliferation by producing angiocrine factors such as HGF and Wnt2<sup>279</sup>. In bone marrow, stress-induced expression of Notch ligands by sinusoidal endothelial cells is necessary for hematopoietic stem cell reconstitution<sup>280</sup>. After a partial lung ablation, pulmonary capillary endothelial cells stimulate proliferation of epithelial progenitor cells through processes involving VEGFR2 and FGFR1 activation, and production of MMP14<sup>281</sup>. Furthermore, production of angiocrine factors by tumor vessels directly leads to tumor progression<sup>252</sup>. In the pancreas, VEGF-A-VEGFR2 signaling is a principal regulator of islet capillary network formation and maintenance 137,207. In addition, endothelial cells are critical for induction of islet endocrine cell differentiation 138,144 and early loss of endothelial cells in developing islets leads not only to reduced β cell mass at birth but also reduced basal β cell proliferation in the adult<sup>148</sup>. Transcriptional profiling of intra-islet endothelial cells suggests that they contribute to β cell regeneration by facilitating monocyte recruitment and M2 macrophage activation, and by producing an array of growth factors and MMPs that increase growth factor bioavailability.

The main challenge of  $\beta$  cell replacement therapy is determining how to generate a sufficient quantity of high-quality mature human  $\beta$  cells. Therefore, understanding mechanisms that modulate  $\beta$  cell regeneration, and fostering this process may help rescue remaining  $\beta$  cell mass in type 1 and type 2 diabetes. Based on our findings, we propose a new model of  $\beta$  cell regeneration (Figure 33) where the

local islet microenvironment, dynamically modulated by VEGF-A, plays an integral part in the  $\beta$  cell regenerative process. Increased VEGF-A production in adult  $\beta$  cells results in intra-islet endothelial cell activation and  $\beta$  cell loss, which demonstrates the essential role of regulated VEGF-A signaling in maintaining islet vascular homeostasis and  $\beta$  cell mass. At the same time, however, islet VEGF-A induction leads to the recruitment of CD45+CD11b+Gr1- macrophages. After withdrawal of the VEGF-A stimulus, these recruited M2-like macrophages persist in islet remnants and produce effector molecules that directly, or in concert with quiescent intra-islet endothelial cells, promote  $\beta$  cell proliferation and regeneration independent of the pancreatic site and systemic factors.

It will be important to further characterize the macrophages responsible for this  $\beta$  cell proliferative effect and determine how to promote their recruitment to pancreatic islets. Furthermore, understanding signals derived from the intra-islet endothelium will allow us to define the mechanism by which these recruited macrophages promote  $\beta$  cell proliferation and develop them as a potential therapeutic for diabetes.

### **CHAPTER IV**

# INTERACTIONS BETWEEN PANCREATIC ISLET $\beta$ CELLS, ENDOTHELIAL CELLS, MACROPHAGES, AND THE EXTRACELLULAR MATRIX PROMOTE $\beta$ CELL PROLIFERATION

### Introduction

Pancreatic islets are highly vascularized mini-organs, and while investigating how vascular endothelial growth factor-A (VEGF-A) regulates this vascularization, we discovered a new model where self-renewal of  $\beta$  cells is stimulated by signals derived from the local microenvironment, as described in Chapter III<sup>153</sup>. In this model, transiently increased  $\beta$  cell VEGF-A production ( $\beta$ VEGF-A model) induces endothelial cell expansion and hypervascularization that result in  $\beta$  cell loss, indicating that proliferative angiogenesis is deleterious to  $\beta$  cells. Remarkably, 6 weeks after withdrawal (WD) of the VEGF-A stimulus, islet morphology, vascularization, mass, and function rapidly normalize as a result of a robust, but transient burst in  $\beta$  cell proliferation. Our initial studies suggested that this process depends on VEGF-A-mediated recruitment of macrophages, which either directly, or cooperatively with quiescent intra-islet endothelial cells, induce  $\beta$  cell proliferation.

The macrophages recruited to  $\beta$ VEGF-A islets express several markers of alternative (M2) activation, which promotes tissue repair/regeneration and some markers of classically activated (M1) pro-inflammatory macrophages, suggesting that these macrophages have a unique regenerative phenotype <sup>153,266,272,277,278</sup>. Although not much is known about the role of macrophages in adult  $\beta$  cell maintenance, during late stages of pancreatic development, mice with severe macrophage deficiency have reduced  $\beta$  cell proliferation,  $\beta$  cell mass, and impaired islet morphogenesis <sup>217</sup>. Furthermore, two recently published studies have confirmed our discovery that macrophages can play an important role in  $\beta$  cell regenerative processes. They both describe a function for M2-like macrophages in  $\beta$  cell proliferation following damage either due to surgically-induced pancreatitis <sup>221</sup>, or ablation of the whole pancreas or  $\beta$  cells using genetic models of diphtheria toxin (DT)-mediated apoptosis <sup>222</sup>. The macrophages in these studies express different phenotypic markers than those in our model and likely work through different mechanisms, but these studies highlight new roles for macrophages in  $\beta$  cell proliferation and the importance of clearly defining the macrophage phenotype and function in the  $\beta$ VEGF-A model.

VEGF-A induces extensive intra-islet endothelial cell proliferation in this  $\beta$ VEGF-A model, leading to  $\beta$  cell loss similar to effects observed previously in VEGF-A-induced neovascularization in the liver and heart<sup>274</sup>. Previous studies have demonstrated that the VEGF-A/VEGFR2 pathway mediates the production of organ-specific angiocrine factors by quiescent endothelial cells that promote local tissue self-renewal and regeneration<sup>252,279-281</sup>. In addition to these direct effects, endothelial cells can facilitate tissue repair indirectly by interacting with macrophages to promote their activation toward a tissue-reparative, M2-like phenotype<sup>278</sup>. In  $\beta$ VEGF-A mice, it is unclear what effects endothelial cells have on  $\beta$  cells, both in their proliferative state during VEGF-A induction and as they become quiescent

as VEGF-A expression normalizes; however, they may participate in the  $\beta$  cell regenerative process indirectly by promoting macrophage recruitment and activation and/or by directly influencing  $\beta$  cell proliferation.

In this Chapter, we describe studies where we tested the hypothesis that  $\beta$  cell self-renewal is mediated by coordinated interactions between macrophages recruited to the site of  $\beta$  cell injury, intra-islet endothelial cells, and the extracellular matrix. To do this, we first developed models for specifically removing macrophages and endothelial cells from the microenvironment to identify whether each cell type is required for  $\beta$  cell proliferation. Because the  $\beta$ VEGF-A islet microenvironment is a complex *in vivo* system with changes in cell composition and function over time, we developed a strategy to identify signals regulating  $\beta$  cell regeneration by examining the microenvironment using transcriptome analysis of purified cell populations— $\beta$  cells, endothelial cells, and macrophages—over the course of VEGF-A induction and normalization and  $\beta$  cell death and regeneration.

### Results

# Genetic model of diphtheria toxin-mediated macrophage depletion fails to adequately remove macrophages or recreate the regenerative $\beta$ VEGF-A islet microenvironment

To determine whether macrophages are required for  $\beta$  cell proliferation in  $\beta$ VEGF-A mice, we created a model of DT-inducible monocyte/macrophage ablation by transplanting lethally irradiated (9 Gy)  $\beta$ VEGF-A mice with bone marrow from WT or CD11b-DTR mice, which express the diphtheria toxin receptor (DTR) on their monocytes and macrophages (Figure 34). After bone marrow reconstitution, treatment with DT during VEGF-A induction reduced both circulating CD11b+Ly6G- monocytes and recruited macrophages (Figure 35A-E and 35J). However, macrophage depletion was not sustained 2 weeks after VEGF-A normalization (Figure 35H-I). More importantly, Dox treatment in these mice did not lead to the same degree of endothelial cell expansion (~55% of islet area vs. 80%) or  $\beta$  cell loss (~35% of islet area vs. 20%) observed in previous studies (Figure 35D-G and Figure 13). Therefore,  $\beta$  cell proliferation remained at its basal level (~2%), even in control mice, 2 weeks after VEGF-A normalization when  $\beta$  cell proliferation is highest in other experiments (Figure 35K and Figure 19)<sup>153</sup>. We concluded that this genetic model of inducible monocyte/macrophage ablation does not adequately reproduce the regenerative islet microenvironment observed previously and therefore would not be useful to evaluate the contribution of macrophages to the  $\beta$  cell proliferative response.

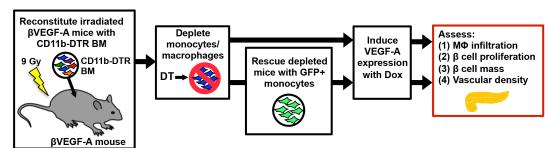


Figure 34. Genetic model of inducible monocyte depletion in  $\beta VEGF-A$  mice. Development of a genetic model of diphtheria toxin (DT)-inducible monocyte depletion in  $\beta VEGF-A$  mice by transplanting lethally irradiated  $\beta VEGF-A$  mice with bone marrow (BM) from CD11b-DTR mice. After bone marrow engraftment monocytes will be depleted by daily DT injections during VEGF-A induction with Dox. A subset of monocyte-depleted mice will be given GFP-labeled monocytes to rescue the phenotype.

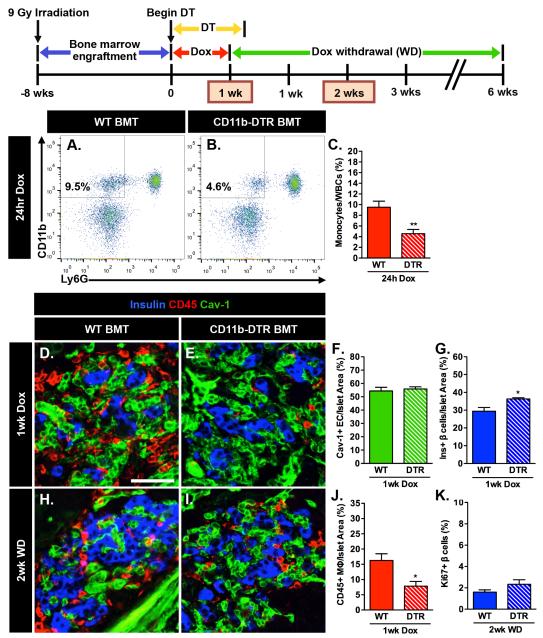


Figure 35. Genetic model of monocyte depletion in βVEGF-A mice does not adequately remove islet macrophages or recreate the islet regenerative microenvironment. Lethally irradiated βVEGF-A mice reconstituted with bone marrow from CD11b-DTR mice (DTR) were treated with daily DT injections (10 ng/g i.v.) and Dox to deplete monocytes and induce VEGF-A overexpression, respectively. Control mice transplanted with WT bone marrow (WT) received the same treatment. (A-C) Circulating CD11b+Ly6G- monocytes were reduced 52% in βVEGF-A mice with CD11b-DTR bone marrow transplants (BMT) 24 hours after beginning DT and Dox treatment (24hr Dox) compared to control mice with WT BMTs. \*\*, p<0.01, CD11b-DTR BMT mice (n=11) vs. WT-BMT mice (n=10) at 24hr Dox. (D-J) One week after beginning DT and Dox treatment (1wk Dox), endothelial cell (EC) expansion to ~55% of islet area (F) and β cell loss to ~35% of islet area (G) in both CD11b-DTR BMT mice and WT BMT mice was not comparable to the endothelial cell expansion (80% of islet area) and β cell loss (20% of islet area) seen in previous studies (see Figure 13). Although macrophage infiltration was reduced 52% in CD11b-DTR BMT mice compared to WT BMT mice at 1wk Dox (J), this reduction was not maintained 2 weeks after Dox withdrawal (2wk WD) (H-I). Labeling for insulin (blue), macrophage (MΦ) marker CD45 (red), and endothelial cell (EC) marker caveolin-1 (Cav-1, green). Scale bar in D is 50 µm and also applies to E, H, and I. \*, p<0.05, CD11b-DTR BMT mice vs. WT-BMT mice at 1wk Dox; n=3 mice/group. (K) Neither CD11b-DTR mice nor WT-BMT mice demonstrated an increase in β cell proliferation over 2% baseline levels at 2wk WD, when proliferation is highest (6%) in previous studies (see Figure 19); CD11b-DTR BMT mice vs. WT-BMT mice at 2wk WD was not significant; n=4-6 mice/group.

## Chemical approach effectively depletes macrophages in $\beta$ VEGF-A islets and demonstrates that macrophages are required for $\beta$ cell proliferation

We next used clodronate-mediated macrophage depletion to evaluate the role of macrophages in β cell proliferation. Clodronate is an ATP/ADP translocase inhibitor, and when packaged into liposomes it is selectively delivered to macrophages and causes apoptosis. We treated βVEGF-A mice with either control or clodronate liposomes starting one day before VEGF-A induction and continuing for 1 week after VEGF-A normalization. Clodronate treatment reduced circulating CD11b+Ly6G- monocytes by 50% within 24 hours (Figure 36A-C) and reduced macrophage infiltration in islets by 94% 1 week after VEGF-A induction (Figure 36D-E and 36H). Macrophage depletion was maintained during VEGF-A normalization, with 86% fewer macrophages in islets from clodronate-treated βVEGF-A mice 1 week after Dox withdrawal (Figure 36I-K). VEGF-A induction in both clodronate-treated and control mice led to an increase in endothelial cells and β cell loss comparable to βVEGF-A mice not treated with liposomes (Figure 36D-G and Figure 13), demonstrating that liposome treatment does not interfere with this model of  $\beta$  cell regeneration and that macrophages are not required for  $\beta$  cell loss. This finding is further confirmed by significant β cell proliferation (8.5±1.4%) in control mice 1 week after VEGF-A normalization (Figure 36L and Figure 19). However, macrophage depletion did significantly reduce this β cell proliferation (2.1±0.2%; Figure 36L), importantly demonstrating that macrophages are required for the  $\beta$  cell proliferative response in  $\beta$ VEGF-A islets.

### Development of a model to evaluate the role of endothelial cells in the \( \beta VEGF-A \) microenvironment

To define the role of proliferative and quiescent endothelial cells in β cell loss, macrophage recruitment, macrophage phenotype activation, and β cell proliferation, we have begun developing a model of endothelial cell-specific VEGFR2 knockdown in βVEGF-A mice (Figure 37). This is being accomplished by introducing floxed VEGFR2 alleles (VEGFR2<sup>fl/fl</sup> mice) and an endothelial cell-specific tamoxifen (Tm)-inducible Cre (EC-SCL-CreER mice) into βVEGF-A mice using the breeding schemes outlined in Table 7. VEGFR2<sup>fl/fl</sup> mice were crossed with EC-SCL-CreER mice to obtain EC-SCL-CreER<sup>tg/wt</sup>; VEGFR2<sup>fl/fl</sup> mice that are currently being crossed with RIP-rtTA mice to obtain EC-SCL-CreER<sup>tg/wt</sup>; VEGFR2<sup>fl/fl</sup>; RIP-rtTA<sup>tg/wt</sup> mice. At the same time, VEGFR2<sup>fl/fl</sup> mice were also crossed with TetO-VEGF mice to obtain TetO-VEGFtg/tg; VEGFR2fl/fl mice that are being maintained for use in final crosses. To confirm that Tm-inducible Cre in EC-SLC-CreER mice is active in islet endothelial cells, we treated EC-SLC-CreER mice that express β-galactosidase upon Cre recombination (EC-SCL-CreER; R26R<sup>lacZ</sup> mice) with 3 x 4 mg Tm. We found X-gal staining in intra-islet endothelial cells (Figure 38), indicating that Cre was successfully activated in islet endothelial cells. To determine whether Cre activity in these cells is sufficient for VEGFR2 knockdown, we are currently treating EC-SCL-CreERtg/wt; VEGFR2fl/fl and EC-SCL-CreERtg/wt; VEGFR2fl/wt mice with Tm and will evaluate these islets for VEGFR2 expression. Once we obtain the desired offspring from these crosses (TetO-VEGFtg/wt; RIP-rtTAtg/wt; EC-SCL-CreERtg/wt; VEGFR2fl/fl mice), we will use this model to prevent VEGF-A mediated endothelial cell activation prior to and after VEGF-A induction to determine: (1) if proliferative intra-islet endothelial cells are required for β cell loss and macrophage recruitment and phenotype activation, and (2) if VEGFR2 signaling in quiescent intra-islet endothelial cells following VEGF-A normalization is required for  $\beta$  cell regeneration (Figure 37).

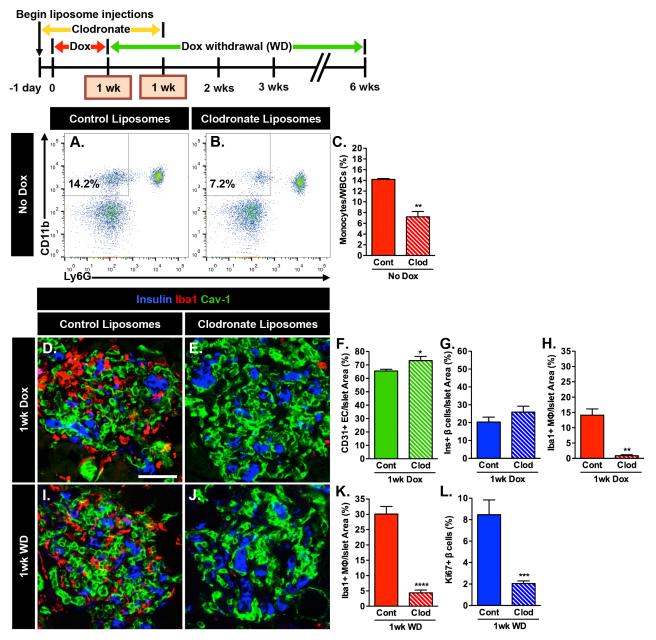
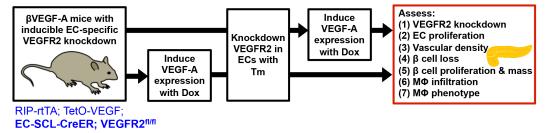


Figure 36. Macrophages are required for β cell proliferation in βVEGF-A mice. βVEGF-A mice were treated with clodronate liposomes (Clod) every other day (150-200 µL i.v.) beginning one day before Dox treatment and continuing 1 week after Dox withdrawal (1wk WD) to deplete macrophages during VEGF-A induction and normalization. Control mice received injections of control (Cont) rather than clodronate liposomes. (A-C) Circulating CD11b+Ly6Gmonocytes were reduced 49% in βVEGF-A mice receiving clodronate vs. control liposomes one day after beginning injections, on the first day of Dox administration (No Dox). \*\*, p<0.01, clodronate vs. control mice at No Dox; n=3 mice/group. (D-H) One week after beginning liposome and Dox treatment (1wk Dox), endothelial cell (EC) expansion to ~70% of islet area (F) and β cell loss to ~23% of islet area (G) in both clodronate-treated βVEGF-A mice and control mice is comparable to the endothelial cell expansion (80% of islet area) and β cell loss (20% of islet area) seen in previous studies (see Figure 13). Macrophage infiltration was reduced 94% in clodronate-treated BVEGF-A mice compared to control mice at 1wk Dox (H). Labeling for insulin (blue), macrophage (ΜΦ) marker lba1 (red), and endothelial cell (EC) marker caveolin-1 (Cav-1, green). Scale bar in D is 50 µm and also applies to E, I, and J. \*, p<0.05 and \*\*, p<0.01, Clod (n=3) vs. Cont (n=6) at 1wk Dox. (I-K) One week after Dox withdrawal (1wk WD), an 86% reduction in macrophage infiltration in clodronate-treated βVEGF-A mice is maintained (K). Labeling for insulin (blue), Iba1 (red), and caveolin-1 (Cav-1, green). \*\*\*\*, p<0.0001, Clod (n=8) vs. Cont (n=7) at 1wk WD. (L) One week after Dox withdrawal (1wk WD),  $\beta$  cell proliferation in control  $\beta$ VEGF-A mice (8.5±1.4%) was comparable to proliferation seen in previous studies (see Figure 19), but was significantly reduced in clodronate-treated mice (2.1±0.2%). \*\*\*, p<0.001, Clod (n=7) vs. Cont (n=6) at 1wk WD.



#### A. VEGFR2 knockdown before VEGF-A induction



### B. VEGFR2 knockdown after VEGF-A induction

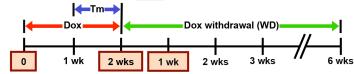


Figure 37. Model of inducible endothelial cell-specific knockdown of VEGFR2 in βVEGF-A mice. Development of a model of inducible endothelial cell (EC)-specific VEGFR2 knockdown by breeding mice with a Tm-inducible endothelial cell-specific Cre recombinase (EC-SCL-CreER) and mice with floxed VEGFR2 alleles (VEGFR2<sup>0/10</sup>) into the βVEGF-A mouse model (RIP-rtTA; TetO-VEGF) will allow us to determine if proliferative intra-islet endothelial cells are required for β cell loss, macrophage recruitment, and macrophage phenotype activation by knocking out VEGFR2 before VEGF-A induction (A) to prevent endothelial cell expansion; and if VEGFR2 signaling in quiescent intra-islet endothelial cells after VEGF-A normalization is required for β cell proliferation by knocking out VEGFR2 after VEGF-A induction (B) to allow for normal endothelial cell expansion and macrophage recruitment.

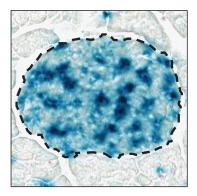


Figure 38 EC-SCL-CreER mice have Cre activity in intra-islet endothelial cells. X-gal staining (blue) in intra-islet ECs of Tm-treated EC-SCL-CreER; R26R<sup>lacZ</sup> mice. Dashed line marks islet.

	Table 7. Breeding scheme for mice	with inducible endother	ding scheme for mice with inducible endothelial cell-specific knockout of VEGFR2	R2
SCH	SCHEME A			
	Breeder 1	Breeder 2	Desired Offspring	Freq
_	EC-SCL-CreER <sup>tg/tg</sup>	VEGFR2fi/fi	EC-SCL-CreERtg/wt; VEGFR2fl/+	100%
7	EC-SCL-CreERtg/wt; VEGFR2fl/+	VEGFR2fi/fi	EC-SCL-CreERtg/wt; VEGFR2fl/fl	25%
က	EC-SCL-CreERtg/wt; VEGFR2fl/fl	RIP-rtTA <sup>tg/tg</sup>	EC-SCL-CreERtg/wt; VEGFR2fl/+; RIP-rtTAtg/wt	%09
4	EC-SCL-CreER®W; VEGFR2®M; RIP-rtTA®M VEGFR2®M	VEGFR2fi/fi	EC-SCL-CreERtg/wt; VEGFR2fl/ff; RIP-rtTAtg/wt	12.5%
SCH	SCHEME B			
	Male Breeder	Female Breeder	Desired Offspring	Freq
_	VEGFR2***	TetO-VEGF <sup>19/19</sup>	TetO-VEGFtg/wt; VEGFR2fl/+	100%
7	TetO-VEGF¹g/wt; VEGFR2fl/+	TetO-VEGF <sup>19/19</sup>	TetO-VEGF <sup>1g/1g</sup> ; VEGFR2 <sup>1l/+</sup>	%09
က	TetO-VEGFtg/wt; VEGFR2fl/+	TetO-VEGF <sup>19/19</sup> ; VEGFR2 <sup>11/+</sup>	TetO-VEGF <sup>1g/1g</sup> ; VEGFR2 <sup>1l/fl</sup>	25%
FINA	FINAL CROSSES			
	Male Breeder	Female Breeder	Desired Offspring	Freq
fl/fl	EC-SCL-CreER®w; VEGFR2IIII; RIP-rtTA®w	TetO-VEGF¹७¹७; VEGFR2ººº	TetO-VEGF'9'w;, RIP-rtTA'9'w;, EC-SCL-CreER'9'w;, VEGFR2"	25%
#/J	EC-SCL-CreER® <sup>wr</sup> ; VEGFR2 <sup>fl/fl</sup> ; RIP-rtTA <sup>tg/wt</sup> TetO-VEGF <sup>tg/tg</sup>	TetO-VEGF <sup>19/19</sup>	TetO-VEGFt@wi; RIP-rtTAt@wi; EC-SCL-CreERt@wi; VEGFR2#/+	25%

Yellow highlight designates offspring mice that have been obtained and are currently in our colony in breeding setups.

### Identifying interactions between $\beta$ cells, endothelial cells, macrophages, and the extracellular matrix in the $\beta$ VEGF-A islet microenvironment

Because the stimulus for  $\beta$  cell proliferation in  $\beta$ VEGF-A mice is localized to the islet microenvironment, and is dependent on macrophage infiltration, we next sought to identify mechanisms through which  $\beta$  cells, endothelial cells, and macrophages are interacting with each other and the extracellular matrix to promote  $\beta$  cell regeneration. After several failed attempts to recreate the  $\beta$ VEGF-A model *in vitro*, we determined that we needed a new strategy to identify these cell-cell and cell-matrix interactions *in vivo*. Therefore, we performed transcriptome analysis on purified, sorted populations of  $\beta$  cells, endothelial cells, and macrophages from  $\beta$ VEGF-A mice over the course of VEGF-A induction and normalization (Figure 39A). By performing fold change analysis on normalized gene expression values for each cell population at each time point, we identified the genes, biological processes, and pathways changing as each individual cell population shifts over the  $\beta$  cell death-to-regeneration timeline (Figure 39B). We then compared these cell populations to determine which of the changes in genes, biological processes, and pathways were specific to individual cell populations, and which were common to multiple populations at each time point analyzed (Figure 39C).

All cell populations analyzed demonstrated distinct transcriptional profiles, reflecting a high degree of separation between cell types and significant transcriptional changes within each cell type over time (Figure 40). Many genes are downregulated as β cells transition from being guiescent (No Dox), to apoptotic (1wk Dox), to proliferative (1wk WD); but a greater number of genes are upregulated. These genes are involved in processes such as cell adhesion, regulation of apoptosis and cell proliferation, extracellular matrix organization, intracellular signal transduction, protein phosphorylation, receptor signaling pathways, and the MAPK cascade (Figure 41). The largest number of genes changed in endothelial cells as they went from quiescent (No Dox) to proliferative (1wk Dox) in response to VEGF-A (Figure 42). Many of these genes are involved in cell cycle progression and cell proliferation as well as extracellular matrix organization and cell adhesion. Following VEGF-A normalization, endothelial cells regress and become guiescent again (1wk WD), which is reflected in few gene changes between these cells and guiescent endothelial cells at baseline (No Dox) (Figure 42). A small population of resident macrophages (No Dox) is supplemented by an influx of recruited macrophages upon VEGF-A induction (1wk Dox), which are required for β cell regeneration to occur upon VEGF-A normalization (1wk WD). Genes changing in this cell population are involved in processes such as immune and inflammatory response, cell adhesion, developmental processes and growth, extracellular matrix organization, and cell proliferation (Figure 43).

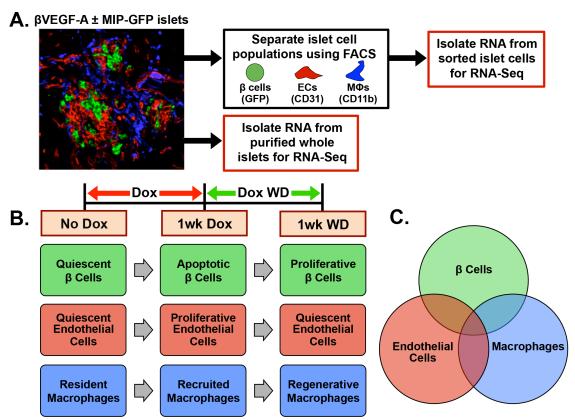


Figure 39. Workflow for sorting and analyzing islet β cells, islet-derived endothelial cells, and islet-derived macrophages from βVEGF-A mice. (A) Islets from βVEGF-A mice with or without GFPexpressing β cells (βVEGF-A±MIP-GFP) were purified and RNA was isolated from whole islets (see Chapter III, Figure 31) or dispersed islet cell populations sorted by FACS for transcriptome analysis (RNA-Seq). (B) Previous studies outlined in Chapter III demonstrate that each islet cell population (B cells, endothelial cells, and macrophages) changes from baseline (No Dox) over the course of VEGF-A induction (1wk Dox) and normalization (1wk WD).  $\beta$  cells transition from being quiescent (No Dox), to apoptotic (1wk Dox), to proliferative (1wk WD). Endothelial cells go from a guiescent state (No Dox) to proliferative in response to VEGF-A (1wk Dox), and then regress once VEGF-A normalizes and become quiescent again (1wk WD). A small population of resident macrophages (No Dox) is supplemented by an influx of recruited macrophages upon VEGF-A induction (1wk Dox), which are required for ß cell regeneration to occur upon VEGF-A normalization (1wk WD). We analyzed transcriptome data from each cell population over the course of VEGF-A induction and normalization to determine what genes, biological processes, and pathways are changing as these populations shift over time. (C) Individual cell populations were then compared to each other to determine which changes were unique to individual cell populations, and which were common to multiple populations at each time point analyzed.

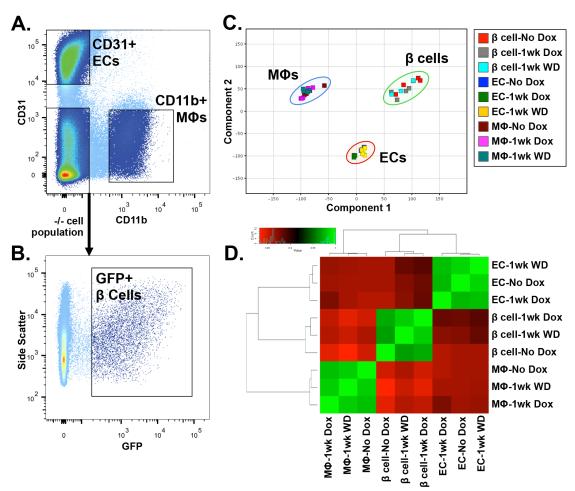


Figure 40. Transcriptome analysis demonstrates a high degree of separation between sorted islet cell populations. (A) Dispersed islet cells from \( \text{SVEGF-A\pmuMIP-GFP} \) mice were immunolabeled with fluorophore-conjugated anti-CD31, and anti-CD11b antibodies to separate endothelial cell (EC) and macrophage (MΦ) populations, respectively. (B) In βVEGF-A+MIP-GFP mice, GFP+ β cells were sorted from the CD31-CD11b- population. (C) Principal component analysis (PCA) plot shows the clustering of samples from sorted β cells (green circle) at No Dox (n=4), 1wk Dox (n=5), and 1wk WD (n=3); sorted endothelial cells (ECs, red circle) at No Dox (n=4), 1wk Dox (n=4), and 1wk WD (n=5); and sorted macrophages (MΦ, blue circle) at No Dox (n=4), 1wk Dox (n=5) and 1wk WD (n=4) from βVEGF-A islets based on their transcriptional profiles. (D) The heat map of the pairwise correlation between all cell populations at all time points based on the Spearman correlation coefficient, which ranks and quantifies the degree of similarity between each pair of samples (perfect correlation=1; green). The highest correlations are between each cell type across different time points (β cells at No Dox, 1wk Dox, and 1wk WD; MΦs at No Dox, 1wk Dox, and 1wk WD; and ECs at No Dox, 1wk Dox, and 1wk WD). Within each cell type, regenerative  $\beta$  cells (1wk WD) are more similar to apoptotic  $\beta$  cells (1wk Dox) than quiescent β cells (No Dox); quiescent endothelial cells before VEGF-A induction (No Dox) are more similar to quiescent endothelial cells following VEGF-A normalization (1wk WD) than proliferative endothelial cells (1wk Dox); and regenerative macrophages (1wk WD) are more similar to resident macrophages (No Dox) than to those initially recruited to islets upon VEGF-A induction (1wk Dox).

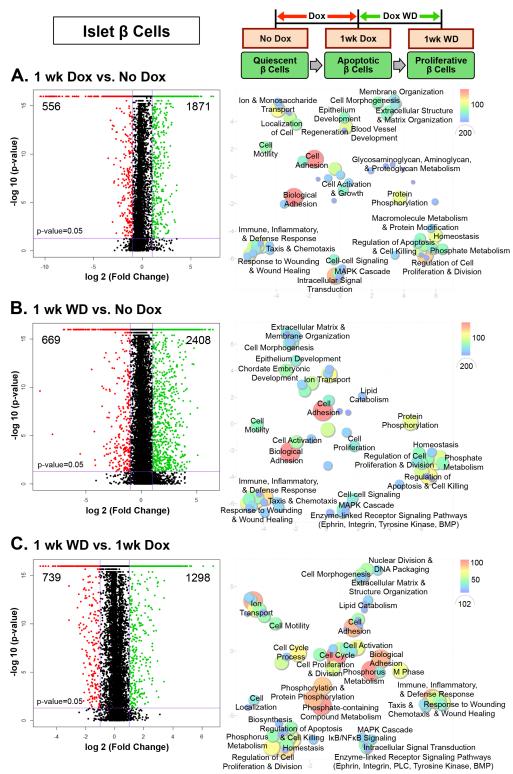


Figure 41. Changes in gene expression and biological processes in islet β cells from βVEGF-A mice during VEGF-A induction and normalization. (Left) Volcano plots display the differential expression of the statistically significant transcripts between β cells at (A) 1wk Dox vs. No Dox, (B) 1wk WD vs. No Dox, and (C) 1wk WD vs. 1wk Dox. Differential expression between conditions was calculated on the basis of fold change (cutoff ≥2.0) and the p-value was estimated by z-score calculations (cutoff 0.05). Each volcano plot shows the total number of upregulated (green) and downregulated transcripts (red) in the upper right and left corner, respectively. (Right) Scatterplot based on semantic similarity of summarized gene ontology (GO) biological processes identified based on the number of genes involved in these processes that were significantly up or downregulated (fold change cutoff ≥2.0) between β cells at (A) 1wk Dox vs. No Dox, (B) 1wk WD vs. No Dox, and (C) 1wk WD vs. 1wk Dox. The most significant GO terms (p≤0.05) were summarized and plotted, with size and color of points based on the number of genes involved (large, red=more genes; small, blue=fewer genes). Genes involved in multiple redundant processes may be represented more than once. Axes have no intrinsic value and are based on a matrix of semantic similarity between GO terms, meaning that semantically similar terms remain close together.

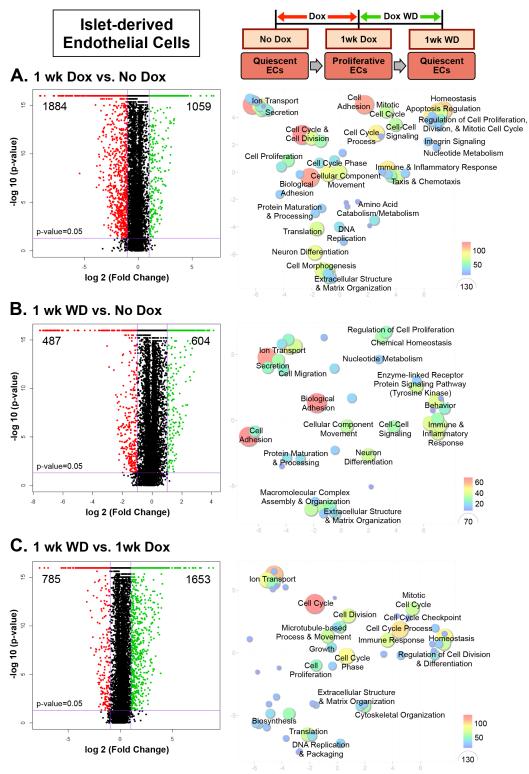


Figure 42. Changes in gene expression and biological processes in islet-derived endothelial cells from βVEGF-A mice during VEGF-A induction and normalization. (Left) Volcano plots display the differential expression of the statistically significant transcripts between endothelial cells at (A) 1wk Dox vs. No Dox, (B) 1wk WD vs. No Dox, and (C) 1wk WD vs. 1wk Dox. Differential expression between conditions was calculated on the basis of fold change (cutoff ≥2.0) and the p-value was estimated by z-score calculations (cutoff 0.05). Each volcano plot shows the total number of upregulated (green) and downregulated transcripts (red) in the upper right and left corner, respectively. (Right) Scatterplot based on semantic similarity of summarized gene ontology (GO) biological processes identified based on the number of genes involved in these processes that were significantly up or downregulated (fold change cutoff ≥2.0) between endothelial cells at (A) 1wk Dox vs. No Dox, (B) 1wk WD vs. No Dox, and (C) 1wk WD vs. 1wk Dox. The most significant GO terms (p≤0.05) were summarized and plotted, with size and color of points based on the number of genes involved (large, red=more genes; small, blue=fewer genes). Genes involved in multiple redundant processes may be represented more than once. Axes have no intrinsic value and are based on a matrix of semantic similarity between GO terms, meaning that semantically similar terms remain close together.

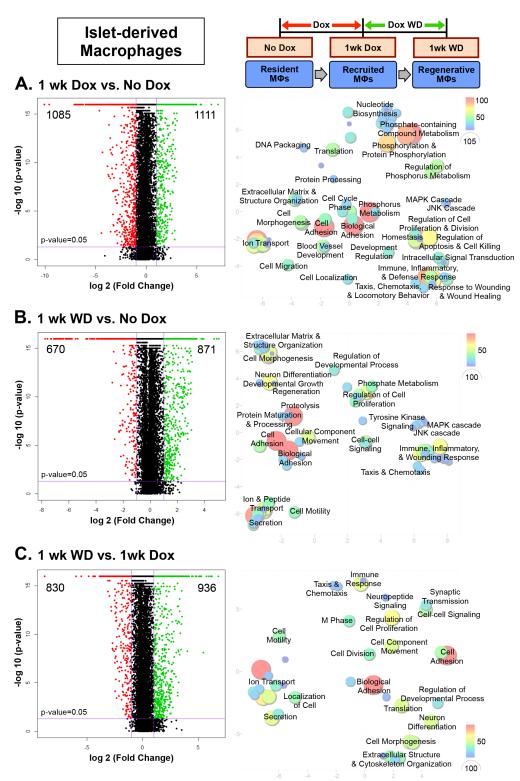


Figure 43. Changes in gene expression and biological processes in islet-derived macrophages from βVEGF-A mice during VEGF-A induction and normalization. (Left) Volcano plots display the differential expression of the statistically significant transcripts between macrophages at (A) 1wk Dox vs. No Dox, (B) 1wk WD vs. No Dox, and (C) 1wk WD vs. 1wk Dox. Differential expression between conditions was calculated on the basis of fold change (cutoff ≥2.0) and the p-value was estimated by z-score calculations (cutoff 0.05). Each volcano plot shows the total number of upregulated (green) and downregulated transcripts (red) in the upper right and left corner, respectively. (Right) Scatterplot based on semantic similarity of summarized gene ontology (GO) biological processes identified based on the number of genes involved in these processes that were significantly up or downregulated (fold change cutoff ≥2.0) between macrophages at (A) 1wk Dox vs. No Dox, (B) 1wk WD vs. No Dox, and (C) 1wk WD vs. 1wk Dox. The most significant GO terms (p≤0.05) were summarized and plotted, with size and color of points based on the number of genes involved (large, red=more genes; small, blue=fewer genes). Genes involved in multiple redundant processes may be represented more than once. Axes have no intrinsic value and are based on a matrix of semantic similarity between GO terms, meaning that semantically similar terms remain close together.

Upon VEGF-A induction, all cell populations increased expression of matrix remodeling enzymes involved in tissue repair and matrix degradation (MMPs, ADAMs, ADAMTS), as well as cell adhesion molecules involved in cell-matrix and cell-cell interactions, including leukocyte extravasation (ICAMs, MCAM, VCAM1, selectins) (Figures 44 and 45)<sup>282</sup>. Endothelial cells were also noted to have changes in integrin expression (Figure 45A), which regulate cell-matrix interactions and can affect cell proliferation and migration<sup>182,186,187</sup>. Some of these integrins are differentially regulated between VEGF-A induction and normalization. Macrophages increased expression of phagocytosis-related genes, M1 and M2 phenotype markers, and both pro- and anti-inflammatory chemokines and cytokines, which act to enhance leukocyte recruitment, among other effects (Figure 45B). These chemokines and cytokines may also influence  $\beta$  cells, which upregulated chemokine and cytokine receptors and also increased expression of chemokines associated with alternative (M2) macrophage phenotype activation (Figure 44).

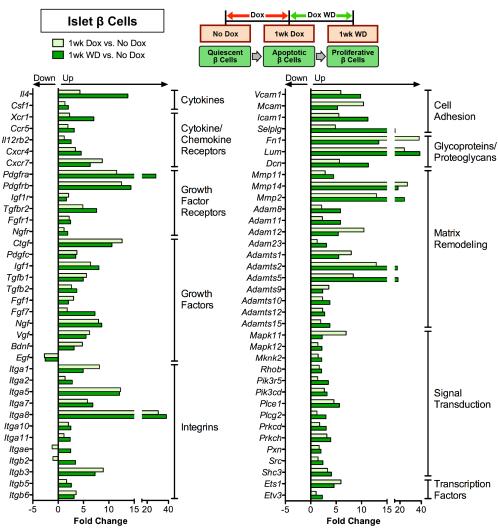


Figure 44. Gene expression profile of islet β cells by RNA-sequencing. Comparison of differential expression of cytokines, cytokine/chemokine receptors, growth factor receptors, growth factors, integrins, cell adhesion molecules, glycoproteins/proteoglycans, matrix remodeling enzymes, signal transduction molecules, and transcription factors downstream of signaling pathways between β cells after VEGF-A induction (1wk Dox, light green) and VEGF-A normalization (1wk WD, dark green). Plotted as fold change (cutoff ≥2.0) between 1wk Dox vs. No Dox baseline (light green) and 1wk WD vs. No Dox baseline (dark green); n=3-5 replicates/ time point.

In addition to matrix remodeling enzymes,  $\beta$  cells upregulated other matrix-interacting proteins including glycoproteins, proteoglycans, and several integrins, some of which are upregulated only as VEGF-A normalizes (Figure 44). All cell types increased expression of growth factors, and  $\beta$  cells also increased expression of growth factor receptors, which are further upregulated once VEGF-A normalizes and  $\beta$  cells begin to proliferate (Figures 44 and 45). Signal transduction molecules, many of which converge on the PI3K/Akt and ERK/MAPK pathways through activation of growth factor receptors and integrin signaling, are also upregulated in  $\beta$  cells along with transcription factors regulated by MAPK signaling (Figure 44)<sup>47,49,283,284</sup>. These data provide evidence for a model where macrophages, endothelial cells, and  $\beta$  cells through paracrine, and in some cases autocrine signaling, as well as through matrix remodeling and cell-matrix interactions promote  $\beta$  cell proliferation (Figure 46).

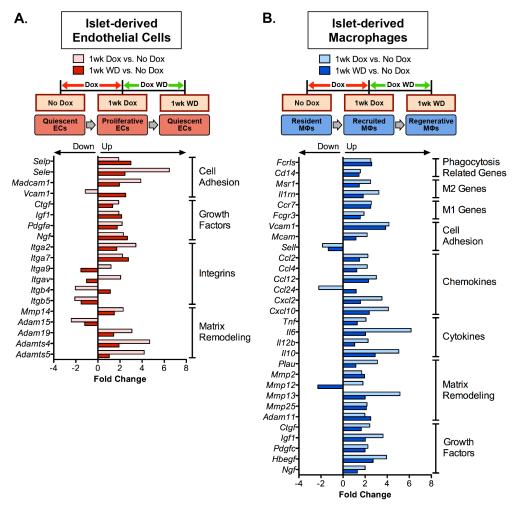


Figure 45. Gene expression profile of islet-derived endothelial cells and macrophages by RNA-sequencing. (A) Comparison of differential expression of cell adhesion molecules, growth factors, integrins, and matrix remodeling enzymes between endothelial cells after VEGF-A induction (1wk Dox, pink) and VEGF-A normalization (1wk WD, red). Plotted as fold change (cutoff ≥2.0) between 1wk Dox vs. No Dox baseline (pink) and 1wk WD vs. No Dox baseline (red); n=4-5 replicates/time point. (B) Comparison of differential expression of phagocytosis-related genes, macrophage phenotype markers (M1, classical; M2, alternative), cell adhesion molecules, chemokines, cytokines, matrix remodeling enzymes, and growth factors between macrophages after VEGF-A induction (1wk Dox, light blue) and VEGF-A normalization (1wk WD, dark blue). Plotted as fold change (cutoff ≥2.0) between 1wk Dox vs. No Dox baseline (light blue) and 1wk WD vs. No Dox baseline (dark blue); n=4-5 replicates/time point.

### **Discussion**

Adult  $\beta$  cell proliferation is extremely limited, and the signals regulating this process are poorly understood (see Chapter I, Expansion of adult  $\beta$  cells). Therefore, new approaches are needed to unravel the pathways and interactions that may be involved in this process. Several growth factors, hormones, nutrients, and other signals have been shown to regulate  $\beta$  cell proliferation<sup>47-49</sup>. However, these regulatory signals and downstream pathways are extremely complex, and can lead to activation of several signaling pathways including PI3K/Akt, ERK/MAPK, and JAK-STAT, among others. Here we discovered a new approach to induce  $\beta$  cell proliferation where the signals promoting this proliferation are generated by an islet microenvironment composed of endothelial cells and recruited macrophages in addition to islet  $\beta$  cells. By separating this complex microenvironment into the component cell types, we identified factors that promote interactions between these cells and the extracellular matrix that cause adult  $\beta$  cell proliferation.

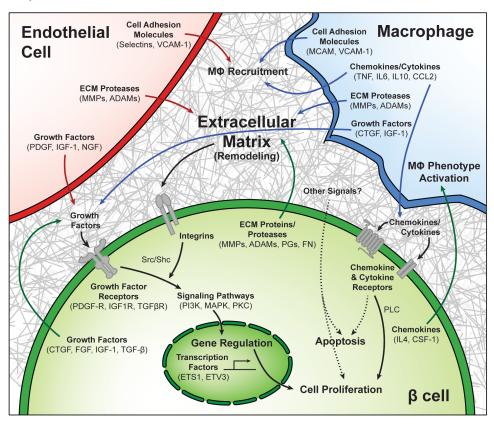


Figure 46. Model of interactions between β cells, macrophages, endothelial cells, and the extracellular matrix in β cell regeneration. Upon VEGF-A induction intra-islet endothelial cells (ECs) proliferate while increasing expression of cell adhesion molecules and growth factors, and altering their expression of integrins and extracellular matrix (ECM) remodeling enzymes. This increase in endothelial cell adhesion molecules aids in the recruitment of macrophages (ΜΦs), which upon islet infiltration also have increased expression of cell adhesion molecules compared to resident macrophages. These recruited macrophages also produce both pro- and anti-inflammatory chemokines and cytokines, which can act on circulating monocytes to increase recruitment to islets, and on  $\beta$  cells, which have increased expression of chemokine and cytokine receptors. In addition to these chemokines and cytokines, which become increasingly less inflammatory as VEGF-A normalizes, macrophages produce growth factors and matrix remodeling enzymes that may play a role in β cell proliferation when VEGF-A normalizes. Upon VEGF-A induction, β cells increase expression of several growth factors and growth factor receptors, which are upregulated even more upon VEGF-A normalization. They also have increased expression of several integrins and other proteins involved in matrix remodeling and cell-matrix interactions. During VEGF-A induction and normalization, β cells produce increasingly more chemokines known to promote a regenerative phenotype (M2, alternative) in macrophages. Growth factors from all cell types acting on an increased number of growth factor receptors being expressed on  $\beta$  cells, as well as an increase in  $\beta$  cell integrin signaling cause activation of several downstream signals converging on the PI3K/Akt and ERK/MAPK pathways, which can lead to β cell proliferation observed after VEGF-A normalization. Other signals from cells in the microenvironment, or from the rapidly remodeling extracellular matrix may also play a role in β cell apoptosis and/or the subsequent β cell proliferation.

By specifically depleting macrophages in  $\beta$ VEGF-A mice, we demonstrated that macrophages are required for  $\beta$  cell proliferation in the islet microenvironment. We had previously noted that these recruited macrophages express markers of both the classical pro-inflammatory (M1) phenotype as well as the alternative (M2) phenotype involved in tissue repair and regeneration<sup>153</sup>. An increasing number of studies using other models of  $\beta$  cell injury have observed a role for macrophages in regulating  $\beta$  cell recovery through a variety of mechanisms<sup>220-222</sup>. Our data supports a model where macrophages are recruited to islets upon VEGF-A induction by increased expression of cell adhesion molecules on both macrophages and endothelial cells, as well as increased production of chemokines and cytokines involved in leukocyte extravasation by macrophages already located in the islet microenvironment (Figure 46)<sup>282</sup>. The future studies we outlined using a model of inducible endothelial cell-specific knockdown of VEGFR2 in these mice will allow us to determine whether endothelial cells are also required for this macrophage infiltration to occur (Figure 37), and further studies will be needed to identify the specific signaling molecules involved.

Although macrophages are required for  $\beta$  cell proliferation, this proliferation does not begin until 1 week after Dox withdrawal when VEGF-A normalizes, despite the increased macrophage infiltration upon VEGF-A induction. This observation indicates that during Dox withdrawal, (1) macrophages experience a shift to a more regenerative phenotype, (2) removal of inhibitory signals or production of permissive signals from endothelial cells occurs as they switch from proliferative back to quiescent, and/or (3)  $\beta$  cells increase their ability to respond to pro-proliferative signals from the microenvironment.

Many genes upregulated in macrophages with VEGF-A induction remain elevated after VEGF-A normalization; however, expression of pro-inflammatory cytokines (e.g., Tnf, Il6) decreased, perhaps in response to increasing expression of signals from  $\beta$  cells known to drive macrophages toward a more tissue reparative phenotype (Il4, Csf1), supporting the theory that macrophage phenotype shifts during Dox withdrawal<sup>214,285</sup>. Because macrophages are the primary producers of cytokines and chemokines in the islet microenvironment, and these molecules have been shown to have widely disparate effects on cells—from inducing apoptosis, to preventing  $\beta$  cell proliferation, to promoting  $\beta$  cell proliferation—we considered the possibility that these phenotypic changes in macrophages may indicate that they are contributing to  $\beta$  cell apoptosis during VEGF-A induction then shifting function to promote  $\beta$  cell proliferation during Dox withdrawal<sup>286-290</sup>. However, equivalent  $\beta$  cell loss occurs when macrophages are removed from the microenvironment (Figure 36G), demonstrating that while these recruited macrophages may alter their gene expression profile and phenotype over the course of VEGF-A induction and normalization, they do not promote  $\beta$  cell apoptosis.

Although VEGF-A-induced endothelial cell expansion was temporally associated with  $\beta$  cell loss in our model, we are unable to determine whether this damage is due to an increase in pro-apoptotic signals from endothelial cells or space constraints within islets from the rapidly expanding endothelium<sup>274</sup>. Our transcriptome analysis did not identify any candidate pro-apoptotic signals increased in proliferative endothelial cells, but these cells do have significant changes in matrix remodeling enzymes which may perturb  $\beta$  cell-matrix interactions. Although not much is known about the role of  $\beta$  cell-matrix interactions in maintaining  $\beta$  cell mass and promoting  $\beta$  cell survival in mature islets *in vivo*, studies of  $\beta$  cells in culture have demonstrated the importance of these cell-matrix interactions in protecting  $\beta$  cells

from apoptosis and promoting  $\beta$  cell survival<sup>291,292</sup>. It is possible that the disturbance in the extracellular matrix caused by the sudden burst in endothelial cell expansion upon VEGF-A induction disrupts crucial  $\beta$  cell-matrix interactions, leading to  $\beta$  cell apoptosis. Disrupting VEGFR2 signaling in endothelial cells both before and after VEGF-A induction (Figure 37) will allow us to further clarify the role of endothelial cells in both  $\beta$  cell loss and proliferation.

Despite the potential deleterious effects of endothelial cells, they also have increased expression of several growth factors known to promote β cell proliferation, including IGF-1, PDGF, and CTGF (Figure 45A)<sup>48,51,111,112</sup>. These and other growth factors are also upregulated in macrophages and β cells upon VEGF-A induction and remain elevated as VEGF-A normalizes. Endothelial cells, macrophages, and β cells also produce molecules that remodel the extracellular matrix, which can lead to the release of growth factors from the matrix in addition to altering cell-matrix interactions<sup>270,271</sup>. Interestingly, throughout the process of VEGF-A induction and normalization,  $\beta$  cells have increasingly higher expression of growth factor receptors, cytokine receptors, chemokine receptors, and integrin receptors, all of which are involved in regulating  $\beta$  cell proliferation<sup>47-49,288,293,294</sup>. This finding suggests that  $\beta$  cells become more responsive to the increase in growth factors, cytokines, chemokines, and signals from the rapidly remodeling extracellular matrix as VEGF-A normalizes. These receptors activate several downstream signaling pathways, many of which converge on the ERK/MAPK pathway. Extensive cross-talk between these pathways, and the fact that regulation of these signals occurs primarily at the protein level makes it difficult to make conclusions about pathway activation based on gene expression. However, we do see significant upregulation of several molecules involved in signal transduction downstream from growth factor receptors, chemokine receptors, and integrins (PI3K/Akt pathway, PLC, MAPK pathway, etc.), and upregulation of transcription factors regulated by the ERK/MAPK pathway<sup>47-49,283,284,295,296</sup>. Each of these signaling pathways promote β cell proliferation by modifying various cell-cycle activators and inhibitors that regulate the G1/S checkpoint<sup>48,297</sup>.

Therefore, we propose a model where  $\beta$  cell proliferation is regulated by simultaneous, and potentially synergistic, activation of signaling pathways due to (1) increased growth factors produced by  $\beta$  cells, endothelial cells, and macrophages, (2) increased production of growth factor receptors on  $\beta$  cells, and (3) increased integrin activation by the extracellular matrix (Figure 46). Potential contributions from chemokines, cytokines, or other signals, either from cells or the extracellular matrix to this process are less clear; however, they could have a role in mediating  $\beta$  cell apoptosis, seen upon VEGF-A induction, or  $\beta$  cell proliferation when VEGF-A normalizes. Although many of these growth factor, and integrin pathways involved in  $\beta$  cell proliferation in the  $\beta$ VEGF-A model have been studied in mouse  $\beta$  cell proliferation, not much is known about how they are activated and regulated in human  $\beta$  cells. Because this regenerative microenvironment is capable of promoting human  $\beta$  cell proliferation, it will be important in future studies to identify which combination of cytokines, growth factors, or other signals in this microenvironment activate relevant mitogenic signaling pathways in human  $\beta$  cells.

### CHAPTER V

# EVALUATION OF ADULT HUMAN β CELL PROLIFERATION IN RESPONSE TO POTENTIAL MITOGENS IN VITRO

### Introduction

Loss of pancreatic  $\beta$  cells occurs in both type 1 diabetes mellitus (DM), which is characterized by autoimmune destruction of  $\beta$  cells, and type 2 DM in which  $\beta$  cell dysfunction and deficiency occur in the context of peripheral insulin resistance. Diabetes affects an estimated 9% of the global population, and therapies targeted at replacing or regenerating lost  $\beta$  cells have the potential to greatly reduce the risk of complications and death in this large patient population<sup>53,54</sup>. Replacement of  $\beta$  cells by human islet transplantation can successfully reverse type 1 DM, however challenges with immunosuppression and a limited supply of islets have prompted the development of alternative strategies for human  $\beta$  cell replacement<sup>65,66</sup>. Efforts to differentiate  $\beta$  cells from human embryonic stem cells or human induced pluripotent stem cells have advanced in recent years, and studies in rodents have suggested the possibility of producing  $\beta$  cells through transdifferentiation of  $\beta$  cells from other pancreatic lineages<sup>97,98,100,102</sup>. Other efforts have focused on developing drugs that induce  $\beta$  cell proliferation for use in expanding the supply of human  $\beta$  cells for transplantation or promoting regeneration of the small population of functional  $\beta$  cells that remain even in patients with longstanding diabetes<sup>104-106</sup>. (See Chapter I, Pancreatic  $\beta$  cell replacement as a therapeutic goal).

Studies of human pancreas samples have found that  $\beta$  cell proliferation peaks neonatally at about 1-3% then sharply declines after the first year of life eventually approaching near 0% and remains at this low level throughout adulthood 32,35,37,38. The extremely low proliferation rate in adult human  $\beta$  cells and their failure to respond to most mitogenic stimuli suggest that even though these cells retain expression of factors required for cell cycle entry, the progression of the cell cycle is halted by cell cycle inhibitors 250,297,298. However, overexpressing cyclins and/or cyclin-dependent kinases (CDKs) can induce adult human  $\beta$  cell proliferation suggesting that even though none have been identified yet, factors or compounds capable of overcoming the inhibitors and reactivating cell cycling in adult human  $\beta$  cells may exist 299-301.

The majority of studies focused on understanding and identifying regulators of  $\beta$  cell proliferation have been performed in animal models, and more recently high-throughput screens have been used with the goal of finding even more potential human  $\beta$  cell mitogens<sup>128,129,135,302,303</sup>. Unfortunately, even though several factors that induce robust proliferation of rodent  $\beta$  cells have been identified, including signaling proteins, hormones, growth factors, neurotransmitters, and small molecules, most have either not been tested on human  $\beta$  cells or are unable to induce adult human  $\beta$  cell proliferation<sup>120,122,128,129,302-308</sup>. Because rodent and human  $\beta$  cells seem to differ so profoundly in their proliferative potential, it is critical that mitogenic factors identified in rodent studies or high-throughput screens be tested in human  $\beta$  cells to establish their therapeutic potential prior to investing further in their development. Though some progress has been made in developing methods for culturing dispersed human islet cells for screening potential mitogens, several challenges remain: (1) Near negligible levels of baseline

human β cell proliferation makes it difficult to develop methods sensitive enough to detect changes in proliferation. Even at its peak neonatally, human β cell proliferation only reaches ~2%, which has been proposed as a target level for therapies<sup>46</sup>. However, identifying compounds able to stimulate β cell proliferation from near zero to only ~2% requires a highly sensitive and specific protocol. (2) Suitable human β cells lines are not available, requiring the use of islets from human donors. The functional variability due to both intrinsic (e.g., genetics, race, age, BMI) and extrinsic (e.g., isolation protocol, time in culture) factors, makes it difficult to consistently reproduce results from a small sample size<sup>135,242</sup>. (3) Confounding artifacts in islet cell culture, including close apposition of non-β endocrine cells as well as highly proliferative fibroblasts, make it difficult to achieve the sensitivity required to automate analysis<sup>129,135,309</sup>.

To address the need to test potential  $\beta$  cell mitogens on adult human  $\beta$  cells, we developed a scalable method for evaluating human  $\beta$  cell proliferation *in vitro* using automated plate imaging and proliferation analysis. All donor islets were evaluated for proper  $\beta$  cell function in a dynamic cell perifusion system and for proliferative potential. To ensure the integrity of  $\beta$  cell identification and avoid artifacts due to proliferating fibroblasts also in culture, we used both cytoplasmic and nuclear markers to identify  $\beta$  cells for proliferation analysis. The automated image analysis produced results comparable to the conventional method of manually counting  $\beta$  cells to quantify proliferation. We then used this method to test 13 potential human  $\beta$  cells mitogens at a variety of concentrations at both basal (5 mM) and high (11 mM) glucose. These proposed mitogens had been identified previously as playing a role in  $\beta$  cell mass regulation and/or proliferation in zebrafish, rodents, or in a few cases, human systems (see Table 8)<sup>45,51,120,122,128,305-307,310-321</sup>. This method allowed us to identify which of the proposed  $\beta$  cell mitogens we tested are capable of promoting adult human  $\beta$  cell proliferation, and provides a solid framework for testing and identifying additional adult human  $\beta$  cell mitogens in the future.

### Results

### Developing a method for evaluating human $\beta$ cell proliferation in vitro

To provide a platform for testing potential adult human  $\beta$  cell mitogens and to minimize the time required to evaluate the effect of these various treatments on human  $\beta$  cell proliferation *in vitro*, we developed a method of dispersing, plating, and treating human islet cells in a 384-well format that provides for quality control of human  $\beta$  cells from different donors and automates plate imaging and proliferation analysis. Prior to treatment with test compounds, islets were purified to homogeneity then islet quality was assessed in a dynamic cell perifusion system for insulin secretory response (Figure 47A). Islets were then dispersed into a single cell suspension with trypsin (Figure 47B), and as an additional quality control measure, an aliquot of islet cells from each donor was co-transduced with adenoviruses expressing cell cycle regulators cyclin D3 and cdk6 to induce cell cycling and evaluate their proliferative potential (Figure 47C). To determine whether glucose had an effect on  $\beta$  cell proliferation at baseline or in response to cyclin D3 and cdk6 overexpression or treatment with potential  $\beta$  cell mitogens, transductions, plating, and treatments were performed at both basal (5 mM) and high (11 mM) glucose concentration.

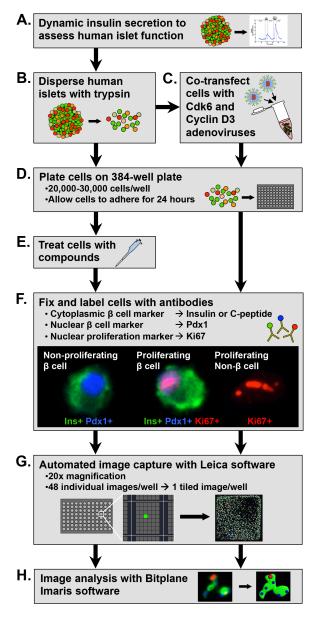


Figure 47. Workflow for semi-automated evaluation of human β cell proliferation. Human islets from each donor were evaluated for  $\beta$  cell function in a cell perifusion system (A), and then dispersed into a single cell suspension with trypsin (B). An aliquot of dispersed cells from each donor was co-transfected with cdk6 and cyclin D3 adenoviruses to evaluate their proliferative potential (C) prior to being plated on 384-well collagen I-coated plates (D) to evaluate β cell proliferative potential. Nontransfected cells were also plated, allowed to adhere for 24 hours and then treated with compounds for 72 hours (E). Following the treatment period, all cells were fixed and labeled with antibodies to identify B cells using both cytoplasmic (insulin or C-peptide) and nuclear (Pdx1) markers and to identify proliferating cells (Ki67) (F). Cells were imaged using Leica LAS AF Matrix Developer software, which automates the capture of 48 images per well at 20x magnification and tiles them to produce a single, merged image of each well (G). These images were then analyzed for β cell proliferation using Bitplane Imaris software (H).

Both transduced and non-transduced cells were plated on a 384-well collagen I-coated plate (Figure 47D). During initial method development we tested other plate coatings, including poly-D-lysine (PDL) and extracellular matrix from HTB-9 human bladder carcinoma cells (ECM), and determined that there was no significant difference in β proliferation measured between the coatings<sup>162</sup>. However we did note that cells had lower adherence throughout the incubation and washing when plated on ECM-coated wells (only half the number of total β cells for quantification as collagen I or PDL-coated plates). Thus, moving forward we used commercially available collagen I-coated plates in all of our experiments. Islet cells were allowed to adhere for 24 hours after plating, and then non-transduced cells were treated with test compounds for 72 hours (Figure 47E). Following the treatment, all cells were fixed with paraformaldehyde and immunolabeled for B cell and proliferation markers (Figure 47F).

Dispersed endocrine cells in culture form dense monolayer clusters, making it difficult to unambiguously assign a cytoplasmic stain to a specific nucleus in the cluster<sup>129</sup>. Another aspect of human islet cell culture that can complicate accurate  $\beta$  cell identification is the presence of rapidly proliferating fibroblastic cells, which are often closely associated with endocrine cell clusters<sup>129,135</sup>. Because baseline proliferation of adult human β cells is so low, misidentification of even a small percentage of these non-β cells will confuse the results and make it difficult to detect differences in β cell proliferation caused by compounds of interest. It is also possible that dedifferentiation or loss of  $\beta$  cell identity may occur during culture as some β cell markers are not stable in culture<sup>309</sup>. To minimize errors from these confounding artifacts of islet cell culture, we used both cytoplasmic insulin or C-peptide and nuclear Pdx1 to identify β cells for quantification in addition to Ki67 as a proliferation marker (Figure 47F). To avoid confusion, in the remainder of the text we only use insulin (rather than insulin or C-peptide) to refer to the β cell-specific cytoplasmic marker used.

For cell imaging in 384-well plates, we set up a template matrix for the entire well using the Multiple Mosaics function. This matrix was made up of one image mosaic per well that encompasses the entire area of the well. Each mosaic captured 48 images at 20x magnification using autofocus to find the focal plane in every field and tiled those images to produce a single, merged image of each well (Figure 47G). Once established, this template matrix enabled the automation of this process, which yielded highly resolved images for analysis. Images were then exported for analysis using Bitplane Imaris 7.6 software (Figure 47H).

In our protocol,  $\beta$  cell proliferation was defined as % proliferating  $\beta$  cells (insulin+Pdx1+Ki67+)/total  $\beta$  cells (insulin+Pdx1+). Prior approaches have quantified proliferating and total  $\beta$  cells by manually counting  $\beta$  cells in each image<sup>45</sup>. We were able to automate this process using Imaris 7.6 software. After loading an image into the Imaris software (Figure 48A) we first defined the insulin+ area using the Surfaces function (Figure 48B). The Spots function was then used to identify Pdx1+ nuclei. These Pdx1+ spots were then filtered by first masking the Pdx1 channel on the insulin surface created previously; second, creating spots on the masked Pdx1 channel; and finally, identifying the original Pdx1+ spots that co-localized with the masked Pdx1+ spots using the Co-localize Spots tool. These insulin+Pdx1+ spots represented the number of total  $\beta$  cells in the well (Figure 48C). Proliferating

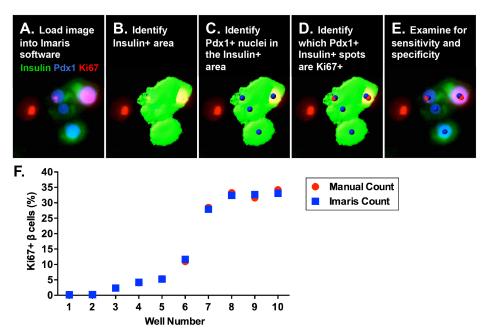


Figure 48. Validation of the Imaris analysis method for quantifying human β cell proliferation. Images were loaded into Imaris software (A), and then Insulin+ area was identified using the Surfaces function (B). The Spots function was then used to identify the Pdx1+ nuclei that were co-localized with Pdx1+ staining masked by the Insulin+ surface. These Pdx1+Insulin+ spots represent the total number of β cells in the well (C). Ki67+ nuclei were then identified using the Spots function, and co-localized with the Pdx1+Insulin+ spots to determine the number of Pdx1+Insulin+Ki67+ proliferating β cells (D). The image with Surface and Spot markups was then examined for sensitivity and specificity of the analysis (E). Quantification of human  $\beta$  cell proliferation using Imaris software was validated using images from 10 different wells with varying β cell proliferation rates due to different levels of cyclinD3 and cdk6 (wells #1-2, no transduction; wells #3-10, transduced with 50-250 MOI). Each well was evaluated by both manual counting and the Imaris algorithm (A-E) to determine the number of proliferating  $\beta$  cells. The average coefficient of variation between manual and Imaris counts for each well was 3.2% (range 0.6-10.7%) indicating that there is no significant difference between manual and Imaris analysis methods (F).

Ki67+ nuclei were then identified using the Spots function and co-localized with the insulin+Pdx1+ spots defined in the previous step using the Co-localize Spots tool. These insulin+Pdx1+Ki67+ spots then represented the number of proliferating  $\beta$  cells in the well (Figure 48D). Once the parameters and thresholding for the Surfaces and Spots functions had been established, the Batch Coordinator was used to process all images from the plate. Following analysis, images with Surface and Spot markups were examined for sensitivity and specificity and to ensure that no staining artifacts have interfered with the analysis (Figure 48E). Low sensitivity indicated that the thresholds for the Surfaces and/or Spots functions were set too low to detect all  $\beta$  cells, and low specificity indicated that thresholds were set too high and were either misidentifying background staining or, in the case of the Surfaces function, were bleeding into unstained areas and incorrectly identifying non- $\beta$  cells as  $\beta$  cells. If necessary, parameters and thresholds were adjusted and images reanalyzed.

### Automated image analysis accurately measures human β cell proliferation

Before using this method to evaluate the effect of potential mitogens on  $\beta$  cell proliferation, we sought to determine whether quantification of human adult  $\beta$  cell proliferation using Imaris software was comparable to the conventional method of manually counting  $\beta$  cells over a wide range of proliferation indices. We performed this analysis validation using images from 10 different wells with varying levels of human adult  $\beta$  cell proliferation, which was achieved by inducing different levels of cyclin D3 and cdk6 expression in dispersed islet cells. Each well was evaluated for  $\beta$  cell proliferation both by manually counting each  $\beta$  cell and by using the Imaris algorithm (Figure 48A-E) to count total and proliferating  $\beta$  cells (Figure 48F). The average coefficient of variation between manual and Imaris counts for each well was 3.2±1.0%, indicating no significant differences between manual and automated analysis methods and demonstrating that adult human  $\beta$  cell proliferation can be accurately measured using this automated protocol.

### Human β cells in purified islet preparations are functional and demonstrate proliferative potential

To minimize the effects of variability between human islet donors, all human islets were purified by handpicking and evaluated for  $\beta$  cell function in a dynamic cell perifusion system<sup>242</sup>. Human islet preparations used to test potential mitogens were examined in a cell perifusion system and had normal basal insulin secretion at 5.6 mM glucose and an elevated insulin secretory response when stimulated with either 16.7 mM glucose (5.8±1.3-fold above baseline) or 16.7 mM glucose + IBMX (12.4±2.7-fold above baseline). Cell cycling was induced in dispersed islet cells from all donors by co-transduction with adenoviruses expressing cyclin D3 and cdk6, which significantly increased human  $\beta$  cell proliferation at basal (5 mM) and high (11 mM) glucose (Figure 49). Baseline  $\beta$  cell proliferation at basal (5 mM) glucose was 0.03±0.01%, which is comparable to reported proliferation indices of adult human  $\beta$  cells from autopsy samples, and increased to 24.5±5.5% with transduction (Figure 49C)<sup>32,35,37,38</sup>. Glucose concentration had no effect on human  $\beta$  cell proliferation of either control or transduced  $\beta$  cells (Figure 49C).

### Evaluation of potential adult human β cell mitogens

After validating the accuracy of our proliferation analysis, we wanted to determine whether this method could be used to effectively evaluate potential human  $\beta$  cell mitogens. We chose to test our method using 13 compounds implicated in  $\beta$  cell mass regulation or  $\beta$  cell proliferation including neurotransmitters, growth factors, hormones, and proteins and small molecules that modulate different signaling pathways (DYRK family, TGF $\beta$  superfamily, adenosine kinase pathway) (Table 8). All of these compounds were previously tested in rodent or zebrafish models, and three (harmine, GABA, PDGF) had also been tested in various *in vitro* and/or *in vivo* human systems<sup>45,51</sup>.

Human islet cells were treated with these potential human  $\beta$  cell mitogens at a range of concentrations at both basal (5 mM) and high (11 mM) glucose (see Table 6; Figure 50). Treatment of human islet cells with harmine caused a significant increase in  $\beta$  cell proliferation at 1  $\mu$ M and 10  $\mu$ M in both glucose concentrations (Figure 50A). Harmine was the only compound that significantly increased  $\beta$  cell proliferation across all conditions tested. GABA, PDGF, UK-432097, and A-134974 each demonstrated a limited increase in  $\beta$  cell proliferation in a single condition (Figure 50B,H,I,K). Other compounds tested, including serotonin, myostatin, activin A, follistatin-like 3, NECA, prolactin, erythropoietin, and exendin-4 had only marginal to no effect on human  $\beta$  cell proliferation (Figure 50). Glucose level did not have a significant effect on  $\beta$  cell proliferation in any treatment condition tested.

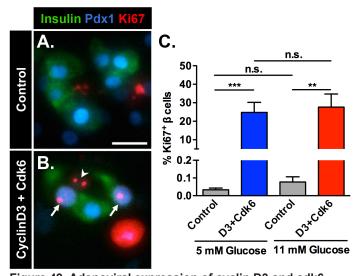
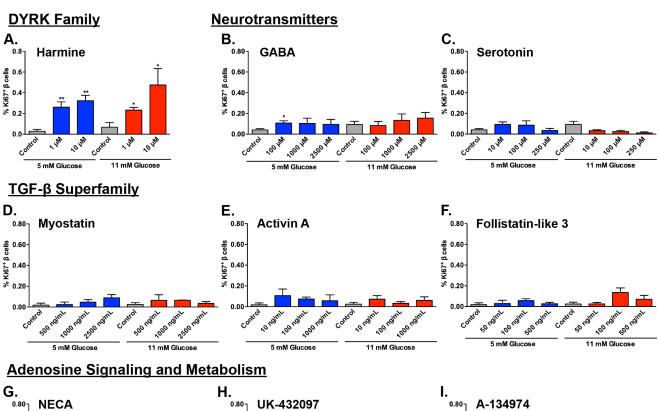
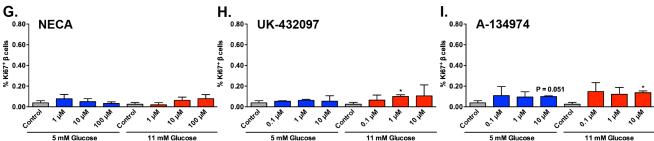


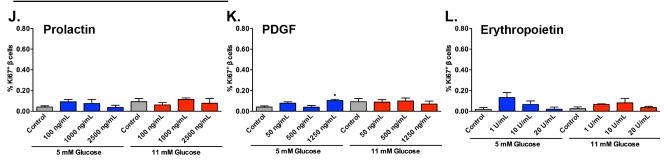
Figure 49. Adenoviral expression of cyclin D3 and cdk6 induce human  $\beta$  cell proliferation. Dispersed islet cells from all human donors were plated following dispersion in basal (5mM) or high (11 mM) glucose. An aliquot of cells at each glucose level was co-transduced with adenoviruses encoding cell cycle regulators cyclin D3 and cdk6 (D3+Cdk6) prior to plating. (A-B) Labeling for cytoplasmic β cell marker, insulin (Ins, green), nuclear β cell marker, Pdx1 (blue), and proliferation marker, Ki67 (red) in control (A) and transduced (B) cells at 5 mM glucose. Arrows mark proliferating β cells, and arrowhead marks a proliferating non-β cell. Scale bar in panel A represents 20 µm and also applies to B. (C) Adenoviral expression of cyclin D3 and cdk6 induces human  $\beta$  cell proliferation in cells from all donors at both basal (5 mM) and high (11 mM) glucose; n=6-9 donors/treatment. \*\* p<0.01 5 mM glucose control vs. D3+Cdk6. \*\*\*p<0.001 11 mM glucose control vs. D3+Cdk6. Comparisons between controls or transfected cells at 5 mM vs. 11 mM glucose were not statistically significant (n.s.).

Tabl	Table 8. Function and reported effects	reported effects of compounds tested on human islet cells	
COMPOUND	FUNCTION	REPORTED EFFECTS	REFERENCES
DYRK Family			
Harmine	Dyrk1a inhibitor	Increases β cell proliferation (mouse, rat, human) Decreases β cell development (mouse)	Wang et al., 2015; Rachdi et al., 2014
Neurotransmitters			
γ-Aminobutyric acid (GABA)	Inhibitory neurotransmitter	Increases β cell proliferation (mouse, human)	Soltani et al. 2011; Tian et al. 2013; Purwana et al., 2014
Serotonin (5HT)	Monoamine neurotransmitter	Regulates pregnancy-related β cell expansion (mouse)	Kim et al., 2010
TGF-β Superfamily			
Myostatin (GDF-8)	Growth differentiation factor	Regulates islet development and insulin sensitivity (mouse)	Brown et al., 2010
Activin A	Signaling and regulation of reproduction, development, and homeostasis	Regulates islet development and insulin secretion (mouse) Increases β cell proliferation (rat)	Brown et al., 2010; Brun et al., 2004
Follistatin-like 3 (FSTL3)	Activin and myostatin antagonist	Regulates β cell mass (mouse)	Mukherjee et al., 2007
Adenosine Signaling/Metabolism			
NECA	Adenosine receptor agonist	Increases $\beta$ cell proliferation (zebrafish, mouse)	Andersson et al., 2012; Tsuji et al., 2014
UK-432097	Selective A <sub>2A</sub> adenosine receptor agonist	Decreases inflammation and promotes wound healing	Xu et al., 2011; Mantell et al., 2010
A-134974	Selective adenosine kinase inhibitor	Increases β cell proliferation (zebrafish)	Andersson et al., 2012
Hormones/Growth Factors			
Prolactin (PRL)	Lactogenic hormone	Regulates pregnancy-related $\beta$ cell expansion (rat, mouse)	Brelje et al., 2004; Huang et al., 2009
Platelet-derived growth factor (PDGF)	Cell growth and division	Regulates age-dependent $\beta$ cell proliferation (mouse, human)	Chen et al., 2011
Erythropoietin (EPO)	Erythropoiesis and angiogenesis	Increases β cell proliferation (mouse)	Choi et al., 2010
Exendin-4 (Ex-4)	GLP-1 agonist	Regulates β cell mass (rat) Increases β cell proliferation (rat)	Xu et al., 1999; Perfetti et al., 2000; Tourrel et al., 2001





### **Hormones and Growth Factors**



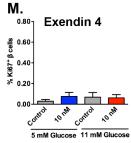


Figure 50. Human β cell proliferation is induced by treatment with some, but not all, compounds tested. Treatment of human islet cells with harmine (A) at 1 µM and 10 µM in 5 mM or 11 mM glucose increased  $\beta$  cell proliferation. \*\*p<0.01 5 mM glucose control vs. 1  $\mu M$ harmine or 10 µM harmine. \*p<0.05 11 mM glucose control vs. 1 µM harmine or 10 µM harmine. Neurotransmitters GABA (B) and serotonin (C) had a limited effect on β cell proliferation, and only treatment with 100 µM GABA at 5 mM glucose was statistically significant \*p<0.05 5 mM glucose control vs. 100 μM GABA. Treatment with members of the TGF-β superfamily myostatin (D), activin A (E), and follistatin-like 3 (F) had no significant effect on β cell proliferation. Compounds involved in adenosine signaling and metabolism NECA (G), UK-432097 (H), and A-134974 (I) had a minimal effect with only 1 µM UK-432097 and 10 µM A-134974 at 11 mM glucose causing a small, but statistically significant increase in β cell proliferation. \*p<0.05 11 mM glucose control vs. 1 μM UK-432097 and control vs. 10 µM A-134974. Hormones prolactin (J), PDGF (K), erythropoietin (L), and exendin-4 (M) had no effect on β cell proliferation other than 1250 ng/mL PDGF at 5 mM glucose, which caused a small, but significant increase in proliferation. \*p<0.05 5 mM glucose control vs. 1250 ng/mL PDGF. Comparisons between controls or compound treatments at 5 mM vs. 11 mM glucose were not statistically significant in any compound tested; n=3-6 donors/treatment condition.

### **Discussion**

As efforts to identify  $\beta$  cell mitogens with the potential to stimulate human  $\beta$  cell regeneration have increased over the last several years, the difficulty of translating findings from animal models to humans has highlighted the need for effective strategies to test these discoveries in human systems. We developed a semi-automated method for evaluating adult human  $\beta$  cell proliferation *in vitro* that provides a platform for testing proposed human  $\beta$  cell mitogens and addresses some of the ongoing challenges of working with human islets in culture.

The effect that differences in human islet isolation procedures and donor attributes (age, sex, BMI, race) and genetic background have on the ability of an islet preparation to respond to any given stimulus is not fully understood. However, a previous study that looked at evaluating human β cell proliferation in vitro noted low reproducibility across donors, suggesting that these variations may influence the ability of a given islet preparation to respond to test compounds<sup>135</sup>. We minimized variability by (1) handpicking all islets upon arrival to homogeneity to minimize the effect of impurities on functional studies or in culture, and (2) performing functional assessments on human islets prior to experimentation to decrease the likelihood of misinterpreting data due to dysfunctional islets<sup>242</sup>. Because adult human β cell proliferation was the parameter we were evaluating and baseline proliferation is low or negligible, in addition to assessing dynamic insulin secretion we also assessed the proliferative potential of β cells from each islet preparation by overexpressing cyclin D3 and cdk6 with adenovirusus, which induces cell cycling. Using this positive control, we demonstrated that β cells from all islet preparations we used were capable of entering the cell cycle. Although variation between samples is an expected feature of primary cell preparations, by employing these quality control measures we ensured that the β cells used to evaluate potential mitogens were functional and able to proliferate.

Using an adult human islet cell culture system to assess human β cell proliferation makes it possible to scale for rapid assessment of multiple compounds at different concentrations. However, as in any in vitro system, we acknowledge that some mitogenic agents may work through mechanisms not recreated in culture. The effects that substrate and the instability of β cell markers have on the responsiveness of human β cells to mitogenic stimuli in culture versus in vivo are unknown, though we noticed no difference in proliferation index across the matrix substrates we tested 162,309. Dispersed human islet cells form a heterogeneous monolayer culture consisting of tight clusters of endocrine cells and rapidly proliferating fibroblastic cells. The close spatial association of these different cell types can make it extremely difficult to definitively identify β cells using only a cytoplasmic marker, and cause misidentification of proliferative fibroblastic cells as β cells<sup>129,135</sup>. These challenges become especially pronounced when automating image analysis and can lead to an artificial elevation of β cell proliferation index, which may either mask the effect a treatment has on β cell proliferation or incorrectly attribute an increase in non- $\beta$  cell proliferation to  $\beta$  cells. To reduce errors in  $\beta$  cell quantification, we used both cytoplasmic (insulin or C-peptide) and nuclear (Pdx1) markers to label β cells and examined each markup image after analysis for artifacts and the sensitivity and specificity of the algorithm. We validated our automated analysis by demonstrating that β cell proliferation quantified by the algorithm was comparable to manually counting each β cell to determine proliferation index.

Another limitation of studying human  $\beta$  cell proliferation *in vitro* is the requirement of using surrogate proliferation markers because it is not feasible to definitively measure an increase in cell number due to the low replication rate in these cells. We used Ki67 to identify proliferating cells in our culture system, which is expressed in cells that have entered the cell cycle. However, the method we describe here can be adapted to substitute other proliferation markers (e.g., BrdU).

We demonstrated the usefulness of our method in evaluating potential adult human  $\beta$  cell mitogens by performing a screen of 13 compounds at different concentrations at both basal and high glucose. We wanted to ensure that we could detect human β cell proliferation in response to treatment in addition to forced overexpression of cell cycle regulators, but because no definitive adult human β cell mitogen has been identified, we selected compounds to test based on their ability in previous studies to promote β cell proliferation or regulate β cell mass. Most of these compounds had only been tested previously in animal models, but three (harmine, GABA, PDGF) had been evaluated in human systems. Our method confirmed that harmine significantly increases adult human β cell proliferation, but the other compounds tested had limited to no effect. Some of the compounds (GABA, PDGF, UK-432097, A-134974) demonstrated marginal increases in β cell proliferation in certain conditions that proved to be statistically significant, however it is unclear whether these results are biologically meaningful. Because human β cell proliferation peaks at around 2% during development, this proliferation rate has been proposed as a therapeutic target for drug development<sup>46</sup>. Due to differences between human islet cells in vivo and in culture using various systems, in addition to inherent variability between donors, further studies will be needed to determine what level of proliferation achieved using our method should be used as a threshold for deciding which compounds should be developed further.

High-throughput screening platforms are being developed, with exciting potential to drive the discovery of  $\beta$  cell mitogens<sup>128,129,135</sup>. Confirming discoveries made using these platforms in primary adult human  $\beta$  cells remains critical to determine which compounds have therapeutic potential in human diabetes. We were able to reduce the effects of variation between islet preparations and confounding artifacts in human islet cell culture to create a scalable method for evaluating adult human  $\beta$  cell proliferation that can be used as an efficient screening system moving forward.

### **CHAPTER VI**

### SIGNIFICANCE AND FUTURE DIRECTIONS

The overall goal of this Dissertation was to advance understanding of how components of the islet microenvironment—including endothelial cells, macrophages, and the extracellular matrix—contribute to the regulation of β cell mass in adult pancreatic islets. In the process of investigating the hypothesis that VEGF-A signaling in intra-islet endothelial cells positively regulates  $\beta$  cell mass and proliferation using a model system of inducible VEGF-A overexpression, we unexpectedly found that increased VEGF-A led not to increased β cell mass, but to reduced β cell mass. Even more surprising was our discovery that withdrawal of the VEGF-A stimulus was followed by robust β cell proliferation, leading to islet regeneration, normalization of β cell mass, and re-establishment of the intra-islet capillary network<sup>153</sup>. Such a robust regenerative response is not seen in other models of β cell loss<sup>82,254,322-326</sup>, making the identification of the signals regulating proliferation in this newly established model of β cell regeneration particularly interesting. Using islet transplantation and bone marrow transplantation approaches, we found that B cell proliferation was dependent on the local microenvironment of endothelial cells, β cells, macrophages recruited to islets upon VEGF-A induction, and a rapidly remodeling extracellular matrix. We also demonstrated that this microenvironment promotes human β cell proliferation. In exploring this model, we discovered exciting new roles for macrophages and endothelial cells in regulating B cell proliferation through interactions with each other and the extracellular matrix. These findings and intriguing future directions of this work are discussed below.

Although several studies have demonstrated the need for careful regulation of VEGF-A signaling between developing endocrine cells and endothelium during pancreas development, our data indicates that the level of VEGF-A in mature islets is also crucial for maintaining islet morphology, vascularization, and β cell mass<sup>153</sup>. Increased VEGF-A/VEGFR2 signaling did cause extensive endothelial cell proliferation and expansion, resulting in β cell loss. Furthermore, transcriptional analysis of these proliferative endothelial cells did not demonstrate upregulation of known pro-apoptotic signals; however, these cells do exhibit significant changes in matrix remodeling enzymes and receptors and adhesion molecules involved in cell-matrix and cell-cell interactions. In normal, healthy tissue, the extracellular matrix provides survival cues through integrins and other signaling molecules, and altering this cell-matrix signaling can push cells toward apoptosis<sup>327,328</sup>. Because endothelial cells are the primary producers of extracellular matrix in islets, dramatic changes in this cell population, and subsequent matrix remodeling may alter β cell-matrix interactions crucial for β cell survival. Not much is known about the role of the extracellular matrix in β cell survival, but in vitro studies have demonstrated increased β cell survival when cultured with collagens, laminin, or other matrix proteins<sup>291,292</sup>. Our findings suggest that endothelial cells play an important role in establishing and maintaining β cellmatrix interactions that are required to promote β cell survival and maintain β cell mass throughout life. However, additional studies will be needed in both our model and others to more fully define this endothelial cell function.

The model we are developing to disrupt VEGFR2 signaling in endothelial cells both before and after VEGF-A induction in  $\beta$ VEGF-A mice (Figure 37) will allow us to further clarify the role endothelial cells play in  $\beta$  cell loss and proliferation in our model. We predict that blocking VEGF-A/VEGFR2 signaling before Dox treatment will prevent endothelial cell expansion and subsequent  $\beta$  cell loss, which would indicate that quiescent islet endothelial cells play a role in maintaining  $\beta$  cell mass. We will also be able to determine whether VEGFR2 signaling in quiescent endothelial cells following  $\beta$  cell loss is required for  $\beta$  cell regeneration. Macrophages play a crucial role in this regeneration and this model will allow us to determine whether endothelial cells are also necessary for macrophage recruitment and phenotypic activation as our transcriptional data suggests. If endothelial cells do play a role in recruiting macrophages and pushing them toward a regenerative phenotype in this model, it is possible that perturbations in islet endothelial cells may contribute to infiltration and activation of harmful phenotypes in immune cells in diabetes, which would warrant further investigation.

Previously, macrophages were primarily thought to be damaging to islets with evidence pointing to their role in the pathogenesis of diabetes 104,218,219. However, it is now known that during the late stages of pancreas development, mice with severe macrophage deficiency have impaired islet morphogenesis and reduced β cell proliferation and mass, suggesting that macrophages may also have a function in β cell survival and/or proliferation<sup>217</sup>. Our findings establish a new role for macrophages in β cell regeneration. We showed that (1) macrophages are recruited to βVEGF-A islets upon VEGF-A induction, and (2) depleting these recruited macrophages inhibits  $\beta$  cell proliferation, thereby demonstrating that macrophages are required for β cell regeneration in this model<sup>153</sup>. Interestingly, two other studies published last year also reported the involvement of macrophages in β cell regeneration using different models of β cell injury. The first of these studies described a function for M2-like macrophages in β cell proliferation following damage due to surgically-induced pancreatitis<sup>221</sup>. The other used diphtheria toxin receptor-mediated ablation of the whole pancreas or β cells and identified a role for macrophages in promoting both acinar and β cell regeneration<sup>222</sup>. These publications independently show that macrophages are important in β cell regeneration and this feature is not unique to the βVEGF-A model, further suggesting the possibility of a wider role for macrophages in establishing and maintaining β cell mass.

Defining a more comprehensive role for macrophages in  $\beta$  cell mass regulation requires addressing several additional questions: (1) what role do macrophages have in establishing  $\beta$  cell mass, (2) are macrophages required to maintain  $\beta$  cell mass in the adult, and (3) do macrophages contribute to  $\beta$  cell proliferation in other models of  $\beta$  cell expansion?

What role do macrophages have in establishing  $\beta$  cell mass? Macrophages are present in the fetal pancreas by embryonic day 12.5, and expansion of these macrophages with colony-stimulating factor (M-CSF) in cultured fetal pancreas explants leads to an increased number of insulin-producing cells<sup>215</sup>. Signaling between macrophages and developing pancreatic epithelium *in vitro* regulates migration and cell cycle progression<sup>216</sup>. Furthermore, mice homozygous for a null mutation in the colony-stimulating factor 1 (CSF-1) gene, leading to a deficiency in the entire mononuclear lineage, have significantly decreased  $\beta$  cell mass, abnormal islet morphogenesis, and impaired postnatal  $\beta$  cell proliferation<sup>217</sup>.

Additional studies depleting macrophages at specific developmental stages *in vivo* will help clarify the role of macrophages in establishing  $\beta$  cell mass. This could be accomplished using mice with diphtheria toxin (DT)-sensitive monocytes/macrophages (e.g., CD11b-DTR, LysM-Cre; iDTR, CD169-DTR)<sup>329-331</sup>.

Are macrophages required to maintain  $\beta$  cell mass in the adult? Tissue-resident macrophages play important roles in immune surveillance and tissue homeostasis and function, and have widely variable tissue- and niche-specific phenotypes. Although the presence of resident macrophages in the pancreas has been noted, these cells have not been well characterized, and no effort has been made to distinguish between resident macrophages of acinar versus islet tissue<sup>215</sup>. Consequently, not much is known about whether macrophages are required to maintain normal  $\beta$  cell mass and function in adult islets. Analyzing mass and function of  $\beta$  cells in macrophage-depleted mice (either via clodronate treatment or in DT-mediated models described above) may provide insight into the role of macrophages in islet homeostasis. Defining the phenotype of islet resident macrophages would also provide key information about their function. Because we collected resident macrophages from  $\beta$ VEGF-A islets at baseline (No Dox), we could compare their transcriptional profile with open access data sets from other tissue-resident, inflammatory, and biologically relevant macrophages. This would allow us to put these islet-resident macrophages in context with those from other systems whose functions have been more thoroughly investigated.

Do macrophages contribute to  $\beta$  cell proliferation in other models of  $\beta$  cell expansion? Although macrophages have now been shown to contribute to  $\beta$  cell proliferation in models of  $\beta$  cell injury and regeneration, it is unknown whether they are required for  $\beta$  cell expansion in models of increased metabolic demand, such as during pregnancy or obesity. Studies in mice have found that during pregnancy,  $\beta$  cell mass expands two- to five-fold, and in obese leptin ( $Lep^{ob/ob}$ ) or leptin-receptor ( $Lep^{rdb/db}$ ) deficient mice it increases three- to five-fold<sup>43,332,333</sup>. Models of high fat diet-induced obesity also display  $\beta$  cell expansion of a little more than two-fold<sup>334-336</sup>. Depleting macrophages during  $\beta$  cell expansion in these models using one of the methods described previously would provide insight into whether macrophages contribute to  $\beta$  cell expansion as well as regeneration.

In any of these proposed studies to determine what role macrophages play in regulating  $\beta$  cell mass, clearly defining macrophage phenotype, signals regulating phenotype activation, and the mechanisms by which they function will be important. For instance, macrophages in the  $\beta$ VEGF-A model of  $\beta$  cell regeneration express different phenotypic markers than those in the pancreatitis and DT-mediated ablation models described above, and likely work through different mechanisms <sup>153,221,222</sup>. The proposed model of macrophage action in pancreatitis is that they promote  $\beta$  cell proliferation by activating SMAD7 through EGF and TGF $\beta$ 1 signaling, whereas in our model they appear to activate the ERK/ MAPK pathway<sup>221</sup>. We actually see a decrease in *Egf* in both macrophages and  $\beta$  cells in our model upon macrophage infiltration and no significant change in *Smad7*. Macrophages in  $\beta$ VEGF-A mice do demonstrate a phenotypic shift going from VEGF-A induction to withdrawal of the VEGF-A stimulus. Additional experiments depleting macrophages specifically during VEGF-A normalization (from 1wk Dox to 1wk WD) when  $\beta$  cells are proliferating would allow us to determine whether macrophages are primarily acting immediately upon infiltration or during VEGF-A withdrawal. Our findings suggest that  $\beta$  cells may be driving macrophage phenotype activation through production of IL4 and CSF-1.

Transplanting  $\beta$ VEGF-A mice with bone marrow from mice with tamoxifen (Tm)-inducible knockout of the CSF-1 receptor or from IL4 receptor deficient mice would allow us to determine whether macrophages unable to respond to these IL4 or CSF-1 signals are still capable of promoting  $\beta$  cell proliferation<sup>337-339</sup>.

The most significant discovery about the regenerative islet microenvironment in βVEGF-A mice is that in addition to causing proliferation in rodent  $\beta$  cells, it is also able to promote human  $\beta$  cell proliferation. Multiple studies have identified physiological settings (e.g., obesity, pregnancy, partial pancreatectomy), and stimuli such as growth factors (e.g., PDGF, IGF-1, CTGF), hormones (e.g., prolactin, growth hormone), and mitogenic agents or small molecules (e.g., glucose, glucokinase activators, adenosine kinase inhibitors) that cause significant β proliferation in rodents, but have limited or no effect on human β cells<sup>46-50</sup>. Because we developed a model that does stimulate significant human β cell proliferation, it is very important to identify the signals driving this process. Since a βVEGF-A model could not be recreated in vitro after multiple attempts, we developed a new strategy to analyze the complex islet microenvironment in order to discover the cell-cell and cell-matrix interactions crucial to both mouse and human  $\beta$  cell proliferation in this model. We did this by performing transcriptome analysis on whole islets and individual islet cell populations—endothelial cells, macrophages, and β cells—over the course of VEGF-A induction and normalization. Data from whole islets allowed us to identify transcriptional changes in the islet microenvironment as a whole, while investigating transcriptional changes in individual cell populations allowed us to identify which of those overall changes in the microenvironment reflected the changing numbers of each cell population over time versus transcriptional changes within and between cell populations during β cell loss and regeneration. Analyzing these data sets further will continue to yield insight into pathways and processes that are being up and downregulated through contributions from multiple cell types over time and provide even more insight into the regulatory mechanisms involved in β cell proliferation in this model.

Surprisingly, we found that a combination of multiple signals from all cell types and the rapidly remodeling extracellular matrix appear to drive  $\beta$  cell proliferation in our model through growth factor receptors, chemokine/cytokine receptors, and integrins. Many of these signals have been identified previously as individually contributing to  $\beta$  cell proliferation in rodents, and either have not been tested in human tissues or fail to stimulate human  $\beta$  cell proliferation on their own<sup>47-49</sup>. It has been proposed that because cell cycle machinery remains intact in human  $\beta$  cells, the failure of these stimuli to drive proliferation occurs at the level of the upstream receptors and signaling cascades<sup>48</sup>. However, our data indicates that multiple, rather than individual signals may be required to promote human  $\beta$  cell proliferation.

Our data also suggests that activation of the PI3K/Akt and ERK/MAPK pathways simultaneous through multiple mediators including growth factors and integrins is required to drive  $\beta$  cell proliferation. While the effect of growth factors on  $\beta$  cell proliferation has been extensively tested, integrins have been largely ignored<sup>47-49,51,111-113,121,340</sup>. Studies on islet integrins have focused primarily on  $\beta$ 1 integrin, which plays a role in regulating rodent  $\beta$  cell mass through the PI3K/Akt and ERK/MAPK pathways, and blocking  $\beta$ 1 integrin signaling in human fetal islet epithelial cell cultures leads to decreased differentiation and survival of these islet cells<sup>187,189,295</sup>. Even though  $\beta$  cells do not alter their consistently

high expression of  $\beta 1$  integrin over the course of VEGF-A induction and normalization in  $\beta$ VEGF-A mice, they do exhibit significant increases in expression of other integrins and integrin ligands. The importance of these integrins and other matrix components in establishing, maintaining, and regenerating  $\beta$  cell mass is unknown and should be investigated.

We have identified important roles for endothelial cells, macrophages, and extracellular matrix components in regulating β cell mass in adult pancreatic islets. Interactions between these cells, islet β cells, and the extracellular matrix create a microenvironment where growth factors, chemokines/ cytokines, and matrix components activate an increasing number of growth factor receptors and integrins expressed on β cells to activate PI3K/Akt and ERK/MAPK pathways, which are able to successfully activate cell cycle machinery to drive β cell replication. Moving forward, we need to determine what combination of signals from this system is necessary for β cell proliferation to occur, and which of those signals are common across different β cell regeneration models (i.e., surgicallyinduced pancreatitis, STZ, DTR-mediated β cell ablation). We can accomplish this by (1) using STZ-mediated β cell ablation in mice with genetically-introduced deficiencies in specific targets we identified in our model (e.g., integrins, growth factor receptors) to identify which of these factors may be important during β cell regeneration in this alternate model, and (2) testing different combinations of growth factors, chemokine/cytokines, and matrix components using the method we developed to evaluate human β cell proliferation *in vitro*. Once the right combination of signals have been identified, this system can also be used to further elucidate the mechanisms by introducing inhibitors and enhancers of the receptors, integrins, and pathways involved, in hopes of using this model to develop new strategies for promoting  $\beta$  cell regeneration in diabetes.

In addition to pursuing the therapeutic potential of mitogenic signals identified, these studies have much broader implications for both understanding the pathogenesis of diabetes and identifying new targets for therapeutic interventions in diabetes. The development of both type 1 and type 2 diabetes mellitus (DM) occurs through a combination of genetic and environmental influences. Current models of type 1 DM pathogenesis include an initial immunological insult in patients with a genetic predisposition, which leads to immune cell infiltration into islets and subsequent autoimmune destruction of B cells mediated by T lymphocytes and other immune cells, including macrophages<sup>341</sup>. Some have suggested that β cell death in type 1 DM can also occur indirectly with increased islet inflammation leading to cytokinemediated or stress-induced β cell apoptosis<sup>342</sup>. Type 2 DM is characterized by insulin resistance and relative insulin deficiency, which develop through genetic and environmental influences and lead to β cell dysfunction and loss. Macrophages in peripheral tissues (e.g., adipose, skeletal muscle, liver) are key regulators of the chronic low-grade inflammation observed in obesity and can contribute to the development of insulin resistance and type 2 DM<sup>343</sup>. This occurs as macrophages switch from an anti-inflammatory (alternative, M2) to pro-inflammatory (classical, M1) phenotype in response to signals from adipose and other tissues altered in obesity. An increased number of macrophages in islets has been observed in patients with type 2 DM, but their phenotypic characteristics and potential role in β cell dysfunction and loss are unknown<sup>344,345</sup>.

Although vascular dysfunction in diabetes leading to complications such as retinopathy, nephropathy, and cardiovascular disease has been well documented, the role of the islet vasculature and its

relationship to islet cells in normal conditions and in diabetes has been understudied<sup>346,347</sup>. Our data demonstrates that changes in islet vascularization and endothelial cell phenotype can have a profound effect on  $\beta$  cell mass, with islet endothelial cells playing a role in producing and maintaining the extracellular matrix, mediating immune cell infiltration, and regulating β cell loss and proliferation<sup>153</sup>. Recent work from others in our group has further demonstrated that islet vasculature dilates, rather than expands, as β cells undergo hypertrophy and hyperplasia in response to insulin resistance<sup>348</sup>. Therefore, it is possible that perturbations in islet vasculature and endothelial cell phenotype occur in diabetes and contribute to immune cell infiltration seen in both type 1 and type 2 DM as well as ß cell dysfunction and loss. Some of these effects could be due to changes or disruption in extracellular matrix–β cell interactions that provide cell survival signals, or activation of harmful pro-inflammatory phenotypes in immune cells. Elucidation of specific signals responsible for β cell apoptosis in the βVEGF-A model may provide important insight into how endothelial cells could be mediating β cell death in diabetes. Furthermore, adjusting the treatment paradigm in \(\text{\BetaVEGF-A}\) mice by (1) increasing the length of VEGF-A induction to cause greater β cell loss and consequent hyperglycemia, or (2) inducing insulin resistance with high-fat diet feeding prior to inducing VEGF-A, may allow these mice to be used more effectively as models of type 1 and type 2 DM, respectively. If endothelial cells do in fact have a pathogenic function in diabetes, they provide an intriguing new target for studying genetic predisposition for diabetes and developing therapies to prevent or halt the disease process.

Macrophages in type 1 DM are thought to contribute to autoimmune destruction of  $\beta$  cells; and in type 2 DM, pro-inflammatory phenotypic changes in macrophages have been well characterized in peripheral tissues, but the role of increased numbers of macrophages in type 2 DM islets is unknown. Our studies define a role for macrophages in  $\beta$  cell regeneration and suggest the possibility of a more comprehensive role for macrophages in regulating  $\beta$  cell mass and maintaining islet tissue homeostasis <sup>153</sup>. If resident macrophages do function to maintain islet homeostasis, then perhaps disruption of this population is responsible for the harmful role macrophages play in the pathogenesis of diabetes. This disruption may occur by (1) infiltration of inflammatory macrophages as seen in both type 1 and type 2 DM, or (2) signals causing a phenotypic shift in these islet macrophages similar to that observed in peripheral tissue macrophages in type 2 DM that transition from anti-inflammatory (M2) to pro-inflammatory (M1) as the disease develops. If alterations in the islet macrophage population do contribute to diabetes pathogenesis, they would provide an exciting target for developing interventions capable of driving macrophage phenotype away from the destructive, inflammatory phenotype thought to contribute to  $\beta$  cell death, and toward a regenerative phenotype capable of promoting  $\beta$  cell proliferation as observed in the  $\beta$ VEGF-A model.

Overall, these studies have provided new targets for expanding  $\beta$  cell mass in patients with diabetes and established a role for macrophages and endothelial cells in regulating  $\beta$  cell mass and regeneration. By continuing to study  $\beta$  cells in the context of the islet microenvironment where they interact with endothelial cells, macrophages, and the extracellular matrix, we will be able to determine how these interactions contribute to  $\beta$  cell function, survival, and proliferation, further our understanding of the pathogenesis of diabetes, and pursue these cell-cell and cell-matrix interactions as new targets for therapeutic intervention in patients with diabetes.

## REFERENCES

- 1 Chen N, Unnikrishnan I R, Anjana RM, Mohan V, Pitchumoni CS. The complex exocrine-endocrine relationship and secondary diabetes in exocrine pancreatic disorders. *J Clin Gastroenterol* 2011; **45**: 850–861.
- 2 Pan FC, Wright CVE. Pancreas organogenesis: from bud to plexus to gland. *Dev Dyn* 2011; **240**: 530–565.
- 3 Slack JM. Developmental biology of the pancreas. *Development* 1995; **121**: 1569–1580.
- 4 Lifson N, Lassa CV, Dixit PK. Relation between blood flow and morphology in islet organ of rat pancreas. *Am J Physiol* 1985; **249**: E43–8.
- Brissova M, Fowler MJ, Nicholson WE, Chu A, Hirshberg B, Harlan DM *et al.* Assessment of human pancreatic islet architecture and composition by laser scanning confocal microscopy. *J Histochem Cytochem* 2005; **53**: 1087–1097.
- 6 Cabrera O, Berman DM, Kenyon NS, Ricordi C, Berggren P-O, Caicedo A. The unique cytoarchitecture of human pancreatic islets has implications for islet cell function. *Proc Natl Acad Sci USA* 2006; **103**: 2334–2339.
- Aronoff SL, Berkowitz K, Shreiner B, Want L. Glucose Metabolism and Regulation: Beyond Insulin and Glucagon. *Diabetes Spectrum* 2004.
- 8 Ahrén B. Autonomic regulation of islet hormone secretion--implications for health and disease. *Diabetologia* 2000; **43**: 393–410.
- 9 Kim W, Egan JM. The role of incretins in glucose homeostasis and diabetes treatment. *Pharmacol Rev* 2008; **60**: 470–512.
- Nolan CJ, Prentki M. The islet beta-cell: fuel responsive and vulnerable. *Trends Endocrinol Metab* 2008; **19**: 285–291.
- Samuel VT, Shulman GI. Mechanisms for insulin resistance: common threads and missing links. *Cell* 2012; **148**: 852–871.
- Fu Z, Gilbert ER, Liu D. Regulation of insulin synthesis and secretion and pancreatic Beta-cell dysfunction in diabetes. *Curr Diabetes Rev* 2013; **9**: 25–53.
- 13 Wilcox G. Insulin and insulin resistance. *Clin Biochem Rev* 2005; **26**: 19–39.
- 14 Rorsman P, Braun M. Regulation of insulin secretion in human pancreatic islets. *Annu Rev Physiol* 2013; **75**: 155–179.
- Bosco D, Armanet M, Morel P, Niclauss N, Sgroi A, Muller YD *et al.* Unique arrangement of alpha- and beta-cells in human islets of Langerhans. *Diabetes* 2010; **59**: 1202–1210.
- Wojtusciszyn A, Armanet M, Morel P, Berney T, Bosco D. Insulin secretion from human beta cells is heterogeneous and dependent on cell-to-cell contacts. *Diabetologia* 2008; **51**: 1843–1852.
- Ferrer J, Benito C, Gomis R. Pancreatic islet GLUT2 glucose transporter mRNA and protein expression in humans with and without NIDDM. *Diabetes* 1995; **44**: 1369–1374.

- De Vos A, Heimberg H, Quartier E, Huypens P, Bouwens L, Pipeleers D *et al.* Human and rat beta cells differ in glucose transporter but not in glucokinase gene expression. *J Clin Invest* 1995; **96**: 2489–2495.
- Shiao M-S, Liao B-Y, Long M, Yu H-T. Adaptive evolution of the insulin two-gene system in mouse. *Genetics* 2008; **178**: 1683–1691.
- 20 Unger RH, Cherrington AD. Glucagonocentric restructuring of diabetes: a pathophysiologic and therapeutic makeover. *J Clin Invest* 2012; **122**: 4–12.
- 21 Saladin K. *Anatomy & Physiology: The Unity of Form and Function, Second Edition.* 2nd ed. McGraw-Hill, 2001.
- Cartailler J-P. Insulin from secretion to action. *Beta Cell Biology Consortium* 2004.https://www.betacell.org/content/articleview/article\_id/1/page/1/glossary/0/.
- Zhou Q, Law AC, Rajagopal J, Anderson WJ, Gray PA, Melton DA. A Multipotent Progenitor Domain Guides Pancreatic Organogenesis. *Developmental Cell* 2007; **13**: 103–114.
- Gittes GK. Developmental biology of the pancreas: a comprehensive review. *Dev Biol* 2009; **326**: 4–35.
- Herrera PL. Adult insulin- and glucagon-producing cells differentiate from two independent cell lineages. *Development* 2000; **127**: 2317–2322.
- Pictet RL, Clark WR, Williams RH, Rutter WJ. An ultrastructural analysis of the developing embryonic pancreas. *Dev Biol* 1972; **29**: 436–467.
- 27 Miller K, Kim A, Kilimnik G, Jo J, Moka U, Periwal V *et al.* Islet formation during the neonatal development in mice. *PLoS ONE* 2009; **4**: e7739.
- Stolovich-Rain M, Hija A, Grimsby J, Glaser B, Dor Y. Pancreatic beta cells in very old mice retain capacity for compensatory proliferation. *J Biol Chem* 2012; **287**: 27407–27414.
- 29 Sarkar SA, Kobberup S, Wong R, Lopez AD, Quayum N, Still T *et al.* Global gene expression profiling and histochemical analysis of the developing human fetal pancreas. *Diabetologia* 2008; **51**: 285–297.
- Jeon J, Correa-Medina M, Ricordi C, Edlund H, Diez JA. Endocrine cell clustering during human pancreas development. *J Histochem Cytochem* 2009; **57**: 811–824.
- Riedel MJ, Asadi A, Wang R, Ao Z, Warnock GL, Kieffer TJ. Immunohistochemical characterisation of cells co-producing insulin and glucagon in the developing human pancreas. *Diabetologia* 2012; **55**: 372–381.
- Gregg BE, Moore PC, Demozay D, Hall BA, Li M, Husain A *et al.* Formation of a human β-cell population within pancreatic islets is set early in life. *J Clin Endocrinol Metab* 2012; **97**: 3197–3206.
- Pan FC, Brissova M. Pancreas development in humans. *Curr Opin Endocrinol Diabetes Obes* 2014; **21**: 77–82.
- Teta M, Long SY, Wartschow LM, Rankin MM, Kushner JA. Very slow turnover of beta-cells in aged adult mice. *Diabetes* 2005; **54**: 2557–2567.

- Meier JJ, Butler AE, Saisho Y, Monchamp T, Galasso R, Bhushan A *et al.* Beta-cell replication is the primary mechanism subserving the postnatal expansion of beta-cell mass in humans. *Diabetes* 2008; **57**: 1584–1594.
- Bouwens L, Rooman I. Regulation of pancreatic beta-cell mass. *Physiol Rev* 2005; **85**: 1255–1270.
- 37 Köhler CU, Olewinski M, Tannapfel A, Schmidt WE, Fritsch H, Meier JJ. Cell cycle control of β-cell replication in the prenatal and postnatal human pancreas. *Am J Physiol Endocrinol Metab* 2011; **300**: E221–30.
- 38 Kassem SA, Ariel I, Thornton PS, Scheimberg I, Glaser B. Beta-cell proliferation and apoptosis in the developing normal human pancreas and in hyperinsulinism of infancy. *Diabetes* 2000; **49**: 1325–1333.
- 39 Cnop M, Igoillo-Esteve M, Hughes SJ, Walker JN, Cnop I, Clark A. Longevity of human islet α-and β-cells. *Diabetes Obes Metab* 2011; **13 Suppl 1**: 39–46.
- Saisho Y, Butler AE, Manesso E, Elashoff D, Rizza RA, Butler PC. β-cell mass and turnover in humans: effects of obesity and aging. *Diabetes Care* 2013; **36**: 111–117.
- Sachdeva MM, Stoffers DA. Minireview: Meeting the demand for insulin: molecular mechanisms of adaptive postnatal beta-cell mass expansion. *Mol Endocrinol* 2009; **23**: 747–758.
- Dor Y, Brown J, Martinez OI, Melton DA. Adult pancreatic beta-cells are formed by self-duplication rather than stem-cell differentiation. *Nature* 2004; **429**: 41–46.
- Parsons JA, Brelje TC, Sorenson RL. Adaptation of islets of Langerhans to pregnancy: increased islet cell proliferation and insulin secretion correlates with the onset of placental lactogen secretion. *Endocrinology* 1992; **130**: 1459–1466.
- Butler AE, Cao-Minh L, Galasso R, Rizza RA, Corradin A, Cobelli C *et al.* Adaptive changes in pancreatic beta cell fractional area and beta cell turnover in human pregnancy. *Diabetologia* 2010; **53**: 2167–2176.
- Wang P, Alvarez-Perez J-C, Felsenfeld DP, Liu H, Sivendran S, Bender A *et al.* A high-throughput chemical screen reveals that harmine-mediated inhibition of DYRK1A increases human pancreatic beta cell replication. *Nat Med* 2015; **21**: 383–388.
- Wang P, Fiaschi-Taesch NM, Vasavada RC, Scott DK, Garcia-Ocaña A, Stewart AF. Diabetes mellitus—advances and challenges in human β-cell proliferation. *Nat Rev Endocrinol* 2015; 11: 201–212.
- 47 Stewart AF, Hussain MA, Garcia-Ocaña A, Vasavada RC, Bhushan A, Bernal-Mizrachi E *et al.* Human β-Cell Proliferation and Intracellular Signaling: Part 3. *Diabetes* 2015; **64**: 1872–1885.
- 48 Kulkarni RN, Mizrachi E-B, Ocana AG, Stewart AF. Human β-cell proliferation and intracellular signaling: driving in the dark without a road map. *Diabetes* 2012; **61**: 2205–2213.
- 49 Bernal-Mizrachi E, Kulkarni RN, Scott DK, Mauvais-Jarvis F, Stewart AF, Garcia-Ocaña A. Human β-cell proliferation and intracellular signaling part 2: still driving in the dark without a road map. *Diabetes* 2014; **63**: 819–831.

- Porat S, Weinberg-Corem N, Tornovsky-Babaey S, Schyr-Ben-Haroush R, Hija A, Stolovich-Rain M *et al.* Control of pancreatic β cell regeneration by glucose metabolism. *Cell Metab* 2011; **13**: 440–449.
- 51 Chen H, Gu X, Liu Y, Wang J, Wirt SE, Bottino R *et al.* PDGF signalling controls age-dependent proliferation in pancreatic β-cells. *Nature* 2011; **478**: 349–355.
- Ashcroft FM, Rorsman P. Diabetes mellitus and the β cell: the last ten years. *Cell* 2012; **148**: 1160–1171.
- 53 Centers for Disease Control and Prevention. National Diabetes Statistics Report, 2014. *Online* 2014; : 1–12.
- World Health Organization. Diabetes Fact Sheet N 312. *Online* 2015; : 1–8.
- Atkinson MA, Eisenbarth GS, Michels AW. Type 1 diabetes. *Lancet* 2014; **383**: 69–82.
- Muoio DM, Newgard CB. Mechanisms of disease: molecular and metabolic mechanisms of insulin resistance and beta-cell failure in type 2 diabetes. *Nat Rev Mol Cell Biol* 2008; **9**: 193–205.
- 57 Prentki M, Nolan CJ. Islet beta cell failure in type 2 diabetes. *J Clin Invest* 2006; **116**: 1802–1812.
- 58 Lain KY, Catalano PM. Metabolic changes in pregnancy. *Clin Obstet Gynecol* 2007; **50**: 938–948.
- Vaxillaire M, D P, Bonnefond A, Froguel P. Breakthroughs in monogenic diabetes genetics: from pediatric forms to young adulthood diabetes. *Pediatr Endocrinol Rev* 2009; **6**: 405–417.
- Vaxillaire M, Froguel P. Monogenic diabetes in the young, pharmacogenetics and relevance to multifactorial forms of type 2 diabetes. *Endocr Rev* 2008; **29**: 254–264.
- 61 Collombat P, Xu X, Heimberg H, Mansouri A. Pancreatic beta-cells: from generation to regeneration. *Semin Cell Dev Biol* 2010; **21**: 838–844.
- Aathira R, Jain V. Advances in management of type 1 diabetes mellitus. *World J Diabetes* 2014; **5**: 689–696.
- 63 Ostenson C-G. Type 2 diabetes: genotype-based therapy. Sci Transl Med 2014; 6: 257fs39.
- 64 Inzucchi SE, Bergenstal RM, Buse JB, Diamant M, Ferrannini E, Nauck M *et al.* Management of hyperglycemia in type 2 diabetes, 2015: a patient-centered approach: update to a position statement of the American Diabetes Association and the European Association for the Study of Diabetes. *Diabetes Care* 2015; **38**: 140–149.
- Shapiro AM, Lakey JR, Ryan EA, Korbutt GS, Toth E, Warnock GL *et al.* Islet transplantation in seven patients with type 1 diabetes mellitus using a glucocorticoid-free immunosuppressive regimen. *N Engl J Med* 2000; **343**: 230–238.
- Pepper AR, Gala-Lopez B, Ziff O, Shapiro AJ. Current status of clinical islet transplantation. *World J Transplant* 2013; **3**: 48–53.
- Harlan DM, Kenyon NS, Korsgren O, Roep BO, Immunology of Diabetes Society. Current advances and travails in islet transplantation. *Diabetes* 2009; **58**: 2175–2184.

- 68 Khan MH, Harlan DM. Counterpoint: clinical islet transplantation: not ready for prime time. *Diabetes Care* 2009; **32**: 1570–1574.
- 69 McCall M, Shapiro AMJ. Islet cell transplantation. Semin Pediatr Surg 2014; 23: 83–90.
- Lakey JRT, Mirbolooki M, Shapiro AMJ. Current status of clinical islet cell transplantation. *Methods Mol Biol* 2006; **333**: 47–104.
- Biarnés M, Montolio M, Nacher V, Raurell M, Soler J, Montanya E. Beta-cell death and mass in syngeneically transplanted islets exposed to short- and long-term hyperglycemia. *Diabetes* 2002; **51**: 66–72.
- Figh T, Eriksson O, Lundgren T, Nordic Network for Clinical Islet Transplantation. Visualization of early engraftment in clinical islet transplantation by positron-emission tomography. *N Engl J Med* 2007; **356**: 2754–2755.
- Carlsson P-O, Palm F, Andersson A, Liss P. Markedly decreased oxygen tension in transplanted rat pancreatic islets irrespective of the implantation site. *Diabetes* 2001; **50**: 489–495.
- Mattsson G, Jansson L, Carlsson P-O. Decreased vascular density in mouse pancreatic islets after transplantation. *Diabetes* 2002; **51**: 1362–1366.
- Korsgren O, Lundgren T, Felldin M, Foss A, Isaksson B, Permert J *et al.* Optimising islet engraftment is critical for successful clinical islet transplantation. *Diabetologia* 2008; **51**: 227–232.
- Korsgren O, Jansson L, Sundler F. Reinnervation of transplanted fetal porcine endocrine pancreas. Evidence for initial growth and subsequent degeneration of nerve fibers in the islet grafts. *Transplantation* 1996; **62**: 352–357.
- Brissova M, Powers AC. Revascularization of transplanted islets: can it be improved? *Diabetes* 2008; **57**: 2269–2271.
- Van der Windt DJ, Bottino R, Kumar G, Wijkstrom M, Hara H, Ezzelarab M *et al.* Clinical islet xenotransplantation: how close are we? *Diabetes* 2012; **61**: 3046–3055.
- 79 Korsgren O, Groth CG. Co-transplantation of human and pig islets. *Xenotransplantation* 2008; **15**: 112.
- Chatenoud L. The long and winding road towards induction of allograft tolerance in the clinic. *Transpl Int* 2008; **21**: 725–727.
- Froud T, Baidal DA, Ponte G, Ferreira JV, Ricordi C, Alejandro R. Resolution of neurotoxicity and beta-cell toxicity in an islet transplant recipient following substitution of tacrolimus with MMF. *Cell transplantation* 2006; **15**: 613–620.
- Nir T, Melton DA, Dor Y. Recovery from diabetes in mice by beta cell regeneration. *J Clin Invest* 2007; **117**: 2553–2561.
- Kroon E, Martinson LA, Kadoya K, Bang AG, Kelly OG, Eliazer S *et al.* Pancreatic endoderm derived from human embryonic stem cells generates glucose-responsive insulin-secreting cells in vivo. *Nat Biotechnol* 2008; **26**: 443–452.

- D'Amour KA, Bang AG, Eliazer S, Kelly OG, Agulnick AD, Smart NG *et al.* Production of pancreatic hormone-expressing endocrine cells from human embryonic stem cells. *Nat Biotechnol* 2006; **24**: 1392–1401.
- Zhang D, Jiang W, Liu M, Sui X, Yin X, Chen S *et al.* Highly efficient differentiation of human ES cells and iPS cells into mature pancreatic insulin-producing cells. *Cell Res* 2009; **19**: 429–438.
- Best M, Carroll M, Hanley NA, Piper Hanley K. Embryonic stem cells to beta-cells by understanding pancreas development. *Mol Cell Endocrinol* 2008; **288**: 86–94.
- Mayhew CN, Wells JM. Converting human pluripotent stem cells into beta-cells: recent advances and future challenges. *Curr Opin Organ Transplant* 2010; **15**: 54–60.
- Pagliuca FW, Millman JR, Gürtler M, Segel M, Van Dervort A, Ryu JH *et al.* Generation of Functional Human Pancreatic β Cells In Vitro. *Cell* 2014; **159**: 428–439.
- 89 Russ HA, Parent AV, Ringler JJ, Hennings TG, Nair GG, Shveygert M *et al.* Controlled induction of human pancreatic progenitors produces functional beta-like cells in vitro. *EMBO J* 2015. doi:10.15252/embj.201591058.
- Oarpenter MK, Frey-Vasconcells J, Rao MS. Developing safe therapies from human pluripotent stem cells. *Nat Biotechnol* 2009; **27**: 606–613.
- 91 Borowiak M, Melton DA. How to make beta cells? Curr Opin Cell Biol 2009; 21: 727–732.
- Takahashi K, Tanabe K, Ohnuki M, Narita M, Ichisaka T, Tomoda K *et al.* Induction of pluripotent stem cells from adult human fibroblasts by defined factors. *Cell* 2007; **131**: 861–872.
- Park I-H, Arora N, Huo H, Maherali N, Ahfeldt T, Shimamura A *et al.* Disease-specific induced pluripotent stem cells. *Cell* 2008; **134**: 877–886.
- 94 Maehr R, Chen S, Snitow M, Ludwig T, Yagasaki L, Goland R *et al.* Generation of pluripotent stem cells from patients with type 1 diabetes. *Proc Natl Acad Sci USA* 2009; **106**: 15768–15773.
- 95 Suzuki A, Nakauchi H, Taniguchi H. Prospective isolation of multipotent pancreatic progenitors using flow-cytometric cell sorting. *Diabetes* 2004; **53**: 2143–2152.
- Jiang F-X, Morahan G. Pancreatic Stem Cells: From Possible to Probable. *Stem Cell Rev* 2011. doi:10.1007/s12015-011-9333-8.
- 97 Thorel F, Népote V, Avril I, Kohno K, Desgraz R, Chera S *et al.* Conversion of adult pancreatic alpha-cells to beta-cells after extreme beta-cell loss. *Nature* 2010; **464**: 1149–1154.
- 98 Chera S, Baronnier D, Ghila L, Cigliola V, Jensen JN, Gu G *et al.* Diabetes recovery by agedependent conversion of pancreatic δ-cells into insulin producers. *Nature* 2014; **514**: 503–507.
- 99 Courtney M, Pfeifer A, Al-Hasani K, Gjernes E, Vieira A, Ben-Othman N *et al.* In vivo conversion of adult α-cells into β-like cells: a new research avenue in the context of type 1 diabetes. *Diabetes Obes Metab* 2011; **13 Suppl 1**: 47–52.
- Courtney M, Gjernes E, Druelle N, Ravaud C, Vieira A, Ben-Othman N *et al.* The inactivation of Arx in pancreatic α-cells triggers their neogenesis and conversion into functional β-like cells. *PLoS Genet* 2013; **9**: e1003934.

- 101 Cozar-Castellano I, Stewart AF. Molecular engineering human hepatocytes into pancreatic beta cells for diabetes therapy. *Proc Natl Acad Sci USA* 2005; **102**: 7781–7782.
- Al-Hasani K, Pfeifer A, Courtney M, Ben-Othman N, Gjernes E, Vieira A *et al.* Adult Duct-Lining Cells Can Reprogram into β-like Cells Able to Counter Repeated Cycles of Toxin-Induced Diabetes. *Developmental Cell* 2013; **26**: 86–100.
- Zhou Q, Brown J, Kanarek A, Rajagopal J, Melton DA. In vivo reprogramming of adult pancreatic exocrine cells to beta-cells. *Nature* 2008; **455**: 627–632.
- Meier JJ, Bhushan A, Butler AE, Rizza RA, Butler PC. Sustained beta cell apoptosis in patients with long-standing type 1 diabetes: indirect evidence for islet regeneration? *Diabetologia* 2005; 48: 2221–2228.
- Keenan HA, Sun JK, Levine J, Doria A, Aiello LP, Eisenbarth G et al. Residual insulin production and pancreatic β-cell turnover after 50 years of diabetes: Joslin Medalist Study. Diabetes 2010; 59: 2846–2853.
- Oram RA, Jones AG, Besser REJ, Knight BA, Shields BM, Brown RJ *et al.* The majority of patients with long-duration type 1 diabetes are insulin microsecretors and have functioning beta cells. *Diabetologia* 2014; **57**: 187–191.
- 107 Assmann A, Hinault C, Kulkarni RN. Growth factor control of pancreatic islet regeneration and function. *Pediatr Diabetes* 2009; **10**: 14–32.
- 108 Assmann A, Ueki K, Winnay JN, Kadowaki T, Kulkarni RN. Glucose Effects on Beta-Cell Growth and Survival Require Activation of Insulin Receptors and Insulin Receptor Substrate 2. *Mol Cell Biol* 2009; **29**: 3219–3228.
- 109 Agudo J, Ayuso E, Jimenez V, Salavert A, Casellas A, Tafuro S *et al.* IGF-I mediates regeneration of endocrine pancreas by increasing beta cell replication through cell cycle protein modulation in mice. *Diabetologia* 2008; **51**: 1862–1872.
- 110 Kulkarni RN, Holzenberger M, Shih DQ, Ozcan U, Stoffel M, Magnuson MA *et al.* beta-cell-specific deletion of the lgf1 receptor leads to hyperinsulinemia and glucose intolerance but does not alter beta-cell mass. *Nat Genet* 2002; **31**: 111–115.
- Guney MA, Petersen CP, Boustani A, Duncan MR, Gunasekaran U, Menon R *et al.* Connective tissue growth factor acts within both endothelial cells and beta cells to promote proliferation of developing beta cells. *Proc Natl Acad Sci USA* 2011; **108**: 15242–15247.
- Riley KG, Pasek RC, Maulis MF, Peek J, Thorel F, Brigstock DR *et al.* Connective tissue growth factor modulates adult β-cell maturity and proliferation to promote β-cell regeneration in mice. *Diabetes* 2015; **64**: 1284–1298.
- 113 Crawford LA, Guney MA, Oh YA, Deyoung RA, Valenzuela DM, Murphy AJ *et al.* Connective tissue growth factor (CTGF) inactivation leads to defects in islet cell lineage allocation and betacell proliferation during embryogenesis. *Mol Endocrinol* 2009; **23**: 324–336.
- 114 Uzan B, Figeac F, Portha B, Movassat J. Mechanisms of KGF mediated signaling in pancreatic duct cell proliferation and differentiation. *PLoS ONE* 2009; **4**: e4734.

- Hart AW, Baeza N, Apelqvist A, Edlund H. Attenuation of FGF signalling in mouse beta-cells leads to diabetes. *Nature* 2000; **408**: 864–868.
- Wagner M, Koschnick S, Beilke S, Frey M, Adler G, Schmid RM. Selective expansion of the betacell compartment in the pancreas of keratinocyte growth factor transgenic mice. *Am J Physiol Gastrointest Liver Physiol* 2008; **294**: G1139–47.
- 117 Krakowski ML, Kritzik MR, Jones EM, Krahl T, Lee J, Arnush M *et al.* Transgenic expression of epidermal growth factor and keratinocyte growth factor in beta-cells results in substantial morphological changes. *J Endocrinol* 1999; **162**: 167–175.
- Movassat J, Beattie GM, Lopez AD, Portha B, Hayek A. Keratinocyte growth factor and beta-cell differentiation in human fetal pancreatic endocrine precursor cells. *Diabetologia* 2003; **46**: 822–829.
- Johansson M, Andersson A, Carlsson P-O, Jansson L. Perinatal development of the pancreatic islet microvasculature in rats. *J Anat* 2006; **208**: 191–196.
- Huang C, Snider F, Cross JC. Prolactin receptor is required for normal glucose homeostasis and modulation of beta-cell mass during pregnancy. *Endocrinology* 2009; **150**: 1618–1626.
- Huang Y, Chang Y. Regulation of pancreatic islet beta-cell mass by growth factor and hormone signaling. *Prog Mol Biol Transl Sci* 2014; **121**: 321–349.
- Brelje TC, Stout LE, Bhagroo NV, Sorenson RL. Distinctive roles for prolactin and growth hormone in the activation of signal transducer and activator of transcription 5 in pancreatic islets of langerhans. *Endocrinology* 2004; **145**: 4162–4175.
- Brelje TC, Scharp DW, Lacy PE, Ogren L, Talamantes F, Robertson M *et al.* Effect of homologous placental lactogens, prolactins, and growth hormones on islet B-cell division and insulin secretion in rat, mouse, and human islets: implication for placental lactogen regulation of islet function during pregnancy. *Endocrinology* 1993; **132**: 879–887.
- Huang Y, Li X, Jiang J, Frank SJ. Prolactin modulates phosphorylation, signaling and trafficking of epidermal growth factor receptor in human T47D breast cancer cells. *Oncogene* 2006; **25**: 7565–7576.
- 125 Clevenger CV. Role of prolactin/prolactin receptor signaling in human breast cancer. *Breast Dis* 2003; **18**: 75–86.
- Lavine JA, Attie AD. Gastrointestinal hormones and the regulation of β-cell mass. *Ann N Y Acad Sci* 2010; **1212**: 41–58.
- 127 Campbell JE, Drucker DJ. Pharmacology, Physiology, and Mechanisms of Incretin Hormone Action. *Cell Metab* 2013; **17**: 819–837.
- Andersson O, Adams BA, Yoo D, Ellis GC, Gut P, Anderson RM *et al.* Adenosine signaling promotes regeneration of pancreatic β cells in vivo. *Cell Metab* 2012; **15**: 885–894.
- Annes JP, Ryu JH, Lam K, Carolan PJ, Utz K, Hollister-Lock J et al. Adenosine kinase inhibition selectively promotes rodent and porcine islet β-cell replication. Proc Natl Acad Sci USA 2012; 109: 3915–3920.

- Lingohr MK, Dickson LM, McCuaig JF, Hugl SR, Twardzik DR, Rhodes CJ. Activation of IRS-2-mediated signal transduction by IGF-1, but not TGF-alpha or EGF, augments pancreatic beta-cell proliferation. *Diabetes* 2002; **51**: 966–976.
- Merighi S, Benini A, Mirandola P, Gessi S, Varani K, Leung E *et al.* Modulation of the Akt/Ras/Raf/MEK/ERK pathway by A<sub>3</sub> adenosine receptor. *Purinergic Signal* 2006; **2**: 627–632.
- Jacques-Silva MC, Bernardi A, Rodnight R, Lenz G. ERK, PKC and PI3K/Akt pathways mediate extracellular ATP and adenosine-induced proliferation of U138-MG human glioma cell line. Oncology 2004; 67: 450–459.
- 133 Abekhoukh S, Planque C, Ripoll C, Urbaniak P, Paul J-L, Delabar J-M *et al.* Dyrk1A, a serine/ threonine kinase, is involved in ERK and Akt activation in the brain of hyperhomocysteinemic mice. *Mol Neurobiol* 2013; **47**: 105–116.
- Kelly PA, Rahmani Z. DYRK1A enhances the mitogen-activated protein kinase cascade in PC12 cells by forming a complex with Ras, B-Raf, and MEK1. *Mol Biol Cell* 2005; **16**: 3562–3573.
- Walpita D, Hasaka T, Spoonamore J, Vetere A, Takane KK, Fomina-Yadlin D *et al.* A Human Islet Cell Culture System for High-Throughput Screening. *Journal of Biomolecular Screening* 2011. doi:10.1177/1087057111430253.
- Bearer EL, Orci L. Endothelial fenestral diaphragms: a quick-freeze, deep-etch study. *J Cell Biol* 1985; **100**: 418–428.
- 137 Brissova M, Shostak A, Shiota M, Wiebe PO, Poffenberger G, Kantz J *et al.* Pancreatic islet production of vascular endothelial growth factor--a is essential for islet vascularization, revascularization, and function. *Diabetes* 2006; **55**: 2974–2985.
- Lammert E, Cleaver O, Melton DA. Induction of pancreatic differentiation by signals from blood vessels. *Science* 2001; **294**: 564–567.
- Nikolova G, Jabs N, Konstantinova I, Domogatskaya A, Tryggvason K, Sorokin L *et al.* The vascular basement membrane: a niche for insulin gene expression and Beta cell proliferation. *Developmental Cell* 2006; **10**: 397–405.
- Murakami T, Miyake T, Tsubouchi M, Tsubouchi Y, Ohtsuka A, Fujita T. Blood flow patterns in the rat pancreas: a simulative demonstration by injection replication and scanning electron microscopy. *Microsc Res Tech* 1997; 37: 497–508.
- 141 Vetterlein F, Pethö A, Schmidt G. Morphometric investigation of the microvascular system of pancreatic exocrine and endocrine tissue in the rat. *Microvasc Res* 1987; **34**: 231–238.
- Bonner-Weir S, Orci L. New perspectives on the microvasculature of the islets of Langerhans in the rat. *Diabetes* 1982; **31**: 883–889.
- Nikolova G, Strilic B, Lammert E. The vascular niche and its basement membrane. *Trends Cell Biol* 2007; **17**: 19–25.
- Yoshitomi H, Zaret KS. Endothelial cell interactions initiate dorsal pancreas development by selectively inducing the transcription factor Ptf1a. *Development* 2004; **131**: 807–817.
- Ferrara N, Gerber H-P, LeCouter J. The biology of VEGF and its receptors. *Nat Med* 2003; **9**: 669–676.

- Pierreux CE, Cordi S, Hick A-C, Achouri Y, Ruiz de Almodovar C, Prévot P-P *et al.* Epithelial: Endothelial cross-talk regulates exocrine differentiation in developing pancreas. *Dev Biol* 2010; **347**: 216–227.
- Lammert E, Cleaver O, Melton DA. Role of endothelial cells in early pancreas and liver development. *Mech Dev* 2003; **120**: 59–64.
- 148 Reinert RB, Brissova M, Shostak A, Pan FC, Poffenberger G, Cai Q *et al.* Vascular endothelial growth factor-a and islet vascularization are necessary in developing, but not adult, pancreatic islets. *Diabetes* 2013; **62**: 4154–4164.
- 149 Sand FW, Hörnblad A, Johansson JK, Lorén C, Edsbagge J, Ståhlberg A *et al.* Growth-limiting role of endothelial cells in endoderm development. *Dev Biol* 2011; **352**: 267–277.
- 150 Cai Q, Brissova M, Reinert RB, Cheng Pan F, Brahmachary P, Jeansson M *et al.* Enhanced expression of VEGF-A in  $\beta$  cells increases endothelial cell number but impairs islet morphogenesis and  $\beta$  cell proliferation. *Dev Biol* 2012; **367**: 40–54.
- Magenheim J, Ilovich O, Lazarus A, Klochendler A, Ziv O, Werman R *et al.* Blood vessels restrain pancreas branching, differentiation and growth. *Development* 2011; **138**: 4743–4752.
- Edsbagge J, Johansson JK, Esni F, Luo Y, Radice GL, Semb H. Vascular function and sphingosine-1-phosphate regulate development of the dorsal pancreatic mesenchyme. *Development* 2005; **132**: 1085–1092.
- Brissova M, Aamodt K, Brahmachary P, Prasad N, Hong J-Y, Dai C *et al.* Islet Microenvironment, Modulated by Vascular Endothelial Growth Factor-A Signaling, Promotes β Cell Regeneration. *Cell Metab* 2014; **19**: 498–511.
- Reinert RB, Cai Q, Hong J-Y, Plank JL, Aamodt K, Prasad N *et al.* Vascular endothelial growth factor coordinates islet innervation via vascular scaffolding. *Development* 2014; **141**: 1480–1491.
- Agudo J, Ayuso E, Jimenez V, Casellas A, Mallol C, Salavert A *et al.* Vascular Endothelial Growth Factor-Mediated Islet Hypervascularization and Inflammation Contribute to Progressive Reduction of β-Cell Mass. *Diabetes* 2012; **61**: 2851–2861.
- 156 Christofori G, Naik P, Hanahan D. Vascular endothelial growth factor and its receptors, flt-1 and flk-1, are expressed in normal pancreatic islets and throughout islet cell tumorigenesis. *Mol Endocrinol* 1995; **9**: 1760–1770.
- Jain R, Lammert E. Cell-cell interactions in the endocrine pancreas. *Diabetes Obes Metab* 2009; **11 Suppl 4**: 159–167.
- van Deijnen JH, Hulstaert CE, Wolters GH, van Schilfgaarde R. Significance of the peri-insular extracellular matrix for islet isolation from the pancreas of rat, dog, pig, and man. *Cell Tissue Res* 1992; **267**: 139–146.
- 159 Kaido T, Yebra M, Cirulli V, Rhodes C, Diaferia G, Montgomery AM. Impact of defined matrix interactions on insulin production by cultured human beta-cells: effect on insulin content, secretion, and gene transcription. *Diabetes* 2006; **55**: 2723–2729.
- Wang RN, Paraskevas S, Rosenberg L. Characterization of Integrin Expression in Islets Isolated from Hamster, Canine, Porcine, and Human Pancreas. *Journal of Histochemistry & Cytochemistry* 1999; **47**: 499–506.

- Bonner-Weir S. Morphological evidence for pancreatic polarity of beta-cell within islets of Langerhans. *Diabetes* 1988; **37**: 616–621.
- 162 Beattie GM, Cirulli V, Lopez AD, Hayek A. Ex vivo expansion of human pancreatic endocrine cells. *J Clin Endocrinol Metab* 1997; **82**: 1852–1856.
- Stagner J, Mokshagundam S, Wyler K, Samols E, Rilo H, Stagner M *et al.* Beta-cell sparing in transplanted islets by vascular endothelial growth factor. *Transplant Proc* 2004; **36**: 1178–1180.
- 164 Virtanen I, Banerjee M, Palgi J, Korsgren O, Lukinius A, Thornell L-E *et al.* Blood vessels of human islets of Langerhans are surrounded by a double basement membrane. *Diabetologia* 2008; **51**: 1181–1191.
- Otonkoski T, Banerjee M, Korsgren O, Thornell L-E, Virtanen I. Unique basement membrane structure of human pancreatic islets: implications for beta-cell growth and differentiation. *Diabetes Obes Metab* 2008; **10 Suppl 4**: 119–127.
- Esni F, Täljedal IB, Perl AK, Cremer H, Christofori G, Semb H. Neural cell adhesion molecule (N-CAM) is required for cell type segregation and normal ultrastructure in pancreatic islets. *J Cell Biol* 1999; **144**: 325–337.
- 167 Cirulli V, Baetens D, Rutishauser U, Halban PA, Orci L, Rouiller DG. Expression of neural cell adhesion molecule (N-CAM) in rat islets and its role in islet cell type segregation. *J Cell Sci* 1994; **107 ( Pt 6)**: 1429–1436.
- Olofsson CS, Håkansson J, Salehi A, Bengtsson M, Galvanovskis J, Partridge C *et al.* Impaired insulin exocytosis in neural cell adhesion molecule-/- mice due to defective reorganization of the submembrane F-actin network. *Endocrinology* 2009; **150**: 3067–3075.
- Dahl U, Sjødin A, Semb H. Cadherins regulate aggregation of pancreatic beta-cells in vivo. *Development* 1996; **122**: 2895–2902.
- Bosco D, Rouiller DG, Halban PA. Differential expression of E-cadherin at the surface of rat betacells as a marker of functional heterogeneity. *J Endocrinol* 2007; **194**: 21–29.
- Jaques F, Jousset H, Tomas A, Prost A-L, Wollheim CB, Irminger J-C *et al.* Dual effect of cell-cell contact disruption on cytosolic calcium and insulin secretion. *Endocrinology* 2008; **149**: 2494–2505.
- Wakae-Takada N, Xuan S, Watanabe K, Meda P, Leibel RL. Molecular basis for the regulation of islet beta cell mass in mice: the role of E-cadherin. *Diabetologia* 2013; **56**: 856–866.
- Bavamian S, Klee P, Britan A, Populaire C, Caille D, Cancela J *et al.* Islet-cell-to-cell communication as basis for normal insulin secretion. *Diabetes Obes Metab* 2007; **9 Suppl 2**: 118–132.
- Serre-Beinier V, Le Gurun S, Belluardo N, Trovato-Salinaro A, Charollais A, Haefliger JA *et al.* Cx36 preferentially connects beta-cells within pancreatic islets. *Diabetes* 2000; **49**: 727–734.
- 175 Charollais A, Gjinovci A, Huarte J, Bauquis J, Nadal A, Martín F *et al.* Junctional communication of pancreatic beta cells contributes to the control of insulin secretion and glucose tolerance. *J Clin Invest* 2000; **106**: 235–243.

- 176 Ravier MA, Güldenagel M, Charollais A, Gjinovci A, Caille D, Söhl G *et al.* Loss of connexin36 channels alters beta-cell coupling, islet synchronization of glucose-induced Ca2+ and insulin oscillations, and basal insulin release. *Diabetes* 2005; **54**: 1798–1807.
- Evans WH, De Vuyst E, Leybaert L. The gap junction cellular internet: connexin hemichannels enter the signalling limelight. *Biochem J* 2006; **397**: 1–14.
- Pasquale EB. Eph-ephrin bidirectional signaling in physiology and disease. *Cell* 2008; **133**: 38–52.
- Konstantinova I, Nikolova G, Ohara-Imaizumi M. EphA-Ephrin-A-Mediated β Cell Communication Regulates Insulin Secretion from Pancreatic Islets. *Cell* 2007.
- Humphries JD, Byron A, Humphries MJ. Integrin ligands at a glance. *J Cell Sci* 2006; **119**: 3901–3903.
- Kilkenny DM, Rocheleau JV. Fibroblast growth factor receptor-1 signaling in pancreatic islet betacells is modulated by the extracellular matrix. *Mol Endocrinol* 2008; **22**: 196–205.
- Kaido T, Perez B, Yebra M, Hill J, Cirulli V, Hayek A *et al.* Alphav-integrin utilization in human beta-cell adhesion, spreading, and motility. *J Biol Chem* 2004; **279**: 17731–17737.
- 183 Kaido T, Yebra M, Cirulli V, Montgomery AM. Regulation of human beta-cell adhesion, motility, and insulin secretion by collagen IV and its receptor alpha1beta1. *J Biol Chem* 2004; **279**: 53762–53769.
- Stendahl JC, Kaufman DB, Stupp SI. Extracellular matrix in pancreatic islets: relevance to scaffold design and transplantation. *Cell transplantation* 2009; **18**: 1–12.
- 185 Wang R, Li J, Lyte K, Yashpal NK, Fellows F, Goodyer CG. Role for beta1 integrin and its associated alpha3, alpha5, and alpha6 subunits in development of the human fetal pancreas. *Diabetes* 2005; **54**: 2080–2089.
- Cirulli V, Beattie GM, Klier G, Ellisman M, Ricordi C, Quaranta V *et al.* Expression and function of alpha(v)beta(3) and alpha(v)beta(5) integrins in the developing pancreas: roles in the adhesion and migration of putative endocrine progenitor cells. *J Cell Biol* 2000; **150**: 1445–1460.
- Diaferia GR, Jimenez-Caliani AJ, Ranjitkar P, Yang W, Hardiman G, Rhodes CJ *et al.* β1 integrin is a crucial regulator of pancreatic β-cell expansion. *Development* 2013. doi:10.1242/dev.098533.
- Riopel M, Krishnamurthy M, Li J, Liu S, Leask A, Wang R. Conditional β1-integrin-deficient mice display impaired pancreatic β cell function. *J Pathol* 2011; **224**: 45–55.
- Saleem S, Li J, Yee S-P, Fellows GF, Goodyer CG, Wang R. beta1 integrin/FAK/ERK signalling pathway is essential for human fetal islet cell differentiation and survival. *J Pathol* 2009; **219**: 182–192.
- 190 Riopel M, Wang R. Collagen matrix support of pancreatic islet survival and function. *Front Biosci* 2014; **19**: 77–90.
- 191 Krishnamurthy M, Li J, Fellows GF, Rosenberg L, Goodyer CG, Wang R. Integrin {alpha}3, but not {beta}1, regulates islet cell survival and function via PI3K/Akt signaling pathways. *Endocrinology* 2011; **152**: 424–435.

- 192 Chin GS, Lee S, Hsu M, Liu W, Kim WJ, Levinson H *et al.* Discoidin domain receptors and their ligand, collagen, are temporally regulated in fetal rat fibroblasts in vitro. *Plast Reconstr Surg* 2001; **107**: 769–776.
- 193 Cheng JYC, Raghunath M, Whitelock J, Poole-Warren L. Matrix components and scaffolds for sustained islet function. *Tissue Eng Part B Rev* 2011; **17**: 235–247.
- van Deijnen JH, Van Suylichem PT, Wolters GH, van Schilfgaarde R. Distribution of collagens type I, type III and type V in the pancreas of rat, dog, pig and man. *Cell Tissue Res* 1994; **277**: 115–121.
- Meyer T, Chodnewska I, Czub S, Hamelmann W, Beutner U, Otto C *et al.* Extracellular matrix proteins in the porcine pancreas: a structural analysis for directed pancreatic islet isolation. *Transplant Proc* 1998; **30**: 354.
- Pinkse GGM, Bouwman WP, Jiawan-Lalai R, Terpstra OT, Bruijn JA, de Heer E. Integrin signaling via RGD peptides and anti-beta1 antibodies confers resistance to apoptosis in islets of Langerhans. *Diabetes* 2006; **55**: 312–317.
- Tunggal P, Smyth N, Paulsson M, Ott MC. Laminins: structure and genetic regulation. *Microsc Res Tech* 2000; **51**: 214–227.
- 198 Parnaud G, Hammar E, Rouiller DG, Armanet M, Halban PA, Bosco D. Blockade of beta1 integrin-laminin-5 interaction affects spreading and insulin secretion of rat beta-cells attached on extracellular matrix. *Diabetes* 2006; **55**: 1413–1420.
- Jiang FX, Cram DS, DeAizpurua HJ, Harrison LC. Laminin-1 promotes differentiation of fetal mouse pancreatic beta-cells. *Diabetes* 1999; **48**: 722–730.
- Jiang FX, Georges-Labouesse E, Harrison LC. Regulation of laminin 1-induced pancreatic betacell differentiation by alpha6 integrin and alpha-dystroglycan. *Mol Med* 2001; **7**: 107–114.
- Jiang FX, Naselli G, Harrison LC. Distinct Distribution of Laminin and Its Integrin Receptors in the Pancreas. *Journal of Histochemistry & Cytochemistry* 2002; **50**: 1625–1632.
- Armanet M, Wojtusciszyn A, Morel P, Parnaud G, Rousselle P, Sinigaglia C *et al.* Regulated laminin-332 expression in human islets of Langerhans. *The FASEB Journal* 2009; **23**: 4046–4055.
- Eberhard D, Kragl M, Lammert E. 'Giving and taking': endothelial and beta-cells in the islets of Langerhans. *Trends Endocrinol Metab* 2010; **21**: 457–463.
- 204 Geutskens SB, Homo-Delarche F, Pleau J-M, Durant S, Drexhage HA, Savino W. Extracellular matrix distribution and islet morphology in the early postnatal pancreas: anomalies in the nonobese diabetic mouse. *Cell Tissue Res* 2004; 318: 579–589.
- 205 Griffith LG, Swartz MA. Capturing complex 3D tissue physiology in vitro. *Nat Rev Mol Cell Biol* 2006; **7**: 211–224.
- 206 Lin X. Functions of heparan sulfate proteoglycans in cell signaling during development. *Development* 2004; **131**: 6009–6021.

- Lammert E, Gu G, McLaughlin M, Brown D, Brekken R, Murtaugh LC *et al.* Role of VEGF-A in vascularization of pancreatic islets. *Curr Biol* 2003; **13**: 1070–1074.
- 208 Beattie GM, Rubin JS, Mally MI, Otonkoski T, Hayek A. Regulation of proliferation and differentiation of human fetal pancreatic islet cells by extracellular matrix, hepatocyte growth factor, and cell-cell contact. *Diabetes* 1996; **45**: 1223–1228.
- Takahashi I, Noguchi N, Nata K, Yamada S, Kaneiwa T, Mizumoto S *et al.* Important role of heparan sulfate in postnatal islet growth and insulin secretion. *Biochem Biophys Res Commun* 2009; **383**: 113–118.
- 210 Corless CL, Mendoza A, Collins T, Lawler J. Colocalization of thrombospondin and syndecan during murine development. *Dev Dyn* 1992; **193**: 346–358.
- Zertal-Zidani S, Bounacer A, Scharfmann R. Regulation of pancreatic endocrine cell differentiation by sulphated proteoglycans. *Diabetologia* 2007; **50**: 585–595.
- Davies LC, Jenkins SJ, Allen JE, Taylor PR. Tissue-resident macrophages. *Nat Immunol* 2013; **14**: 986–995.
- 213 Murray PJ, Wynn TA. Protective and pathogenic functions of macrophage subsets. *Nat Rev Immunol* 2011; **11**: 723–737.
- 214 Murray PJ, Wynn TA. Obstacles and opportunities for understanding macrophage polarization. *J Leukoc Biol* 2011; **89**: 557–563.
- 215 Geutskens SB, Otonkoski T, Pulkkinen M-A, Drexhage HA, Leenen PJM. Macrophages in the murine pancreas and their involvement in fetal endocrine development in vitro. *J Leukoc Biol* 2005; **78**: 845–852.
- 216 Mussar K, Tucker A, McLennan L, Gearhart A, Jimenez-Caliani AJ, Cirulli V *et al.* Macrophage/epithelium cross-talk regulates cell cycle progression and migration in pancreatic progenitors. *PLoS ONE* 2014; **9**: e89492.
- 217 Banaei-Bouchareb L, Gouon-Evans V, Samara-Boustani D, Castellotti MC, Czernichow P, Pollard JW *et al.* Insulin cell mass is altered in Csf1op/Csf1op macrophage-deficient mice. *J Leukoc Biol* 2004; **76**: 359–367.
- 218 Campbell-Thompson ML, Atkinson MA, Butler AE, Chapman NM, Frisk G, Gianani R *et al.* The diagnosis of insulitis in human type 1 diabetes. *Diabetologia* 2013; **56**: 2541–2543.
- 219 Halban PA, Polonsky KS, Bowden DW, Hawkins MA, Ling C, Mather KJ *et al.* β-cell failure in type 2 diabetes: postulated mechanisms and prospects for prevention and treatment. 2014, pp 1983–1992.
- Tessem JS, Jensen JN, Pelli H, Dai X-M, Zong X-H, Stanley ER *et al.* Critical roles for macrophages in islet angiogenesis and maintenance during pancreatic degeneration. *Diabetes* 2008; **57**: 1605–1617.
- 221 Xiao X, Gaffar I, Guo P, Wiersch J, Fischbach S, Peirish L *et al.* M2 macrophages promote betacell proliferation by up-regulation of SMAD7. *Proc Natl Acad Sci USA* 2014; **111**: E1211–E1220.

- 222 Criscimanna A, Coudriet GM, Gittes GK, Piganelli JD, Esni F. Activated macrophages create lineage-specific microenvironments for pancreatic acinar- and β-cell regeneration in mice. *Gastroenterology* 2014; **147**: 1106–18.e11.
- 223 Efrat S, Fusco-DeMane D, Lemberg H, Emran al O, Wang X. Conditional transformation of a pancreatic beta-cell line derived from transgenic mice expressing a tetracycline-regulated oncogene. *Proc Natl Acad Sci USA* 1995; **92**: 3576–3580.
- Milo-Landesman D, Surana M, Berkovich I, Compagni A, Christofori G, Fleischer N *et al.*Correction of hyperglycemia in diabetic mice transplanted with reversibly immortalized pancreatic beta cells controlled by the tet-on regulatory system. *Cell transplantation* 2001; **10**: 645–650.
- Nyman LR, Wells KS, Head WS, McCaughey M, Ford E, Brissova M *et al.* Real-time, multidimensional in vivo imaging used to investigate blood flow in mouse pancreatic islets. *J Clin Invest* 2008; **118**: 3790–3797.
- Ohno-Matsui K, Hirose A, Yamamoto S, Saikia J, Okamoto N, Gehlbach P *et al.* Inducible expression of vascular endothelial growth factor in adult mice causes severe proliferative retinopathy and retinal detachment. *Am J Pathol* 2002; **160**: 711–719.
- Zhang H, Fujitani Y, Wright CVE, Gannon M. Efficient recombination in pancreatic islets by a tamoxifen-inducible Cre-recombinase. *genesis* 2005; **42**: 210–217.
- Gannon M, Gamer LW, Wright CVE. Regulatory regions driving developmental and tissue-specific expression of the essential pancreatic gene pdx1. *Dev Biol* 2001; **238**: 185–201.
- 229 Soriano P. Generalized lacZ expression with the ROSA26 Cre reporter strain. 1999; 21: 70–71.
- Hara M, Wang X, Kawamura T, Bindokas VP, Dizon RF, Alcoser SY *et al.* Transgenic mice with green fluorescent protein-labeled pancreatic beta -cells. *Am J Physiol Endocrinol Metab* 2003; **284**: E177–83.
- Göthert JR, Gustin SE, van Eekelen JAM, Schmidt U, Hall MA, Jane SM *et al.* Genetically tagging endothelial cells in vivo: bone marrow-derived cells do not contribute to tumor endothelium. *Blood* 2004; **104**: 1769–1777.
- Hooper AT, Butler JM, Nolan DJ, Kranz A, Iida K, Kobayashi M *et al.* Engraftment and reconstitution of hematopoiesis is dependent on VEGFR2-mediated regeneration of sinusoidal endothelial cells. *Cell Stem Cell* 2009; **4**: 263–274.
- Okabe M, Ikawa M, Kominami K, Nakanishi T, Nishimune Y. 'Green mice' as a source of ubiquitous green cells. *FEBS Lett* 1997; **407**: 313–319.
- Duffield JS, Tipping PG, Kipari T, Cailhier JF, Clay S, Lang R *et al.* Conditional ablation of macrophages halts progression of crescentic glomerulonephritis. *Am J Pathol* 2005; **167**: 1207–1219.
- 235 Shultz LD, Lyons BL, Burzenski LM, Gott B, Chen X, Chaleff S *et al.* Human lymphoid and myeloid cell development in NOD/LtSz-scid IL2R gamma null mice engrafted with mobilized human hemopoietic stem cells. *J Immunol* 2005; **174**: 6477–6489.
- 236 King M, Pearson T, Shultz LD, Leif J, Bottino R, Trucco M *et al.* A new Hu-PBL model for the study of human islet alloreactivity based on NOD-scid mice bearing a targeted mutation in the IL-2 receptor gamma chain gene. 2008; **126**: 303–314.

- Wang YV, Leblanc M, Fox N, Mao J-H, Tinkum KL, Krummel K *et al.* Fine-tuning p53 activity through C-terminal modification significantly contributes to HSC homeostasis and mouse radiosensitivity. *Genes Dev* 2011; **25**: 1426–1438.
- 238 Reinert RB, Kantz J, Misfeldt AA, Poffenberger G, Gannon M, Brissova M *et al.* Tamoxifen-Induced Cre-loxP Recombination Is Prolonged in Pancreatic Islets of Adult Mice. *PLoS ONE* 2012; **7**: e33529.
- Brissova M, Shiota M, Nicholson WE, Gannon M, Knobel SM, Piston DW *et al.* Reduction in pancreatic transcription factor PDX-1 impairs glucose-stimulated insulin secretion. *J Biol Chem* 2002; **277**: 11225–11232.
- 240 Brissova M, Fowler M, Wiebe P, Shostak A, Shiota M, Radhika A *et al.* Intraislet endothelial cells contribute to revascularization of transplanted pancreatic islets. *Diabetes* 2004; **53**: 1318–1325.
- Wang T, Lacík I, Brissova M, Anilkumar AV, Prokop A, Hunkeler D *et al.* An encapsulation system for the immunoisolation of pancreatic islets. *Nat Biotechnol* 1997; **15**: 358–362.
- 242 Kayton NS, Poffenberger G, Henske J, Dai C, Thompson C, Aramandla R *et al.* Human islet preparations distributed for research exhibit a variety of insulin-secretory profiles. *Am J Physiol Endocrinol Metab* 2015; **308**: E592–E602.
- 243 Mortazavi A, Williams BA, McCue K, Schaeffer L, Wold B. Mapping and quantifying mammalian transcriptomes by RNA-Seq. *Nat Methods* 2008; **5**: 621–628.
- Malone JH, Oliver B. Microarrays, deep sequencing and the true measure of the transcriptome. *BMC Biol* 2011; **9**: 34.
- Trapnell C, Pachter L, Salzberg SL. TopHat: discovering splice junctions with RNA-Seq. *Bioinformatics* 2009; **25**: 1105–1111.
- Robinson MD, Oshlack A. A scaling normalization method for differential expression analysis of RNA-seq data. *Genome Biol* 2010; **11**: R25.
- Dillies M-A, Rau A, Aubert J, Hennequet-Antier C, Jeanmougin M, Servant N *et al.* A comprehensive evaluation of normalization methods for Illumina high-throughput RNA sequencing data analysis. *Brief Bioinformatics* 2012. doi:10.1093/bib/bbs046.
- 248 Benjamini Y, Hochberg Y. A direct approach to false discovery rates. 1995; **57**: 289–300.
- Supek F, Bošnjak M, Škunca N, Šmuc T. REVIGO summarizes and visualizes long lists of gene ontology terms. *PLoS ONE* 2011; **6**: e21800.
- Fiaschi-Taesch NM, Kleinberger JW, Salim FG, Troxell R, Wills R, Tanwir M *et al.* Human pancreatic β-cell G1/S molecule cell cycle atlas. *Diabetes* 2013; **62**: 2450–2459.
- 251 Rieck S, Kaestner KH. Expansion of beta-cell mass in response to pregnancy. 2010; **21**: 151–158.
- Butler JM, Kobayashi H, Rafii S. Instructive role of the vascular niche in promoting tumour growth and tissue repair by angiocrine factors. *Nat Rev Cancer* 2010; **10**: 138–146.

- Barleon B, Sozzani S, Zhou D, Weich HA, Mantovani A, Marmé D. Migration of human monocytes in response to vascular endothelial growth factor (VEGF) is mediated via the VEGF receptor flt-1. *Blood* 1996; **87**: 3336–3343.
- Peshavaria M, Larmie BL, Lausier J, Satish B, Habibovic A, Roskens V *et al.* Regulation of pancreatic beta-cell regeneration in the normoglycemic 60% partial-pancreatectomy mouse. *Diabetes* 2006; **55**: 3289–3298.
- Ward TH, Cummings J, Dean E, Greystoke A, Hou JM, Backen A *et al.* Biomarkers of apoptosis. 2008; **99**: 841–846.
- Lu C, Zhu F, Cho Y-Y, Tang F, Zykova T, Ma W-Y *et al.* Cell apoptosis: requirement of H2AX in DNA ladder formation, but not for the activation of caspase-3. 2006; **23**: 121–132.
- Hesse JE, Faulkner MF, Durdik JM. Increase in double-stranded DNA break-related foci in early-stage thymocytes of aged mice. 2009; **44**: 676–684.
- Wilson AJ, Holson E, Wagner F, Zhang Y-L, Fass DM, Haggarty SJ *et al.* The DNA damage mark pH2AX differentiates the cytotoxic effects of small molecule HDAC inhibitors in ovarian cancer cells. 2011; **12**: 484–493.
- 259 Carmeliet P, Tessier-Lavigne M. Common mechanisms of nerve and blood vessel wiring. 2005; **436**: 193–200.
- Dhawan S, Tschen S-I, Bhushan A. Bmi-1 regulates the Ink4a/Arf locus to control pancreatic beta-cell proliferation. *Genes Dev* 2009; **23**: 906–911.
- 261 Chen H, Gu X, Su I-H, Bottino R, Contreras JL, Tarakhovsky A *et al.* Polycomb protein Ezh2 regulates pancreatic beta-cell Ink4a/Arf expression and regeneration in diabetes mellitus. *Genes Dev* 2009; **23**: 975–985.
- Dai C, Brissova M, Hang Y, Thompson C, Poffenberger G, Shostak A *et al.* Islet-enriched gene expression and glucose-induced insulin secretion in human and mouse islets. *Diabetologia* 2012; **55**: 707–718.
- Sharpe EE III, Teleron AA, Li B, Price J, Sands MS, Alford K *et al.* The Origin and in Vivo Significance of Murine and Human Culture-Expanded Endothelial Progenitor Cells. *Am J Pathol* 2006; **168**: 1710–1721.
- Vasir B, Jonas JC, Steil GM, Hollister-Lock J, Hasenkamp W, Sharma A *et al.* Gene expression of VEGF and its receptors Flk-1/KDR and Flt-1 in cultured and transplanted rat islets. 2001; **71**: 924–935.
- Diamond JR, Pesek-Diamond I. Sublethal X-irradiation during acute puromycin nephrosis prevents late renal injury: role of macrophages. *Am J Physiol* 1991; **260**: F779–86.
- 266 Ricardo SD, van Goor H, Eddy AA. Macrophage diversity in renal injury and repair. *J Clin Invest* 2008; **118**: 3522–3530.
- 267 Nakayama S, Uchida T, Choi JB, Fujitani Y, Ogihara T, Iwashita N *et al.* Impact of whole body irradiation and vascular endothelial growth factor-A on increased beta cell mass after bone marrow transplantation in a mouse model of diabetes induced by streptozotocin. *Diabetologia* 2009; **52**: 115–124.

- Urbán VS, Kiss J, Kovács J, Gócza E, Vas V, Monostori E *et al.* Mesenchymal stem cells cooperate with bone marrow cells in therapy of diabetes. *Stem Cells* 2008; **26**: 244–253.
- Nucera S, Biziato D, De Palma M. The interplay between macrophages and angiogenesis in development, tissue injury and regeneration. *Int J Dev Biol* 2011; **55**: 495–503.
- 270 Kveiborg M, Albrechtsen R, Couchman JR, Wewer UM. Cellular roles of ADAM12 in health and disease. 2008; **40**: 1685–1702.
- Apte SS. A disintegrin-like and metalloprotease (reprolysin-type) with thrombospondin type 1 motif (ADAMTS) superfamily: functions and mechanisms. 2009; **284**: 31493–31497.
- Tsunawaki S, Sporn M, Ding A, Nathan C. Deactivation of macrophages by transforming growth factor-beta. *Nature* 1988; **334**: 260–262.
- 273 Bardin N, Blot-Chabaud M, Despoix N, Kebir A, Harhouri K, Arsanto J-P *et al.* CD146 and its soluble form regulate monocyte transendothelial migration. *Arteriosclerosis, Thrombosis, and Vascular Biology* 2009; **29**: 746–753.
- Grunewald M, Avraham I, Dor Y, Bachar-Lustig E, Itin A, Yung S *et al.* VEGF-Induced Adult Neovascularization: Recruitment, Retention, and Role of Accessory Cells. *Cell* 2006; **124**: 175–189.
- 275 Hess DA, Li L, Martin M, Sakano S, Hill D, Strutt B *et al.* Bone marrow-derived stem cells initiate pancreatic regeneration. *Nat Biotechnol* 2003; **21**: 763–770.
- 276 Hasegawa Y, Ogihara T, Yamada T, Ishigaki Y, Imai J, Uno K *et al.* Bone marrow (BM) transplantation promotes beta-cell regeneration after acute injury through BM cell mobilization. *Endocrinology* 2007; **148**: 2006–2015.
- 277 Sica A, Mantovani A. Macrophage plasticity and polarization: in vivo veritas. *J Clin Invest* 2012; **122**: 787–795.
- He H, Xu J, Warren CM, Duan D, Li X, Wu L *et al.* Endothelial cells provide an instructive niche for the differentiation and functional polarization of M2-like macrophages. *Blood* 2012; **120**: 3152–3162.
- 279 Ding B-S, Nolan DJ, Butler JM, James D, Babazadeh AO, Rosenwaks Z et al. Inductive angiocrine signals from sinusoidal endothelium are required for liver regeneration. *Nature* 2010; 468: 310–315.
- 280 Butler JM, Nolan DJ, Vertes EL, Varnum-Finney B, Kobayashi H, Hooper AT *et al.* Endothelial cells are essential for the self-renewal and repopulation of Notch-dependent hematopoietic stem cells. *Cell Stem Cell* 2010; **6**: 251–264.
- Ding B-S, Nolan DJ, Guo P, Babazadeh AO, Cao Z, Rosenwaks Z *et al.* Endothelial-derived angiocrine signals induce and sustain regenerative lung alveolarization. *Cell* 2011; **147**: 539–553.
- 282 Shi C, Pamer EG. Monocyte recruitment during infection and inflammation. *Nat Rev Immunol* 2011; **11**: 762–774.

- Foulds CE, Nelson ML, Blaszczak AG, Graves BJ. Ras/mitogen-activated protein kinase signaling activates Ets-1 and Ets-2 by CBP/p300 recruitment. *Mol Cell Biol* 2004; **24**: 10954–10964.
- Carlson SM, Chouinard CR, Labadorf A, Lam CJ, Schmelzle K, Fraenkel E *et al.* Large-scale discovery of ERK2 substrates identifies ERK-mediated transcriptional regulation by ETV3. *Science Signaling* 2011; **4**: rs11.
- 285 Martinez FO, Sica A, Mantovani A, Locati M. Macrophage activation and polarization. *Front Biosci* 2008; **13**: 453–461.
- Grunnet LG, Aikin R, Tonnesen MF, Paraskevas S, Blaabjerg L, Størling J *et al.* Proinflammatory cytokines activate the intrinsic apoptotic pathway in beta-cells. *Diabetes* 2009; **58**: 1807–1815.
- Vetere A, Choudhary A, Burns SM, Wagner BK. Targeting the pancreatic β-cell to treat diabetes. *Nat Rev Drug Discov* 2014; **13**: 278–289.
- Dirice E, Kahraman S, Jiang W, Ouaamari El A, De Jesus DF, Teo AKK *et al.* Soluble factors secreted by T-cells promote β-cell proliferation. *Diabetes* 2013. doi:10.2337/db13-0204.
- Morimoto J, Yoneyama H, Shimada A, Shigihara T, Yamada S, Oikawa Y *et al.* CXC chemokine ligand 10 neutralization suppresses the occurrence of diabetes in nonobese diabetic mice through enhanced beta cell proliferation without affecting insulitis. *J Immunol* 2004; **173**: 7017–7024.
- Wada T, Penninger JM. Mitogen-activated protein kinases in apoptosis regulation. *Oncogene* 2004; **23**: 2838–2849.
- Weber LM, Hayda KN, Anseth KS. Cell-matrix interactions improve beta-cell survival and insulin secretion in three-dimensional culture. *Tissue Eng Part A* 2008; **14**: 1959–1968.
- 292 Hammar E, Parnaud G, Bosco D, Perriraz N, Maedler K, Donath M *et al.* Extracellular matrix protects pancreatic beta-cells against apoptosis: role of short- and long-term signaling pathways. *Diabetes* 2004; **53**: 2034–2041.
- Liu Z, Stanojevic V, Avadhani S, Yano T, Habener JF. Stromal cell-derived factor-1 (SDF-1)/ chemokine (C-X-C motif) receptor 4 (CXCR4) axis activation induces intra-islet glucagon-like peptide-1 (GLP-1) production and enhances beta cell survival. *Diabetologia* 2011; **54**: 2067–2076.
- 294 Yano T, Liu Z, Donovan J, Thomas MK, Habener JF. Stromal cell derived factor-1 (SDF-1)/ CXCL12 attenuates diabetes in mice and promotes pancreatic beta-cell survival by activation of the prosurvival kinase Akt. *Diabetes* 2007; **56**: 2946–2957.
- 295 Schlaepfer DD, Hanks SK, Hunter T, van der Geer P. Integrin-mediated signal transduction linked to Ras pathway by GRB2 binding to focal adhesion kinase. *Nature* 1994; **372**: 786–791.
- 296 Playford MP, Schaller MD. The interplay between Src and integrins in normal and tumor biology. *Oncogene* 2004; **23**: 7928–7946.
- 297 Cozar-Castellano I, Fiaschi-Taesch N, Bigatel TA, Takane KK, Garcia-Ocaña A, Vasavada R et al. Molecular control of cell cycle progression in the pancreatic beta-cell. Endocr Rev 2006; 27: 356–370.

- Fiaschi-Taesch NM, Kleinberger JW, Salim FG, Troxell R, Wills R, Tanwir M *et al.* Cytoplasmic-nuclear trafficking of G1/S cell cycle molecules and adult human β-cell replication: a revised model of human β-cell G1/S control. *Diabetes* 2013; **62**: 2460–2470.
- Fiaschi-Taesch NM, Salim F, Kleinberger J, Troxell R, Cozar-Castellano I, Selk K *et al.* Induction of human beta-cell proliferation and engraftment using a single G1/S regulatory molecule, cdk6. *Diabetes* 2010; **59**: 1926–1936.
- 300 Fiaschi-Taesch N, Bigatel TA, Sicari B, Takane KK, Salim F, Velazquez-Garcia S *et al.* Survey of the human pancreatic beta-cell G1/S proteome reveals a potential therapeutic role for cdk-6 and cyclin D1 in enhancing human beta-cell replication and function in vivo. *Diabetes* 2009; **58**: 882–893.
- Takane KK, Kleinberger JW, Salim FG, Fiaschi-Taesch NM, Stewart AF. Regulated and Reversible Induction of Adult Human β-Cell Replication. *Diabetes* 2012; **61**: 418–424.
- 302 Shen W, Tremblay MS, Deshmukh VA, Wang W, Filippi CM, Harb G *et al.* Small-molecule inducer of β cell proliferation identified by high-throughput screening. *J Am Chem Soc* 2013; **135**: 1669–1672.
- Wang W, Walker JR, Wang X, Tremblay MS, Lee JW, Wu X *et al.* Identification of small-molecule inducers of pancreatic beta-cell expansion. *Proc Natl Acad Sci USA* 2009; **106**: 1427–1432.
- Jiao Y, Le Lay J, Yu M, Naji A, Kaestner KH. Elevated mouse hepatic betatrophin expression does not increase human β-cell replication in the transplant setting. *Diabetes* 2014; **63**: 1283–1288.
- Kim H, Toyofuku Y, Lynn FC, Chak E, Uchida T, Mizukami H *et al.* Serotonin regulates pancreatic beta cell mass during pregnancy. *Nat Med* 2010; **16**: 804–808.
- 306 Choi D, Schroer SA, Lu SY, Wang L, Wu X, Liu Y *et al.* Erythropoietin protects against diabetes through direct effects on pancreatic beta cells. *J Exp Med* 2010; **207**: 2831–2842.
- 307 Xu G, Stoffers DA, Habener JF, Bonner-Weir S. Exendin-4 stimulates both beta-cell replication and neogenesis, resulting in increased beta-cell mass and improved glucose tolerance in diabetic rats. *Diabetes* 1999; **48**: 2270–2276.
- Guthalu Kondegowda N, Joshi-Gokhale S, Harb G, Williams K, Zhang XY, Takane KK *et al.* Parathyroid hormone-related protein enhances human ß-cell proliferation and function with associated induction of cyclin-dependent kinase 2 and cyclin E expression. *Diabetes* 2010; **59**: 3131–3138.
- Russ HA, Bar Y, Ravassard P, Efrat S. In vitro proliferation of cells derived from adult human beta-cells revealed by cell-lineage tracing. *Diabetes* 2008; **57**: 1575–1583.
- 310 Rachdi L, Kariyawasam D, Guez F, Aïello V, Arbonés ML, Janel N *et al.* Dyrk1a haploinsufficiency induces diabetes in mice through decreased pancreatic beta cell mass. *Diabetologia* 2014; **57**: 960–969.
- 311 Soltani N, Qiu H, Aleksic M, Glinka Y, Zhao F, Liu R *et al.* GABA exerts protective and regenerative effects on islet beta cells and reverses diabetes. *Proc Natl Acad Sci USA* 2011; **108**: 11692–11697.

- Tian J, Dang H, Chen Z, Guan A, Jin Y, Atkinson MA *et al.* γ-Aminobutyric acid regulates both the survival and replication of human β-cells. *Diabetes* 2013; **62**: 3760–3765.
- Purwana I, Zheng J, Li X, Deurloo M, Son DO, Zhang Z *et al.* GABA promotes human β-cell proliferation and modulates glucose homeostasis. *Diabetes* 2014; **63**: 4197–4205.
- Brown ML, Schneyer AL. Emerging roles for the TGFbeta family in pancreatic beta-cell homeostasis. *Trends Endocrinol Metab* 2010; **21**: 441–448.
- 315 Brun T, Franklin I, St-Onge L, Biason-Lauber A, Schoenle EJ, Wollheim CB *et al.* The diabetes-linked transcription factor PAX4 promotes {beta}-cell proliferation and survival in rat and human islets. *J Cell Biol* 2004; **167**: 1123–1135.
- 316 Mukherjee A, Sidis Y, Mahan A, Raher MJ, Xia Y, Rosen ED *et al.* FSTL3 deletion reveals roles for TGF-beta family ligands in glucose and fat homeostasis in adults. *Proc Natl Acad Sci USA* 2007; **104**: 1348–1353.
- Tsuji N, Ninov N, Delawary M, Osman S, Roh AS, Gut P *et al.* Whole organism high content screening identifies stimulators of pancreatic Beta-cell proliferation. *PLoS ONE* 2014; **9**: e104112.
- 318 Xu F, Wu H, Katritch V, Han GW, Jacobson KA, Gao Z-G *et al.* Structure of an agonist-bound human A2A adenosine receptor. *Science* 2011; **332**: 322–327.
- Mantell S, Jones R, Trevethick M. Design and application of locally delivered agonists of the adenosine A(2A) receptor. *Expert Rev Clin Pharmacol* 2010; **3**: 55–72.
- Perfetti R, Merkel P. Glucagon-like peptide-1: a major regulator of pancreatic beta-cell function. *Eur J Endocrinol* 2000; **143**: 717–725.
- Tourrel C, Bailbé D, Meile M-J, Kergoat M, Portha B. Glucagon-like peptide-1 and exendin-4 stimulate beta-cell neogenesis in streptozotocin-treated newborn rats resulting in persistently improved glucose homeostasis at adult age. *Diabetes* 2001; **50**: 1562–1570.
- Like AA, Rossini AA. Streptozotocin-induced pancreatic insulitis: new model of diabetes mellitus. *Science* 1976; **193**: 415–417.
- Cano DA, Rulifson IC, Heiser PW, Swigart LB, Pelengaris S, German M *et al.* Regulated betacell regeneration in the adult mouse pancreas. *Diabetes* 2008; **57**: 958–966.
- Finegood DT, Weir GC, Bonner-Weir S. Prior streptozotocin treatment does not inhibit pancreas regeneration after 90% pancreatectomy in rats. *Am J Physiol* 1999; **276**: E822–7.
- Leahy JL, Bumbalo LM, Chen C. Beta-cell hypersensitivity for glucose precedes loss of glucose-induced insulin secretion in 90% pancreatectomized rats. *Diabetologia* 1993; **36**: 1238–1244.
- Wang ZV, Mu J, Schraw TD, Gautron L, Elmquist JK, Zhang BB *et al.* PANIC-ATTAC: a mouse model for inducible and reversible beta-cell ablation. *Diabetes* 2008; **57**: 2137–2148.
- Meredith JE, Fazeli B, Schwartz MA. The extracellular matrix as a cell survival factor. *Mol Biol Cell* 1993; **4**: 953–961.
- Gilmore AP, Owens TW, Foster FM, Lindsay J. How adhesion signals reach a mitochondrial conclusion--ECM regulation of apoptosis. *Curr Opin Cell Biol* 2009; **21**: 654–661.

- Duffield JS, Forbes SJ, Constandinou CM, Clay S, Partolina M, Vuthoori S *et al.* Selective depletion of macrophages reveals distinct, opposing roles during liver injury and repair. *J Clin Invest* 2005; **115**: 56–65.
- Goren I, Allmann N, Yogev N, Schürmann C, Linke A, Holdener M *et al.* A transgenic mouse model of inducible macrophage depletion: effects of diphtheria toxin-driven lysozyme M-specific cell lineage ablation on wound inflammatory, angiogenic, and contractive processes. *Am J Pathol* 2009; **175**: 132–147.
- 331 Miyake Y, Asano K, Kaise H, Uemura M, Nakayama M, Tanaka M. Critical role of macrophages in the marginal zone in the suppression of immune responses to apoptotic cell–associated antigens. *J Clin Invest* 2007; **117**: 2268–2278.
- Golson ML, Misfeldt AA, Kopsombut UG, Petersen CP, Gannon M. High Fat Diet Regulation of β-Cell Proliferation and β-Cell Mass. *Open Endocrinol J* 2010; **4**. doi:10.2174/187421650100401 0066.
- Karnik SK, Chen H, McLean GW, Heit JJ, Gu X, Zhang AY *et al.* Menin controls growth of pancreatic beta-cells in pregnant mice and promotes gestational diabetes mellitus. *Science* 2007; **318**: 806–809.
- Terauchi Y, Takamoto I, Kubota N, Matsui J, Suzuki R, Komeda K *et al.* Glucokinase and IRS-2 are required for compensatory cell hyperplasia in response to high-fat diet-induced insulin resistance. *J Clin Invest* 2007; **117**: 246–257.
- Sone H, Kagawa Y. Pancreatic beta cell senescence contributes to the pathogenesis of type 2 diabetes in high-fat diet-induced diabetic mice. *Diabetologia* 2005; **48**: 58–67.
- 336 Hull RL, Kodama K, Utzschneider KM, Carr DB, Prigeon RL, Kahn SE. Dietary-fat-induced obesity in mice results in beta cell hyperplasia but not increased insulin release: evidence for specificity of impaired beta cell adaptation. *Diabetologia* 2005; **48**: 1350–1358.
- Li J, Chen K, Zhu L, Pollard JW. Conditional deletion of the colony stimulating factor-1 receptor (c-fms proto-oncogene) in mice. *genesis* 2006; **44**: 328–335.
- Ventura A, Kirsch DG, McLaughlin ME, Tuveson DA, Grimm J, Lintault L *et al.* Restoration of p53 function leads to tumour regression in vivo. *Nature* 2007; **445**: 661–665.
- Mohrs M, Ledermann B, Köhler G, Dorfmüller A, Gessner A, Brombacher F. Differences between IL-4- and IL-4 receptor alpha-deficient mice in chronic leishmaniasis reveal a protective role for IL-13 receptor signaling. *J Immunol* 1999; **162**: 7302–7308.
- van Haeften TW, Twickler TB. Insulin-like growth factors and pancreas beta cells. *Eur J Clin Invest* 2004; **34**: 249–255.
- 341 Bluestone JA, Herold K, Eisenbarth G. Genetics, pathogenesis and clinical interventions in type 1 diabetes. *Nature* 2010; **464**: 1293–1300.
- Atkinson MA, Bluestone JA, Eisenbarth GS, Hebrok M, Herold KC, Accili D *et al.* How does type 1 diabetes develop?: the notion of homicide or β-cell suicide revisited. *Diabetes* 2011; **60**: 1370–1379.
- Olefsky JM, Glass CK. Macrophages, inflammation, and insulin resistance. *Annu Rev Physiol* 2010; **72**: 219–246.

- Ehses JA, Perren A, Eppler E, Ribaux P, Pospisilik JA, Maor-Cahn R *et al.* Increased number of islet-associated macrophages in type 2 diabetes. *Diabetes* 2007; **56**: 2356–2370.
- Donath MY, Schumann DM, Faulenbach M, Ellingsgaard H, Perren A, Ehses JA. Islet inflammation in type 2 diabetes: from metabolic stress to therapy. *Diabetes Care* 2008; **31 Suppl 2**: S161–4.
- Fowler MJ. Microvascular and macrovascular complications of diabetes. *Clinical diabetes* 2008.
- Avogaro A, Albiero M, Menegazzo L, de Kreutzenberg S, Fadini GP. Endothelial dysfunction in diabetes: the role of reparatory mechanisms. *Diabetes Care* 2011; **34 Suppl 2**: S285–90.
- Dai C, Brissova M, Reinert RB, Nyman L, Liu EH, Thompson C *et al.* Pancreatic islet vasculature adapts to insulin resistance through dilation and not angiogenesis. *Diabetes* 2013; **62**: 4144–4153.